ANNUAL PROGRESS REPORT
1973

BONE MINERAL LABORATORY
UNIVERSITY OF WISCONSIN
MADISON, WISCONSIN

PROGRESS REPORT

NASA Grant No. Y-NGR-50-002-051

"SKELETAL STATUS AND SOFT TISSUE

COMPOSITION IN ASTRONAUTS"

AND

NASA Grant No. Y-NGR-50-002-183

"TISSUE AND FLUID CHANGES BY

RADIONUCLIDE ABSORPTIOMETRY IN VIVO"

August 1, 1973

John R. Cameron
Richard B. Mazess
Charles R. Wilson

Department of Radiology
University of Wisconsin Medical Center
Madison, Wisconsin 53706

FORWARD

This progress report is a summary of research on the measurement of bone mineral content and body composition, in vivo, at the University of Wisconsin from July 15, 1972 through July 15, 1973. Research support for our laboratories comes from the National Aeronautics and Space Administration through Grant Y-NGR-50-002-051 and Y-NGR-50-002-183 and the University of Wisconsin. The research work represents primarily the efforts of the following: Dr. Philip F. Judy, Dr. Mark Mueller, Dr. Everett L. Smith, Robert M. Witt, John M. Sandrik, Kianpour Kianian, William Kan, James Hansen, Ralph Mathison, Howie Gollup, Norbert Pelc, and Clifford E. Vought. We wish to express appreciation for their efforts.

We would like to thank Mrs. Linda Robbins, Mrs. Mary Wheaton, Miss Barbara Epstein, and Miss Joyce Reilly for their secretarial help in preparing these reports and Stephanie Wurdinger and Quentin Verdier for assembling these reports. We would also like to thank Orlando Canto for the illustration.

Certain parts of this report represent work in progress which will be continued during the coming year, and work which resulted from previous support through AEC-(11-1)-1422.

John R. Cameron Richard B. Mazess Charles R. Wilson

September 19, 1973

ANNUAL PROGRESS REPORT ON AEC CONTRACT AT(11-1)-1422

Table of Contents

11. COO-1422-145 Detectors Suitable for Body Composition Measurements with the Photon Absorptiometry Technique.

. . . R. M. Witt

12. COO-1422-146 A Compact Scanner for Measurement of Bone Mineral Content and Soft-Tissue Composition.

. . . D. A. Hennies, R. B. Mazess and C. R. Wilson

13. COO-1422-147 Direct Readout of Bone Mineral Content with Dichromatic Absorptiometry.

. . . W. C. Kan, C. R. Wilson, R. M. Witt and R. B. Mazess

14. COO-1422-148 Absorptiometry Using ^{125}I and ^{241}Am to Determine Tissue Composition In Vivo.

. . . Norbert J. Pelc

15. COO-1422-149 Bone Mineral Content of North Alaskan Eskimos.

. . . Richard B. Mazess and Warren E. Mather

16. COO-1422-150 The Bone Mineral and Soft Tissue Composition of the Siemens-Reiss Reference Step Wedges.

. . . R. H. Jurisch, R. M. Witt and J. R. Cameron

17. COO-1422-151 The Expected Precision of Dual-Photon-Absorptiometry for Fat-Lean Composition.

. . . James Hanson

18. COO-1422-152 Video-Roentgen Absorptiometry for the Measurement of Bone Mineral Mass.

. . . C. R. Wilson, J. R. Cameron, E. L. Ritman, R. E. Sturm and R. A. Robb

19. COO-1422-153 Effects of the Polyenergetic Character of the Spectrum of ^{125}I on the Measurement of Bone Mineral Content.

. . . John M. Sandrik and Philip F. Judy

20. COO-1422-154 Rectilinear and Linear Scanning in the Determination of Bone Mineral Content.

. . . J. M. Sandrik, C. R. Wilson and J. R. Cameron

21. COO-1422-155 Determination of Lung Tumor Mass by Roentgen Video Absorptiometry.

. . . J. M. Sandrik, C. R. Wilson and J. R. Cameron

22. C00-1422-156 Bone Loss in Rheumatoid Arthritis Accelerated by Corticosteroid Treatment.

. . . M. N. Mueller, R. B. Mazess and J. R. Cameron

23. C00-1422-157 Evaluation of Bone Mass in Arthritis Using Monoenergetic Photon-Absorptiometry.

. . . M. N. Mueller

24. C00-1422-158 Early Recognition of Osteoporosis in the Aged Female.

. . . Everett Smith, Steven Babcock and John Cameron

25. C00-1422-159 Effects of Physical Activity on Bone Loss in the Aged.

. . . E. L. Smith and S. W. Babcock

COO-1422-135

DIRECT READOUT OF BONE MINERAL CONTENT USING RADIONUCLIDE ABSORPTIOMETRY +

R. B. Mazess and J. R. Cameron*

and

H. M. Miller

International Journal of Applied Radiation and Isotopes, 1972, Vol. 23, pp. 471-479

A B S T R A C T

A device has been constructed and tested which provides immediate readout of bone mineral content and bone width from absorptiometric scans with low-energy radionuclides (such as ^{125}I). The basis of this analog system is a logarithmic converter-integrator coupled with a precision linear ratemeter. The system provided accurate and reliable results on standards and ashed bone sections. The standard deviation for measurements on standards over a year was about 1 percent; the standard deviation for the residuals about the regression line predicting the ash weight of bone sections was about 1.5 percent, but part of this appeared due to variability in the bone sections rather than due to limitations of the instrumentation. Clinical measurements were made on about 100 patients with the direct readout system, and these were highly correlated with the results from digital scan data on the same patients. The direct readout system has been used successfully in field studies and surveys as well as for clinical observations. Such an analog system has several advantages over previously-used digital handling of scan data, including lower operational and equipment costs, greater mobility, and immediate availability of results.

* Reprint available upon request

+ Preprint appeared in 1972 Bone Mineral Progress Report, COO-1422-114

COO-1422-136

WEIGHT AND DENSITY OF SADLERMIUT ESKIMO LONG BONES[+]

By:

Richard B. Mazess and Robert Jones[*]

Human Biology, September, 1972, Vol. 44, No. 3, pp. 537-548

A B S T R A C T

The weights of six long bones and the densities (water displacement) of three of these were measured in the Sadlermiut Eskimo skeletal series (67 adults). Weights and densities of these appendicular bones were intercorrelated. Older adults of both sexes had about 10 to 15% lower bone weights and densities than younger adults. As in previous work on bone sections, the Sadlermiut had bone densities comparable to those of elderly Negroes and higher than those of elderly Whites, but if correction is made for age and for methodological differences the Sadlermiut were more nearly comparable to Whites and lower in density than Negroes. Sex differences in Sadlermiut bone weights and densities were smaller than in Whites or Negroes.

[*] Reprint available upon request

[+] Preprint appeared in 1972 Bone Mineral Progress Report, COO-1422-115

COO-1422-137

THE EFFECTS OF TEMPORARY PROTEIN DEPRIVATION ON BONE WIDTH AND BONE MINERAL CONTENT IN RHESUS MACAQUES

Walter Leutenegger
Robert M. Larsen
Sylvia Bravo

Department of Anthropology
University of Wisconsin
Madison, Wisconsin

Protein malnutrition retards bone growth (Jha et al, 1968) and reduces mineral densities (du Boulay, 1972) in primates. Similar bone disturbances have been reported in humans (Jones and Dean, 1959; Gillman and Gillman, 1951), in pigs (Pratt and McCance, 1964), and in rats (McCance and Widdowson, 1962; Dickerson et al, 1972). The chronological timing and duration of deprivation influence the extent and permanence of bone alterations (Pratt and McCance, 1964).

Normal bone growth and maturation (Kerr et al, 1972), as well as bone growth in protein deficiency (Kerr et al,1973) have been recorded in rhesus macaques. The impact of temporary protein deprivation, followed by a normal diet, on the bone, however, has not been well documented for these animals. The objective of this study was to provide measurements of bone dimension and bone mineral in macaques recovered from temporary protein malnutrition in their first year.

SAMPLES AND METHODS

Seventeen rhesus macaques were selected for a study on temporary protein deprivation. This study was part of a larger research effort considering calorie-protein malnutrition carried out by the Wisconsin Regional Primate Center. These animals were divided into two dietary groups, the dietary regimes of which are presented in Table 1. Control animals were fed foodstuffs which contained 18.2% protein during their first year. The composition of their control diet (Similac-Ross Laboratories) can be found in Kerr et al (1969). Deprived animals received the control diet but with only 50% or 25% of the control protein level between 30 and 210 days of age. This deficient protein diet was made isocaloric with lactose. The diet, before and after the deprivation, until one year of age, was the control diet. All animals received daily vitamin supplements (Paladac) during the first year, and returned to a Purina monkey chow and fruit diet after one year. The animals were sacrificed at an average age of 4.5 years, approximately 1400 days after deprivation. Sample sizes, age at sacrifice and weight at sacrifice are presented in Table 1.

Bone mineral values and bone widths of the humerus and femur were taken from the sacrificed animals. In vivo determinations of bone width and bone mineral were possible utilizing direct photon absorptiometry. Description and discussion of the technique can be found elsewhere (Cameron et al, 1968; Mazess, 1964; Mazess, 1971).

RESULTS

Bone widths and bone mineral values for both groups are presented in Table 2 and Table 3. No significant differences in width dimension occurred between the two groups. The bone mineral contents of the control animals were higher at all three sites on both bones. Significantly greater values were recorded at proximal and midshaft sites of the femur of control animals.

DISCUSSION

In this study a group of infant rhesus macaques were placed on a low protein diet (4.0%or 9,1% protein) between 30 and 210 days of age, after which they received a normal diet. Deprivation was severe enough to retard weight gain during the experiment and to prohibit normal weight recovery. The protein deprivation did not adversely affect skeletal dimensions, as indicated by width measurements, but did reduce bone mineral values in the rehabilitated animals.

A similar study on rats (Dickerson et al, 1972) found that protein deprivation had a small but permanent stunting effect on some of the bones (pelvis, hind limb) but not on the forelimb. Comparison of the two studies is difficult, however, since bone width was the only common measurement. The significantly lower bone mineral values in the deprived animals after an early deprivation and a four year recovery period are of interest. These values suggest that a reduction of bone mineral content may be not completely reversible with respect to the recovery of normal bone mass in some bones.

ACKNOWLEDGEMENTS

This work was supported in part by grant RR-00167 from the National Institutes of Health, United States Health Service to the Wisconsin Regional Primate Research Center and by grant 130628 from the Research Committee of the Graduate School of the University of Wisconsin, Madison. Substantial help was given by Drs. John R. Cameron, R. W. Goy, W. D. Houser and R. B. Mazess.

TABLE I

Sample sizes, dietary regimes, ages of sacrifice, and average weights at sacrifice of control and deprived animals

N	Dietary regime (Days)	Age of sacrifice	Average weight at sacrifice
Control 9	0-365 days control diet*	1650 ± 314 days	5.45 kg
	365 - Purina chow and fruit		
Deprived 8	0-30 days control diet	1603 ± 223 days	4.61 kg
	30-210 days control diet with 1/4-1/2 less protein+		
	210-365 days control diet		
	365 - Purina chow and fruit		

* Control diet is commercially called Similac (Ross Laboratories)

\+ Ross Laboratories also provided the 1/2 and 1/4 protein deficient formulas.

TABLE 2

Mean bone widths (cm) at six sites of control and deprived rhesus macaques. None of the differences were significant.

Site	CONTROL		DEPRIVED		
	Mean	S.D.	Mean	S.D.	t-value
Humerus					
Proximal	1.034	0.179	1.041	0.224	-0.06
Midshaft	0.899	0.152	0.956	0.182	-0.65
Distal	0.863	0.092	0.855	0.140	0.13
Femur					
Proximal	1.099	0.092	1.103	0.084	-0.08
Midshaft	1.141	0.116	1.102	0.070	0.77
Distal	1.139	0.102	1.172	0.118	-0.59

TABLE 3

Mean bone mineral values (g/cm) at six sites of control and deprived rhesus macaques. Two of the femoral differences were significant

Site	CONTROL		DEPRIVED		
	Mean	S.D.	Mean	S.D.	t-value
Humerus					
Proximal	0.610	0.122	0.552	0.084	1.06
Midshaft	0.585	0.130	0.546	0.073	0.69
Distal	0.600	0.105	0.553	0.109	0.85
Femur					
Proximal	0.734	0.070	0.650	0.047	2.69*
Midshaft	0.679	0.098	0.576	0.037	2.62*
Distal	0.629	0.086	0.588	0.091	0.90

* Indicates a significance level of less than 0.02

REFERENCES

Cameron, J.R., Mazess, R.B. and Sorenson, J.A. Precision and Accuracy of Bone Mineral Determination by Direct Photon Absorptiometry. Invest. Radiol. 3: 141-150 (1968).

Dickerson, J.W.T., Hughes, P.S.R. and McAnulty, P.A. The Growth and Development of Rats Given a Low-Protein Diet. Br. J. Nutr. 27: 527-536 (1972).

du Boulay, G.H., Hime, J.M. and Verity, P.M. Spondylosis in Captive Wild Animals: A Possible Relationship with Nutritional Osteodystrophy. Br. J. Radiol. 45: 841-847 (1972).

Gillman, J. and Gillman, T. Perspective in Human Malnutrition. Grune, New York (1951).

Jha, G.J., Deo, M.G. and Ramalingaswami, V. Bone Growth in Protein Deficiency. Amer. J. Path. 53: 1111-1123 (1968).

Jones, P.R.M. and Dean, R.F.A. The Effect of Kwashiorkor on the Development of the Bones of the Knee. J. Pediat. 54: 176-184 (1959).

Kerr, G.R., Scheffler, G. and Waisman, H.A. Growth and Development of Infant M. Mulatta Fed a Standardized Diet. Growth 33: 185-199 (1969).

Kerr, G.R., Wallace, J.H., Chesney, C.F. and Waisman, H.A. Growth and Development of the Fetal Rhesus Monkey III. Maturation and Linear Growth of the Skull and Appendicular Skeleton. Growth 36: 59-76 (1972).

Kerr, G.R., Waisman, H.A., Allen, J.A., Wallace, J. and Scheffler, G. Malnutrition Studies in Mucaca Mulatta II. The Effect on Organ Size and Skeletal Growth. Amer. J. Clin. Nutr. 26: 620-630 (1973).

Mazess, R.B. Accuracy of Bone Mineral Measurement. Science 145: 388-389 (1964).

Mazess, R.B. Estimation of Bone and Skeletal Weight by Direct Photon Absorptiometry. Invest. Radiol. 6: 52-60 (1971).

McCance, R.A. and Widdowson, E.M. The Bearing of the Plane of Nutrition on Growth and Endocrine Development. In Protein Metabolism, F. Gross (ed.), Spiner and Berlin, 109-117 (1972).

Pratt, C.W. and McCance, R.A. Severe Undernutrition in Growing and Adult Animals. XIV. The Shafts of the Long Bones in Pigs. Br. J. Nutr. 18: 613-624 (1964).

COO-1422-138

AGE RELATED CHANGES IN THE COMPRESSIVE STRENGTH AND BONE MINERAL PER UNIT VOLUME OF COMPACT BONE*

By:

Charles R. Wilson
Department of Radiology
University of Wisconsin

The bone mineral content (determined by the University of Wisconsin photon absorptiometric technique) and the maximum compressive strength of compact bone samples from 24 skeletons ranging in age from 35 to 89 years were measured. The maximum compressive strength was found to decrease by about 7 percent per decade after age 35. There was also a decline in the amount of bone mineral per unit volume of compact bone tissue of about 3.3 percent per decade. The results of these measurements will be presented in terms of a model of compact bone which mathematically describes the age related changes in its strength and bone mineral per unit bolume after maturity. In the model, bone in considered to be a material with nearly uniform physical properties in which cylindrical voids corresponding to haversian canals, incompletely closed osteons and resorption spaces are preferentially oriented along the long axis of the bone. The model predicts that the bone mineral content will provide a better estimate of the maximum compressive load of a bone specimen than its area, and this was experimentally verified.

*Presented at the Annual Winter Meeting of the AAPM, Chicago, Illinois December, 1972

COO-1422-139

ESTIMATION OF THE BONE MINERAL CONTENT OF THE FEMORAL NECK AND SPINE FROM THE BONE MINERAL CONTENT OF THE RADIUS OR ULNA[+]

Charles R. Wilson

J. Bone Joint Surg. (in press)[*]

A B S T R A C T

The interrelationships between the bone mineral content (BMC) of the radius and ulna and that of the femoral neck and lower thoracic vertebrae of twenty-four skeletons were investigated to determine the utility of the peripheral bones in predicting the BMC of the femoral neck and spine. The BMC of the radius and ulna were highly related to that of the femoral neck (average correlation coefficients, $\bar{r}$, were 0.82 and 0.81 respectively) and moderately related to the mineral content of the vertebrae ($\bar{r}$ = 0.57 and 0.51 respectively). Regression analysis showed that the radius BMC provides an estimate (%SEE - 16%) of the BMC of the femoral neck. The combination of the radius BMC and age provides a similar predictive accuracy (%SEE 17%) for the BMC of the vertebrae.

[*]Reprints of this article available upon request

[+]Preprint appeared in 1972 Bone Mineral Progress Report, COO-1422-131

COO-1422-140

Analysis of the Effects of Adipose Tissue on the Absorptiometric Measurement of Bone Mineral Mass

W. W. Wooten, MS,* P. F. Judy, PhD,† and M. A. Greenfield, PhD*

The effects of adipose tissue on the absorptiometric measurement of bone mineral mass has been estimated mathematically. The error caused by adipose tissue in the bone has been determined from a formula derived from the exponential equations describing the attenuation of mono-energetic x-rays. At the radius site, 6 cm from the proximal end, the accuracy error ranged from 1.5 to 5.5% at 27 kev, and from 2.5 to 8.5% at 60 kev. This accuracy error can be affected by calibration techniques. The imprecision due to adipose tissue in the bone was 1.2% at 27 kev, and 1.8% at 60 kev, and is independent of calibration techniques.

Key words: bone (analysis), bone (radiography), radioisotopes (diagnostic), radioisotope scanning, osteoporosis.

THE BONE MINERAL MASS AT A PARTICULAR site in a bone has been estimated in vivo by the attenuation of x-rays by the bone. The precision of such measurements improved significantly when Cameron developed his method in 1963.[1] A nearly mono-energetic radionuclide source was substituted for the polyenergetic x-ray tube source, and a collimated scintillation detector was substituted for the x-ray film. The attenuation of these beams by a single substance can be described by a single exponential formula and the mass attenuation coefficients measured are consistent with the tabulated values.[2]

For photon energies that are practical (less than 60 kev), the mass attenuation coefficient of bone mineral is at least two times larger than all other tissues present. Cameron assumed the system can be treated mathematically as though there were only two types of attenuators present in the body, "bone mineral" and "soft tissue." The mathematical derivation has been presented in detail and will only be summarized here; m_b is the amount of mineral in the path of the photon beam (in units of g/cm²) and is related to the transmission rates I_o^* and I (Fig. 1) according to the equation:

$$m_b = \rho_b \frac{\ln\left(\frac{I_o^*}{I}\right)}{(\mu/\rho)_b\ \rho_b - (\mu/\rho)_s\ \rho_s}$$

Some confusion may arise from the notation: $(\mu/\rho)_b$ and $(\mu/\rho)_s$ represent the mass attenuation coefficients (cm²/g) of bone mineral and soft tissue, respectively. This notation is chosen to be consistent with most references and deviates from the articles published by Cameron and his group[1] in that they choose μ_b and μ_s to represent the mass attenuation coefficients.

Several features of the derivation should be noted.

1. The mass attenuation coefficients for both bone mineral and soft tissue are determined by two independent factors—the composition of the mineral and the photon energy.

2. The densities ρ_b and ρ_s are the densities of pure bone mineral (ρ_b = 3.2 g/cm³)[4] and soft tissue (ρ_s = 1.0 g/cm³). These may be thought of as the microscopic densities and are constant for all samples of bone. Compact bone is not pure bone mineral but a mixture of bone mineral, collagen, and other minerals, and has a hydrated density of about

* Department of Radiological Sciences, UCLA School of Medicine, Center for the Health Sciences, Los Angeles, Calif.

† Department of Radiology, University of Wisconsin, Madison, Wis.

2.0 g/cm³ [4] which may be thought of as the macroscopic density. Each cubic centimeter of compact bone contains about 1.2 g of bone mineral[4] and about .8 g of other tissues and water. The derivation assumes that these other tissues can be treated as equivalent to soft tissue. All samples of compact bone need not have the same (macroscopic) density because the relative abundance of bone mineral and other minerals can vary.

3. For an instrument that has been calibrated with an ash study, the result of a measurement is the mass of bone mineral present, not the mass of compact bone. The measurement is independent of the distribution of bone mineral, and by implication the bone mineral present could be compressed into a thickness with the density of pure bone mineral (3.2 g/cm³).

Effect of Adipose Tissue

This treatment is exact if there are only two types of attenuators present—soft tissue and bone mineral. In fact, there are many types of tissue present and the resulting error is not completely understood. The attenuation characteristics of adipose tissue differ from those of soft tissue as a result of two factors: 1. the composition shows an increased lipid content which leads to a decreased mass attenuation coefficient at low photon energies, and 2. the density of adipose tissue is about 0.9 g/cm³ while that of soft tissue is about 1.0. This decreases the attenuation at all energies and is the dominant factor at high energies.

Adipose tissue can be considered as a third phase, distinct from soft tissue, or bone mineral; and the same derivation that led to equation (I) can be repeated including the effect of the adipose tissue. This amounts to a correction to the two-component or two-phase model and predicts a deviation from the two-phase model as a function of energy. The calculation is fairly simple and is presented in detail in the appendix. The size of the deviation, however, depends on the amount of adipose tissue present and its distribution which are quite difficult to predict.

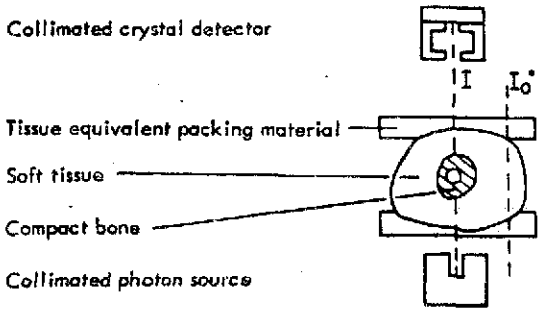

FIG. 1. Schematic of measuring geometry.

Plausible distributions of adipose tissue are assumed in order to insert in the calculation and predict a range of deviation that can be expected. Two situations must be considered: 1. the thickness or mass of adipose tissue that is uniform across the scan, and 2. the thickness of adipose tissue that changes at different locations in the scan.

In the first situation (an evenly distributed mass of adipose tissue), there is no effect on the measurement. The calculated value for m_b always depends on the ratio of the intensity measured beside the bone to the intensity at some location through the bone $\left(\frac{I_o^*}{I}\right)$. Any uniform overlying third phase, such as adipose tissue, will attenuate both I_o^* and I by the same factor and cancel out of the ratio $\left(\frac{I_o^*}{I}\right)$. To the extent that the adipose tissue present is uniform across the scan, it has no effect on the bone mineral mass measurement.

The effect of adipose tissue which is not uniform across the scan is more important and leads to a deviation from the two-phase

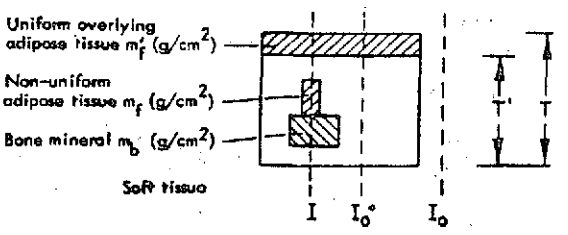

FIG. 2. The distribution of tissues in a scan is abstracted to illustrate that the mass of adipose tissue in the beam is not constant across the scan.

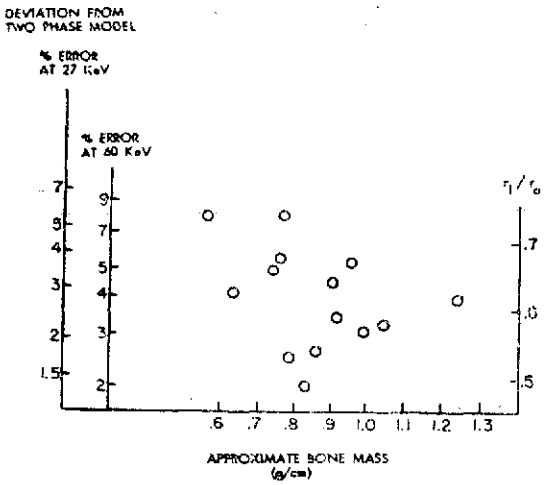

FIG. 3. Accuracy error in bone mineral scan of the proximal radius.

model which may be regarded as an error. At some point in the scan (see the photon beam labeled I in Fig. 2), the beam encounters a mass of adipose tissue greater or less than the mass of adipose tissue in the beam where I_o^* is measured. The mass of adipose tissue in the beam where I_o^* is measured is m_f'. The mass of adipose tissue in the beam at location I is $(m_f' + m_f)$. The calculated bone mineral is m_b', the actual bone mineral present is m_b, and Appendix I demonstrates that the deviation in a point measurement is proportional to the mass of non-uniform adipose tissue in the beam.

$$m_b' - m_b = K m_f \qquad \text{(AII)}$$

The fractional error in m_b' at that point is:

$$\frac{m_b' - m_b}{m_b} = K \frac{m_f}{m_b}$$

The proportionality constant K is evaluated for several commonly used radionuclides in Table 1.

A measurement normally involves scanning across the bone and the total amount of bone seen in the scan is reported as the "bone mass."

$$M_b \propto \int_{\text{scan}} m_b \, ds$$

The accuracy error in a measurement of "bone mass" is given by equation (AIII).

$$\% \text{ error } (M_b) = K \frac{\int_{\text{scan}} m_f \, ds}{\int_{\text{scan}} m_b \, ds} \qquad \text{(A III)}$$

A calculation of this error is now possible based on the total mass of bone mineral, and on the distribution of adipose tissue present in a scan.

Experimental

To illustrate the magnitude of the errors predicted, adipose tissue outside the bone will be assumed uniform and errors calculated solely on the basis of marrow cavity fat. Adipose tissue contained in the marrow cavity of a bone (yellow marrow) is not uniform across the scan, and this mass of non-uniform adipose tissue can be easily estimated from the bone dimensions.

A shaft bone can be modeled as a hollow cylinder, completely filled with yellow marrow (adipose tissue); $m_f = 0$ at all points except those where the medullary adipose tissue intercepts the beam. When a cross section of bone is measured by performing an absorption scan, the per cent error in the measurement is given by equation (AIII), which upon integration reduces to:

$$\% \text{ error} = \frac{0.9}{1.2} \cdot \frac{r_i^2}{r_o^2 - r_i^2} K \qquad \text{(II)}$$

where r_i and r_o are the inner and outer radii of the hollow cylinder, respectively. This is the same error predicted by Sorenson and Mazess[7] using a slightly different mathematical approach. The factor 0.9 in equation (II) is the mass of adipose tissue per cubic centimeter of yellow marrow, and the factor 1.2 is the mass of bone mineral per cubic centimeter of compact bone. In order to estimate the magnitude of r_i and r_o, the dimenisons of a typical bone were surveyed. A site approximately 6 cm from the proximal end of the radius was chosen because, at this location, the radius is quite uniform. It is approximately cylindrical and nearly free from trabeculation in the medullary cavity.

Radiographs of 14 women were surveyed. The women were all volunteer hospital workers at the UCLA Center for the Health

Sciences and ranged from 49 to 76 years of age. The results, based on equation (II), using dimensions taken from radiographs, are shown in Fig. 3 and illustrate the accuracy error due to medullary fat when making a monochromatic bone mineral measurement at this location.

Note should be made of the abundance of adipose tissue outside the bone. A layer of subcutaneous adipose tissue is distinguishable radiographically, and, in middle-aged women, the subcutaneous layer is about 6 mm thick on both sides of the forearm.[3] In comparison with this total of 12 mm subcutaneous adipose tissue, the marrow cavity diameter is usually about 8 mm. Non-uniformities in the subcutaneous layer and other adipose tissue outside the bone could easily contribute errors as great as, or greater than, the errors due to marrow cavity fat.

Summary

Attenuation measurements of bone mineral mass must be calibrated with an ash study, because the quality of the beam is uncertain, the scatter detected alters the attenuation, and adipose tissue is in the beam. The presence of adipose tissue in the beam causes an accuracy error which we have illustrated in Fig. 3 and ranges from 1.5 to 5.5% at 27 kev, and from 2.5 to 8.5% at 60 kev.

The reproducibility of serial measurements on a single patient is about 2%[2, 6] and is mainly a result of the ability to reposition the instrument over the same location on the bone. In a long-term study of a single patient, the fat distribution is expected to change very slowly and contribute an accuracy error typical of that shown in Fig. 3, but no significant imprecision. The scatter shown in Fig. 3 will contribute an imprecision in a population study. The different proportion of yellow marrow to bone mineral that occurs in each patient leads to a scatter of 1.2% S. D. at 27 kev, and 1.8% S. D. at 60 kev. In a population study, this scatter will introduce an imprecision which combines with the imprecision due to positioning.

In principle, one could reduce the accuracy error by calibrating against bones that contained fat in the marrow cavity. The advantage to be gained in such a procedure is limited by the scatter in Fig. 3. The standard deviation quoted above would then describe both the accuracy error and the imprecision in a population study.

A method of eliminating the fat error has been suggested.[1, 2] By adding the information of a second attenuation measurement at another energy, with the same geometry, another unknown can be added to the mathematical system. This would allow one to distinguish between soft tissue and adipose tissue and eliminate the error discussed here. The feasibility of such a dichromatic method has not yet been demonstrated, and one expects that the statistical uncertainty due to the limited number of photons that can be collected will be a much greater problem.

REFERENCES

1. Cameron, J. R., and J. Sorenson: Measurement of Bone Mineral In Vivo. An Improved Method. *Science* 142:230, 1968.

2. Cameron, J. R., R. B. Mazess, and J. A. Sorenson: Precision and Accuracy of Bone Mineral Determination by Direct Photon Absorptiometry. *Invest. Radiol.* 3:141, 1968.

3. Garn, S. M.: Fat Weight and Fat Placement in the Female. *Science* 125:1091, 1957.

4. Gong, J. K., J. S. Arnold, and S. H. Cohn: The Density of Organic and Volatile and Non-volatile Inorganic Components of Bone. *Anat. Rec.* 149:39, 1964.

5. Hubbell, J. H.: Photon Cross Sections, Attenuation Coefficients, and Energy Absorption Coefficients from 10 KeV to 100 GeV. U. S. Dept. of Commerce, National Bureau of Standards, NSRDS-NBS 29, 1969.

6. Johnston, C. C., Jr., D. M. Smith, Pao-Lo Yu, and W. P. Deiss, Jr.: In Vivo Measurement of Bone Mass in the Radius. *Metabolism* 17:1140, 1968.

7. Sorenson, J. A., and R. B. Mazess: Effects of Fat on Bone Mineral Measurements. *In* Proceedings of Bone Measurement Conference, J. R. Comeron, Ed. A. E. C. Conf.-700515, 1970; p. 248.

8. Tipton, I. H.: Elemental Composition of Total Body and Certain Tissues. *In* Health Physics Division Annual Progress Report for Period Ending July 31, 1969. Oak Ridge National Laboratory, ORNL-4446, 1969; p. 299.

APPENDIX I. Expansion of Tissue Modeling from a Two-phase to a Three-phase System

The original derivation presented by Cameron and Sorenson,[1] and summarized here in equation (I), assumes that only two types of material are present to intercept the photon beam. That treatment is expanded here by allowing the presence of

TABLE I. Tissue Characteristics and Proportionality Constant At Three Energies

Radionuclide	Photon energy (kev)		μ/ρ Mass attenuation coefficients* (cm^2/g)	Density (g/cm^3)	K Proportionality constant
^{125}I	27	adipose tissue†	.343	.9	−.059
		soft tissue‡	.448	1.0	
		bone mineral††	2.78	3.2	
^{241}Am	60	adipose tissue	.198	.9	−.085
		soft tissue	.204	1.0	
		bone mineral	.403	3.2	
^{137}Cs	661	adipose tissue	.0870	.9	−.145
		soft tissue	.0849	1.0	
		bone mineral	.0772	3.2	

* Cross sections are those compiled by Hubbell.[5] † Composition is that recommended by Tipton.[8]
‡ Hydroxylapatite.

three types of material: soft tissue, adipose tissue, and bone mineral. The geometry to be considered is illustrated in Fig. 2, and the manner in which the tissues attenuate is described below.

At the location I, or at any other point in the scan, the total linear thickness of all tissues is related to the mass and microscopic density of each type of tissue as follows:

$$T = \frac{m_s}{\rho_s} + \frac{m_b}{\rho_b} + \frac{m_t}{\rho_t} + \frac{m_f'}{\rho_f}$$

T has units of cm and is constant across the scan. Substracting off the thickness of the uniform adipose layer:

$$T' = T - \frac{m_f'}{\rho_f}$$

T′ also has units of cm and is constant across the scan. The attenuation is described by the following equations:

$$I = I_o\, e^{-(\mu/\rho)_s\, m_s - (\mu/\rho)_b\, m_b - (\mu/\rho)_t\, m_t - (\mu/\rho)_f\, m_f'}$$

$$I_o^* = {}_o\, e^{-(\mu/\rho)_s\, \rho_s\, T' - (\mu/\rho)_f\, m_f'}$$

Combining the above four equations:

$$\frac{I_o^*}{I} = e^{-(\mu/\rho)_s\, \rho_s \left(\frac{m_b}{\rho_b} + \frac{m_t}{\rho_t}\right) + (\mu/\rho)_b\, m_b + (\mu/\rho)_t\, m_t} \qquad \text{(A1)}$$

These equations describe the "actual" attenuation of the beam including the effect of the non-uniform adipose tissue as a third phase. The effect of the third phase (non-uniform adipose tissue) can be seen by inserting the expression for $\frac{I_o^*}{I}$ from the three-phase model into the two-phase calculation. That is, we are putting the intensities from the "actual" situation, equation (A1), into the two-phase calculation, equation (I). Let m_b' be the bone mineral calculated using the two-phase model, while m_b is the actual bone mineral present.

$$m_b' = \rho_b \frac{\ln\left(\frac{I_o^*}{I}\right)}{(\mu/\rho)_b\,\rho_b - (\mu/\rho)_s\,\rho_s} \tag{I}$$

$$m_b' = \rho_b \frac{\ln\left(e^{-(\mu/\rho)_s\,\rho_s\left(\frac{m_b}{\rho_b} + \frac{m_f}{\rho_f}\right) + (\mu/\rho)_b\,m_b + (\mu/\rho)_f\,m_f}\right)}{(\mu/\rho)_b\,\rho_b - (\mu/\rho)_s\,\rho_s}$$

$$m_b' = m_b + \left[\frac{(\mu/\rho)_f\,\rho_f - (\mu/\rho)_s\,\rho_s}{(\mu/\rho)_b\,\rho_b - (\mu/\rho)_s\,\rho_s}\right]\frac{\rho_b}{\rho_f}\,m_f$$

The error in m_b' calculated by the two-phase model is:

$$m_b' - m_b = \left[\frac{(\mu/\rho)_f\,\rho_f - (\mu/\rho)_s\,\rho_s}{(\mu/\rho)_b\,\rho_b - (\mu/\rho)_s\,\rho_s}\right]\frac{\rho_b}{\rho_f}\,m_f = K\,m_f \tag{AII}$$

and the fractional error in m_b' at a single point is:

$$\frac{m_b' - m_b}{m_b} = \left[\frac{(\mu/\rho)_f\,\rho_f - (\mu/\rho)_s\,\rho_s}{(\mu/\rho)_b\,\rho_b - (\mu/\rho)_s\,\rho_s}\right]\frac{\rho_b}{\rho_f}\frac{m_f}{m_b} = K\,\frac{m_f}{m_b}$$

The proportionality constant K is evaluated for several commonly used radionuclides and presented in Table I.

The deviation from the two-phase model amounts to an accuracy error which at one point is proportional to m_f, and a per cent error, proportional to $\frac{m_f}{m_b}$. Again, m_f is the difference between the mass of adipose tissue in the beam and the mass of adipose tissue next to the bone (the location where I_o^* is measured); m_f is positive if there is more adipose tissue in the beam than there was beside the bone, or m_f can be negative if a greater mass of adipose tissue is encountered beside the bone.

A measurement normally involves scanning across the bone and the total amount of bone seen in the scan is reported as the "bone mass."

$$M_b \propto \int_{\text{scan}} m_b\,ds$$

The accuracy error in such a measurement is obtained by integrating equation (AII) across the scan.

$$\text{error} = \int_{\text{scan}} (m_b' - m_b)\,ds = K \int_{\text{scan}} m_f\,ds$$

The fractional error in such a measurement is:

$$\%\ \text{error} = K\,\frac{\int_{\text{scan}} m_f\,ds}{\int_{\text{scan}} m_b\,ds} \tag{AIII}$$

A METHOD TO ESTIMATE THE ERROR CAUSED BY ADIPOSE TISSUE IN THE ABSORPTIOMETRIC MEASUREMENT OF BONE MINERAL MASS

Philip F. Judy and John R. Cameron
Department of Radiology
University of Wisconsin, Madison

John M. Vogel
University of California, Davis

Bone absorptiometry using ^{125}I has been used extensively to measure the bone mineral mass of various bones (Cameron and Sorenson, 1963). The accuracy of the technique has been estimated to be 2% - 3% and the reproducibility of the technique has been typically 2% (Sorenson and Cameron, 1967). With care in repositioning patient reproducibility of 0.1% to 0.5% has been achieved (Vogel and Anderson, 1969).

Variation in the adipose tissue content adjacent to, over and inside the bone has been reported to cause a significant error in the measurement of the bone mineral mass of the radius (Zeitz, 1972). The magnitude of the error was determined by the method of estimating the baseline, that is the transmission of soft tissue alone, and by the distribution of the adipose tissue. A general mathematical description of the effects of the variation of adipose tissue in soft tissue has been proposed (Wooten et al, 1973). This analysis provided a basis of a possible method of measuring directly the magnitude of the error by the use of the absorptiometric measurement of bone mineral mass at several photon energies.

Method

The error caused by the variation of adipose tissue over the bone has been estimated from Equation 1 (Wooton, et al, 1973)

$$(1) \quad \langle M_{BM} \rangle - M_{BM} = K \int \Delta m_a \cdot ds$$

where,

$\langle M_{BM} \rangle$ = the absorptiometric estimate of bone mineral mass

M_{BM} = the actual bone mineral mass

K = constant

$\Delta m_a \cdot ds$ = the difference of the mass of adipose tissue at the baseline measurement and over the bone integrated over the scan path (adipose defect)

This formula describes a linear relationship between the constant, K, and the absorptiometric estimate of bone mineral mass. The constant is determined by the densities of bone mineral, water, and adipose tissue and their mass attenuation coefficients. The constant, K, can also be estimated experimentally for each energy photon beam. Using linear regression analysis of the difference between the actual and measured mineral mass versus the adipose defect K is the slope.

The bone mineral mass of the os calcis of six normal male subjects undergoing a bedrest study was measured with the photon beams from ^{125}I and ^{153}Gd. Two photon energies (43 keV and 100 keV) were available from ^{153}Gd (Mazess, 1970). The results of that study have been described elsewhere (Vogel, 1972). Each beam was calibrated with a reference standard (Witt, 1972). A reference standard is required because a simple exponential formula does not describe the transmission of these photon beams because of the hardening effects (Sandrik and Judy, 1973) and finite size of the photon beam (Judy, 1970). The reference standard consists of three bone equivalent annuluses with a bone mineral mass assigned to each. A linear regression of the assigned values versus the actual measurements was performed to determine a and b in Equation 2.

$$(2)\quad \langle M_{BM} \rangle = a \sum \log (I_o^*/I) + b$$

where

$\sum \log (I_o^*/I)$ = actual measurement.

The values for K from Equation 1 were estimated experimentally. Polymethyl methacrylate tubes were filled with soybean oil or water and placed in a water bath which covered the reference standard. The difference of the two measurements was an estimate of error caused by the simulated fat defect. The fat defects ranged from 0.5 g/cm to 1.9 g/cm.

The values for K for the ^{125}I beam and the ^{153}Gd beams are shown in Table I. The effective linear attenuation coefficients for these beams in water and soybean oil are also given.

TABLE I

	K	μ(water) cm^{-1}	μ(Oil) cm^{-1}
^{125}I (28 keV)	0.041 ± 0.009	0.414 ± 0.001	0.275 ± 0.002
^{153}Gd (43 keV)	0.078 ± 0.022	0.248 ± 0.001	0.198 ± 0.004
^{153}Gd (100 keV)	0.21 ± 0.09	0.1687 ± 0.0004	0.51 ± 0.0004

The reproducibility of the estimate of adipose defect was determined by repeat measurement of the os calcis less than a week apart during the control period of the bedrest study. No changes in the adipose defect or the bone mineral mass would be expected during the interval between measurements. The reproducibility for the in vivo measurements was estimated to be 2.0 g/cm (± 1 Standard Deviation).

The adipose defect was estimated for two different methods of determination of the baseline count rate (I_o^*). In the first method I_o^* was estimated from the mean of the transmission counts for a 3 mm interval on each edge of the bone. In the second method I_o^* was determined from the minimum value of the transmission counts for a 3 mm interval at the edge of the bone. The average fat defect was estimated for the six subjects during the control period and twice during the bedrest study. These results along with the increase these fat defects would cause in the ^{125}I measurement of bone mineral mass are shown in Table II and III. The variation of adipose defect for a particular individual for three measurements over the 13 weeks was not significantly different from the short term reproducibility. No significant difference between the adipose defects was observed between individuals. The mean value of the measurement of bone mineral mass was 3.5 g/cm for these subjects.

Errors

The reproducibility of the measurement of adipose defect was determined by the reproducibility of ^{153}Gd measurements of bone mineral mass. The variation is caused by the stochastic nature of the process (Judy, 1970). The magnitude of this variability transformed into the ^{125}I measurement of bone mineral mass resulted in an error of 2.2%. Therefore, if the method were used to correct an individual measurement of bone mineral mass of the os calcis, the correction would introduce a variability of 2%.

The calibration of the method to estimate adipose defect with soybean oil results in an over-estimate of 30% in the error caused in ^{125}I measurement. In as much as the variation in the composition of soft tissue over the bone is a result of the variation of protein, it will mitigate the error in calibration caused by using soybean to simulate adipose tissue.

The measurement of bone mineral mass with different photon beams has systematic error for other reasons than variation in adipose composition. The calibration of absorptiometric measurement accounted for most of this error, but this method of estimating the effects of adipose defect will be in error to the extent that other systematic errors were not determined.

Summary

This report describes a method to estimate the magnitude of the error caused by the variation of adipose tissue in the photon beam path for the absorptiometric measurement of bone mineral mass. The method was applied to the rectilinear scan of the os calcis using ^{125}I. The error was estimated at three times on six subjects during a bedrest study. The mean error was $1.3\% \pm 0.5\%$ (SD_m). The baseline was estimated from the minimum transmission through the soft tissue alone for a 3 mm interval at the edge of the bone, the error was $6\% \pm 0.5\%$. If the transmissions at both edges of the bone were used to estimate the baseline no significant variation in the error in the ^{125}I measurement was observed during the duration of bedrest study or between individuals.

The results indicate that the method of measuring the bone mineral mass with the absorptiometric method was useful to estimate the error caused by variation in the composition of soft tissue. The method is not recommended to correct the error of an individual measurement, because it will reduce the precision of the measurement of bone mineral mass.

References

1. Cameron, J. R. and Sorenson J. A. Measurement of Bone Mineral In Vivo: An Improved Method. Science 142(1963) 230.

2. Judy, P. F. Theoretical Accuracy and Precision in the Photon Attenuation Measurement of Bone Mineral. Proceeding of the Bone Measurement Conference, Cameron (Edit) USAEC, Division of Technical Information, p. 1, Oak Ridge, Tennesee, 1970, CONF-700515.

3. Sandrik, J. M. and Judy, P. F. Effects of the Polyenergetic Character of the Spectrum of ^{125}I on the Measurement of Bone Mineral Content. Investigative Radiology. 8(1973)143.

4. Sorenson, J. A. and Cameron,J. R. A Reliable In Vivo Measurement of Bone Mineral Content. J. Bone Jt. Surg 49(1967)481.

5. Vogel, J. M. and Anderson J. Rectilinear Transmission Scanning of Irregular Bones for Quantification of Mineral Content. J. Nucl. Med. 13(1972)13.

6. Witt, R.M., private communication.

7. Wooten, W. W., Judy, P.F. and Greenfield, M.A. Analysis of the Effect of Adipose Tissue on Absorptiometric Measurements of Bone Mineral Mass. Investigative Radiology 8(1973)84.

8. Zeitz, L. Effect of Subcutaneous Fat on Bone Mineral Content Measurements with 'Single-Energy' Photon Absorptiometry Technique. Acta Radiologica. Ther. Phys. Biol. 11(1972)401.

TABLE II

Fat Defects (g/cm)

Time	I_o^* (both edges) g/cm	I_o^* (Minimum)
Control Period	4.7 ± 1.9	0.43 ± 1.9
7 weeks	6.53 ± 3.5	2.38 ± 3.2
12 weeks	4.43 ± 1.8	0.42 ± 2.8

TABLE III

Error of Absorptiometric Measurement of Bone Mineral Mass Using ^{125}I(g/cm)

Time	I_o^* (both edges)	I_o^* (Minimum)
Control Period	0.19 ± 0.08	0.02 ± 0.08
7 weeks	0.26 ± 0.14	0.10 ± 0.14
12 weeks	0.18 ± 0.07	0.02 ± 0.11

BONE MINERAL CONTENT IN NORMAL SUBJECTS

R. B. Mazess and J. R. Cameron
Departments of Radiology and Physics
University of Wisconsin Hospitals
Madison, Wisconsin

Over the past five years a large number of apparently normal U.S. white subjects have been measured. The adult sample was derived from several sources: a) hospital or laboratory visitors, b) homes for the elderly, and c) scientific meetings. The childrens sample was derived from: a) hospital and laboratory visitors, b) a survey of school age children between ages 6 and 14, and c) a study of little league baseball players between 8 and 19 years of age. None of the subjects had a history of spontaneous fractures, renal disease, or immobilization.

Results

a. Adults: The heights and weights of the adults by decades are given in Table 1. There was a decrease of stature by about 2 cm per decade in females, and 1 cm per decade in males, after the thirties. This may be a secular trend, but was also no doubt a reflection of vertebral collapse and height loss. The mineral content, bone width, and the mineral-width ratio for the radius shaft, distal radius, ulna, and humerus are given in Tables 2, 3, 4, and 5. In females the bone mineral content and mineral-width ratio were relatively constant through the thirties and into the early forties. This was followed by a period of relatively rapid bone loss between the mid-forties and mid-seventies, with a somewhat slower decrease thereafter. In males the bone mineral content and mineral-width ratio stayed relatively constant through the fifties with bone loss progressing from the sixties on. In both sexes the bone widths did not change with age appreciably; the apparent decrease of the bone width of the distal radius in later life may actually be an artifact of the edge criterion used to start and stop a scan. The distal radius width is critically dependent on the edge criterion, especially in the elderly. An 85% edge criterion, rather than the usual 70% edge, should probably be used for ^{125}I scans of the distal radius in demineralized subjects.

The coefficients of variation differed with age and measurement site. Relatively high mineral variation was evident for the distal radius and ulna; in the younger adults it was 15 to 20% while the variation in older adults was even larger (20 to 30%). This variation may reflect the difficulties of measuring the distal bone sites, rather than a real biological pattern. The variation was not reduced by using the mineral-width ratio. At the other measurement sites the variation was only 10 to 15% for younger adults and 15 to 20% for the elderly groups; in general the variation of the mineral-width ratio was a few percent lower than that of the mineral content itself.

b. Children: The heights and weights of the children are given in Table 6; the Wisconsin children were somewhat taller and heavier than those examined by others (McCammon, 1970). Skeletal ages of a sub-sample of these children were entirely normal (Mazess and Cameron, 1971). The bone mineral, width, and mineral-width ratio for the midshaft of the radius, ulna and humerus are given in Tables 7, 8, and 9. There was insufficient data on the distal ulna and radius in children to warrant compilation.

Prior to the adolescent growth spurt there appears to be a similar rate of growth (about 8% annually) for the radius, ulna and humerus in both boys and girls. From ages 13 to 16 boys grow at about 13% annually, and from 17 to 20 years the growth is about 4% annually. Females have an earlier growth spurt; from ages 11 to 14 they grow at about 11% annually, but only at 1 to 2% annually thereafter til age 20. The changes of bone width are of lesser magnitude and there is a less well-defined growth spurt, at least in this gross-sectional data. Boys and girls increase width by about 4% annually until adolescence; from adolescence to adulthood boys increase width at about 2% annually and girls at about 1% annually.

The pattern of mineral-width ratio changes was somewhat similar to the above. This ratio changed by about 4% annually prior to adolescence in both sexes; this growth rate doubled during peak adolescent growth. Post-adolescent changes amounted to about 2 to 3% annually in males and 1 to 2% in females.

The coefficients of variation for each age-sex group amounted to about 10 to 15% for bone mineral, 8 to 12% for bone width, and about 10% for the mineral-width ratio. In general the use of the mineral-width ratio decreased the variation indicating that the variation in bone mineral at each age was a reflection of bone size differences. This reduced variation, however, does not make this ratio a more sensitive indicator than the bone mineral itself. Bone mineral content during this period of growth doubles in females and almost triples in males. In contrast the mineral-width ratio changes are only half as large. As a consequence the signal (age change) to noise (variation) ratio is greater for the mineral content than for the mineral-width ratio.

Discussion and Conclusions

a. Adults: A decrease of the amount of bone with age has been demonstrated using both direct and indirect methods for many populations (Barzel, 1970). The extent and magnitude of the bone loss, the age at which loss begins, and the nature of sex differences have not been defined with exactitude. Indirect methods, such as radiographic photodensitometry or measurement of compact bone area, are inaccurate indicators of the amount of bone and are subject to large systematic, as well as random, errors. Hence the great majority of results on age trends of bone loss, which have been obtained with these methods are in question. For example Dequeker (1972) examined populations in the Netherlands, Nigeria and Belgium and found that women lost 5.7% and men 3.1% per decade of their compact bone between the ages of 40 and 80 years. The same rate of loss was found in iliac crest biopsies. Garn et al (1967) showed that in U.S. white and negro and in Central American populations the rate of loss was similar and amounted to about 3% per decade for males and 8% per decade for females. However, this referred to changes of compact bone thickness, rather than area. Changes in the latter, which are more directly related to the amount of bone, were about 2.8% per decade in males and 6.3% per decade in females (Garn, 1970, p. 64). The present results showed a decrease over the 4 decades from 40 to 80 years which was relatively constant for different sites and different bones amounting to about 8.6% per decade in females and 3.2% per decade in males. However, our data showed that the onset of bone loss was different in males and females, and that there were two phases to the rate of bone loss in females. Females lost bone rapidly (about 9.5% per decade between the ages of 45 and 75) and more slowly (4.4% per decade) thereafter. Males did not lose bone

until after the fifties, with a loss between 55 and 85 years amounting to about 4.7% per decade.

The plateau of bone mineral loss in the very old females may represent two somewhat distinct phenomena. First, there may be a selection process in which women with bone mineral values lower than those seen in the elderly groups either die, or are not included in the sample because of fractures. Interestingly the level of this plateau in bone loss was about equal to the discriminant value between fracture and non-fracture groups in women (Smith and Cameron, 1973). Secondly, there may actually be two distinct phases to bone loss, with a more rapid loss in the post-menopausal decades, and a slower loss, analagous to that evident in elderly males, in subsequent decades. Such a two-component analysis indicated that females lose bone by about 10 to 15% per decade due to a rapid process between 45 and 70 years, and at about 4% per decade after age 50 by a slower process.

Comparable data on the patterns of aging bone loss are not available. Johnston and Goldsmith (1971) surveyed large samples of white, negro and oriental populations in California using photon absorptiometry on the distal radius. However, the sample sizes above age 60 were very small. Their data on white males and females up to age 80 does support the present findings. The data of Johnston et al (1968) and Smith et al (1972) are even more limited, and do not allow conclusions.

b. Children: A number of investigators have attempted to examine skeletal growth, but in general the methods used have limited precision, accuracy and sensitivity (Mazess and Cameron, 1971, 1972). Bone lengths give only linear growth, and bone widths give only an approximation of appositional changes. Garn (1970) summarized extensive findings on compact bone thickness and area; he also found that appositional growth ended at about age 15 in females and at 20 years in males. The rate of pre-adolescent bone growth seems to be somewhat over estimated by compact bone measures, and the extent of sexual dimorphism appeared inaccurate, especially toward the end of growth. Compact bone area, despite its numerous shortcomings, does indicate about the same magnitude of bone increase during growth from 6 to 18 years as does photon absorptiometry, that is, about 260% in males and 215% in females. The magnitude of changes in actual skeletal weight is somewhat larger than this, about 400% in males and 330% in females (Trotter and Peterson, 1970). The difference is due to the linear element of skeletal growth which can be measured by height or bone length changes, and which is about half the magnitude of the appositional bone growth.

ACKNOWLEDGEMENTS

This research was supported by NASA-Y-NGR-50-002-051 and AEC-AT-(11-1)-1422. Many persons have aided in the collection and processing of this data over the years, including: Joyce Fischer, Sue Kennedy, Bob Witt, Warren Mather, Kian Kianapour, Ellie Sosne, Barbara Binns, N. Suntharalingam, Bob Jones, Monica Jaehnig, Mrs. J. R. Cameron, Mrs. F. Lantz, the staff of the St. Bernards School, the Sisters of Notre Dame Home, and John Jurist, James Sorenson, Philip Judy, Hugh Hickey and Mark Mueller. Ron Watson, University of Western Ontario, contributed the data collected in our laboratory on 220 little league baseball players. Everett Smith, University of Wisconsin, kindly contributed data on 100 elderly women to the compilation. Howie Gollup has added substantially in collation and calculation of these final results.

REFERENCES

Barzell, U. S. (ed.), 1970. Osteoporosis. Grune and Stratton, N.Y.

Dequeker, J., 1972. Bone Loss in Normal and Pathological Conditions.

Garn, S. M., 1970. The Earlier Gain and the Later Loss of Cortical Bone.

Garn, S. M., Rohmann, C. G. and Wagner, B., 1967. Bone loss as a general phenomenon in man. Fed. Proc. 25:1729-1736.

Johnston, C. C., Smith, D. M., Yu, P. L. and Deiss, W. P., Jr., 1968. In vivo measurement of bone mass in the radius. Metabolism 17:1140-1153.

Johnston, J. O. and Goldsmith, N. F., 1971. The Osteoporosis Prevalence Survey Conducted at the Multiphasic Clinic of Kaiser Foundation Hospital. Final Report on USPHS Contract PH 86-68-181.

Mazess, R. B. and Cameron, J. R., 1971. Skeletal growth in school children: maturation and bone mass. Am. J. Phys. Anthrop. 35:399-408.

Mazess, R. B. and Cameron, J. R., 1972. Growth of bone in school children: comparison of radiographic morphometry and photon absorptiometry. Growth 36:77-92.

McCammon, R. W., 1970. Human Growth and Development. C. C. Thomas, Springfield.

Smith, D. M., Johnston, C. C. and Yu, P. L., 1972. In vivo measurement of bone mass. J.A.M.A. 219:325-329.

Smith, E. and Cameron, J. R., 1973. Interpretation of fracture index charts. (submitted for publication)

Trotter, M. and Peterson, R. R., 1970. Weight of the skeleton during post-natal development. Am. J. Phys. Anthrop. 33:313-324.

HEIGHTS AND WEIGHTS OF ADULTS

AGE GROUP	N	HEIGHT (cm) $\bar{X}$	SD	CV	WEIGHT (kg) $\bar{X}$	SD	CV
MALES							
20-29*	102	178.9	7.6	4.2	76.3	11.3	14.8
30-39+	117	179.6	7.1	4.0	79.8	12.4	15.5
40-49+	117	177.0	8.4	4.7	78.8	10.5	13.3
50-59+	46	177.5	6.0	3.4	79.5	8.2	10.3
60-69*	40	175.2	8.8	5.0	75.9	15.5	20.4
70-79*	50	174.8	8.0	4.6	74.1	12.6	17.1
80-89*	3	163.4	2.9	1.8	61.5	5.9	9.6
FEMALES							
20-39*	123	163.6	6.6	4.0	58.1	10.4	17.9
30-39*	29	164.9	6.4	3.9	65.2	10.6	16.2
40-49*	42	160.3	8.3	5.2	63.8	10.6	16.6
50-59*	60	161.0	5.6	3.5	63.8	11.9	18.6
60-69*	78	159.1	6.9	4.3	62.8	11.3	18.0
70-79*	100	158.2	6.9	4.4	62.6	11.3	18.0
80-89*	74	155.4	7.4	4.8	56.8	9.4	16.6
90-99*	16	152.7	8.4	5.5	55.4	10.3	18.6

SOURCES: * from mid-radius data
+ from humerus data

TABLE 1: Heights and Weights of Adult Male and Female Groups by Decades

RADIUS SHAFT ADULTS

AGE GROUP	N	AGE	MINERAL (mg/cm)			WIDTH ($mx10^{-5}$)			MINERAL/WIDTH		
			$\bar{X}$	SD	CV	$\bar{X}$	SD	CV	$\bar{X}$	SD	CV
MALES											
20-29	105	24.6	1307	173	13.2	1476	144	9.7	.885	.078	8.8
30-39	72	34.0	1322	138	10.5	1479	125	8.5	.895	.070	7.6
40-49	64	44.2	1304	146	11.2	1485	147	9.9	.880	.077	8.7
50-59	31	54.7	1313	159	12.1	1489	116	7.8	.880	.064	7.3
60-69	46	64.1	1226	229	18.7	1569	297	18.9	.790	.122	15.4
70-79	22	74.2	1256	188	15.0	1553	148	9.5	.811	.110	13.6
80-89	16	84.1	1182	219	18.5	1577	177	11.2	.751	.110	14.6
FEMALES											
20-29	126	22.9	952	108	11.3	1230	109	8.8	.774	.055	7.1
30-39	29	33.7	1000	121	12.1	1304	156	12.0	.769	.064	8.3
40-49	42	44.4	977	95	9.7	1298	240	18.6	.763	.074	9.8
50-59	63	55.0	885	136	15.3	1252	119	9.5	.706	.078	11.0
60-69	93	64.6	769	142	18.5	1259	125	9.9	.610	.086	14.1
70-79	134	72.2	722	126	17.4	1255	112	8.9	.575	.085	14.7
80-89	121	83.8	681	143	21.1	1271	156	12.2	.538	.104	19.5
90-99	29	92.2	675	129	19.2	1295	112	8.6	.521	.084	16.2

TABLE 2: Absorptiometric Measurements on the Distal Third of the Radius Shaft in Adult Males and Females by Decades

DISTAL RADIUS ADULTS

AGE GROUP	N	AGE	MINERAL (mg/cm)			WIDTH ($mx10^{-5}$)			MINERAL/WIDTH		
			$\bar{X}$	SD	CV	$\bar{X}$	SD	CV	$\bar{X}$	SD	CV
MALES											
20-29	27	24.3	1386	204	14.7	2342	413	17.6	.600	.079	13.3
30-39	19	33.8	1317	186	14.1	2283	364	15.9	.588	.106	18.0
40-49	12	43.8	1298	154	11.9	2162	339	15.7	.608	.076	12.5
50-59	10	55.5	1330	177	13.3	2201	352	16.0	.614	.108	17.7
60-69	30	64.9	1191	288	24.2	2362	435	18.4	.516	.134	26.0
70-79	14	74.3	1187	279	23.5	2330	550	23.6	.536	.183	34.1
80-89	14	84.5	1134	282	24.9	1989	456	22.9	.578	.116	20.1
FEMALES											
20-29	54	23.2	984	126	12.8	1857	267	14.4	.539	.092	17.0
30-39	6	32.7	955	84	8.8	1635	195	12.0	.564	.091	16.2
40-49	11	45.9	933	174	18.7	1953	462	23.6	.494	.114	23.0
50-59	37	55.5	886	146	16.5	1855	255	13.7	.482	.080	16.7
60-69	71	64.6	742	116	15.7	1902	364	19.1	.402	.088	21.9
70-79	96	75.1	718	175	24.4	1820	316	17.4	.402	.103	25.6
80-89	87	83.7	645	144	22.4	1724	370	21.5	.388	.111	28.6
90-99	18	92.5	668	173	25.9	1775	343	19.3	.392	.127	32.5

TABLE3: Absorptiometric Measurements on the Distal Radius in Adult Males and Females *by Decades*

MIDSHAFT ULNA

AGE GROUP	N	AGE	MINERAL (mg/cm)			WIDTH ($mx10^{-5}$)			MINERAL/WIDTH		
			$\bar{X}$	SD	CV	$\bar{X}$	SD	CV	$\bar{X}$	SD	CV
FEMALES											
20-29	22	23.2	843	121	14.3	1074	179	16.7	.791	.094	11.8
30-49	6	39.7	868	95	11.0	1108	138	12.5	.794	.135	17.0
50-59	18	54.9	804	126	15.7	1105	131	11.8	.728	.078	10.8
60-69	24	63.8	702	106	15.1	1109	119	10.7	.625	.093	14.9
70-79	38	75.4	615	121	19.6	1103	108	9.8	.562	.120	21.4
80-89	30	83.7	590	116	19.7	1130	128	11.3	.525	.105	20.1
90-99	7	92.7	560	86	15.4	1126	115	10.2	.499	.069	13.8

DISTAL ULNA

AGE GROUP	N	AGE	MINERAL (mg/cm)			WIDTH ($mx10^{-5}$)			MINERAL/WIDTH		
			$\bar{X}$	SD	CV	$\bar{X}$	SD	CV	$\bar{X}$	SD	CV
FEMALES											
20-29	20	23.2	511	154	30.0	999	183	18.3	.511	.112	22.0
30-49	6	39.7	510	86	16.9	1013	141	13.9	.513	.114	22.3
50-59	17	55.1	452	89	19.7	971	134	13.8	.469	.086	18.3
60-69	22	64.0	364	60	16.4	1000	127	12.7	.366	.059	16.1
70-79	38	75.4	330	96	29.1	1038	134	12.9	.318	.090	28.4
80-89	29	83.7	303	78	25.8	1026	116	11.4	.296	.068	23.1
90-99	7	92.7	287	113	39.4	1029	102	9.9	.274	.082	29.9

TABLE 4: Absorptiometric Measurements on the Shaft and on the Distal End of the Ulna in Adult Females by Decades. (Only a few males in each of the decade groups were measured.)

HUMERUS

AGE GROUP	N	AGE	MINERAL (mg/cm)			WIDTH ($mx10^{-5}$)			MINERAL/WIDTH		
			$\bar{X}$	SD	CV	$\bar{X}$	SD	CV	$\bar{X}$	SD	CV
MALES											
20-29	100	25.9	2766	333	12.0	2305	215	9.3	1.200	.093	7.7
30-39	118	34.6	2732	383	14.0	2300	226	9.8	1.188	.113	9.5
40-49	118	44.3	2731	340	12.5	2315	198	8.5	1.181	.114	9.6
50-59	49	54.6	2779	335	12.1	2343	183	7.8	1.189	.137	11.5
60-69	28	63.6	2579	408	15.8	2300	193	8.4	1.122	.157	14.0
70-79	16	74.4	2622	415	15.8	2348	135	5.7	1.114	.143	12.8
80-89	18	85.6	2287	456	20.0	2337	181	7.8	.980	.186	18.9
FEMALES											
20-29	31	23.0	2098	243	11.6	1987	176	8.8	1.056	.079	7.5
30-39	11	34.7	2117	260	12.3	1969	169	8.6	1.074	.074	6.9
40-49	19	42.7	2081	240	11.5	2013	132	6.6	1.033	.089	8.6
50-59	12	55.6	1811	307	17.0	1940	219	11.3	.943	.183	19.4
60-69	22	65.9	1539	464	30.2	2070	521	25.2	.748	.160	21.4
70-79	47	74.8	1384	300	21.7	1964	207	10.6	.707	.140	19.8
80-89	39	84.1	1296	211	16.3	2012	168	8.3	.644	.089	13.8
90-99	10	92.5	1271	227	17.9	2000	168	8.4	.639	.116	18.1

TABLE 5: Absorptiometric Measurements on the Midshaft of the Humerus in Adult Males and Females by Decades

HEIGHTS AND WEIGHTS OF CHILDREN

AGE GROUP	N	HEIGHT (cm) $\bar{X}$	SD	CV	WEIGHT (kg) $\bar{X}$	SD	CV
MALES							
6*	15	121.1	5.0	4.2	23.0	2.6	11.2
7*	27	127.8	5.2	4.0	25.9	3.9	14.9
8+	39	135.5	6.2	4.6	29.2	5.5	18.9
9+	42	140.3	6.3	4.5	33.0	6.3	19.0
10*	50	144.2	5.9	4.1	35.4	7.1	20.0
11+	44	149.2	6.4	4.3	38.3	5.9	15.3
12*	37	154.5	7.7	5.0	44.8	8.4	18.8
13*	35	158.8	9.6	6.0	47.4	9.8	20.6
14*	35	168.9	6.0	3.6	58.3	6.7	11.6
15*	43	175.2	7.2	4.1	66.5	10.8	16.2
16*	36	176.3	7.3	4.1	68.3	7.4	10.8
17*	39	179.4	6.2	3.5	73.6	9.5	12.9
18*	31	180.6	6.1	3.4	77.4	10.0	12.9
19*	19	181.3	8.9	4.9	79.4	10.3	12.9
FEMALES							
6*	14	123.6	6.3	5.1	22.9	3.8	16.7
7+	20	128.9	6.2	4.8	25.3	3.9	15.4
8*	18	134.5	9.0	6.7	27.2	4.4	16.0
9*	20	137.7	7.5	5.5	31.3	6.4	20.3
10*	24	143.0	6.2	4.3	34.0	6.3	18.6
11*	20	150.4	5.9	3.9	41.0	9.5	23.1
12*	15	160.4	7.7	4.8	45.5	8.2	18.0
13*	18	160.9	5.6	3.5	46.5	7.7	16.5
14*	28	165.2	8.2	5.0	52.9	7.7	14.6
15*	25	165.7	6.6	4.0	55.7	5.9	10.6
16*	13	167.8	5.3	3.2	56.7	6.7	11.9
17*	22	167.9	6.5	3.8	55.9	6.9	12.3
18*	16	164.3	7.3	4.4	58.6	8.6	14.7
19*	32	164.2	8.6	5.3	60.0	10.3	17.2

SOURCES: * from midshaft radius data
+ from humerus data

TABLE 6: Heights and Weights of Male and Female Children by Year

MIDSHAFT RADIUS CHILDREN

AGE GROUP	N	MINERAL (mg/cm) $\bar{X}$	SD	CV	WIDTH ($mx10^{-5}$) $\bar{X}$	SD	CV	MINERAL/WIDTH $\bar{X}$	SD	CV
MALES										
6	16	472	59	12.4	954	97	10.1	.495	.040	8.0
7	27	509	73	14.3	1000	87	8.7	.508	.042	8.2
8	38	565	71	12.6	1033	89	8.6	.546	.042	7.6
9	39	592	70	11.8	1059	95	9.0	.559	.044	7.9
10	52	640	78	12.2	1112	98	8.8	.577	.062	10.8
11	43	702	107	15.3	1146	119	10.4	.610	.051	8.4
12	39	746	95	12.8	1200	103	8.5	.620	.050	8.1
13	39	813	112	13.8	1268	115	9.1	.640	.049	7.7
14	35	898	126	14.1	1301	101	7.8	.688	.065	9.5
15	43	1048	146	10.3	1420	146	10.3	.738	.064	8.7
16	36	1154	143	12.4	1468	146	9.9	.787	.064	8.1
17	39	1196	130	10.9	1447	99	6.8	.826	.068	8.3
18	31	1247	116	9.3	1480	123	8.3	.843	.051	6.0
19	19	1296	187	14.4	1542	256	16.6	.845	.073	8.6
FEMALES										
6	14	434	79	8.2	911	115	12.6	.474	.044	9.3
7	20	452	63	13.8	912	90	9.8	.497	.141	10.2
8	18	485	66	13.6	924	96	10.4	.525	.049	9.4
9	20	548	70	12.7	972	104	10.8	.564	.125	7.1
10	24	564	93	16.5	999	106	10.6	.563	.163	9.2
11	22	653	125	19.1	1074	106	9.9	.607	.194	15.5
12	15	745	114	15.4	1145	163	14.3	.655	.150	12.2
13	18	738	93	12.6	1144	121	10.6	.646	.128	7.6
14	28	844	112	13.3	1185	119	10.1	.710	.138	5.4
15	25	869	76	8.7	1191	86	7.2	.730	.089	6.2
16	13	882	86	9.8	1214	85	7.0	.727	.101	7.7
17	22	893	99	11.0	1223	89	7.3	.730	.108	7.1
18	16	911	134	14.7	1214	138	11.4	.749	.153	8.4
19	32	937	107	11.4	1228	121	9.8	.764	.115	7.0

TABLE 7: Absorptiometric Measurements the Distal Third of the Radius Shaft in Male and Female Children by Year

MIDSHAFT ULNA CHILDREN

AGE GROUP	N	MINERAL (mg/cm) $\bar{X}$	SD	CV	WIDTH ($mx10^{-5}$) $\bar{X}$	SD	CV	MINERAL/WIDTH $\bar{X}$	SD	CV
MALES										
6	4	355	30	8.5	830	50	6.0	.428	.037	8.7
7	14	418	56	13.5	864	109	12.6	.485	.043	8.9
8	26	474	51	10.7	941	51	10.7	.506	.051	10.0
9	29	480	66	13.8	921	86	9.4	.521	.055	10.6
10	30	532	59	11.1	938	66	7.0	.567	.056	9.8
11	29	578	66	11.4	986	82	8.3	.587	.058	9.9
12	24	588	48	8.1	992	55	5.6	.593	.043	7.2
13	20	670	77	11.5	1022	65	6.4	.655	.055	8.3
14	17	746	106	14.2	1107	77	6.9	.672	.065	9.6
15	18	879	127	14.4	1174	90	7.7	.748	.085	11.4
16	17	959	102	10.7	1229	92	7.5	.782	.080	10.3
17	18	978	196	20.0	1257	158	12.6	.790	.176	22.3
18	15	1024	183	17.9	1269	100	7.9	.810	.149	18.3
19	15	1111	147	13.3	1255	103	8.2	.888	.115	12.9
FEMALES										
6	5	354	57	16.0	760	54	7.1	.466	.070	15.0
7	12	374	52	13.8	818	73	8.9	.459	.056	12.3
8	8	413	70	16.9	879	82	9.4	.472	.082	17.4
9	8	481	43	9.0	841	108	12.9	.575	.040	6.9
10	14	473	76	16.0	865	108	12.5	.546	.052	9.5
11	11	540	141	26.1	964	112	11.7	.551	.088	16.0

TABLE 8: Absorptiometric Measurements on the Distal Third of the Ulna Shaft in Male and Female Children by Year. (Only a few females above age 11 have been scanned.)

HUMERUS CHILDREN

AGE GROUP	N	MINERAL (mg/cm)			WIDTH ($mx10^{-5}$)			MINERAL/WIDTH		
		$\bar{X}$	SD	CV	$\bar{X}$	SD	CV	$\bar{X}$	SD	CV
MALES										
6	14	1009	128	12.7	1421	172	12.1	.712	.055	7.8
7	27	1112	168	15.1	1472	212	14.4	.757	.055	7.3
8	39	1268	137	10.8	1574	155	9.9	.806	.051	6.3
9	42	1311	155	11.8	1608	137	8.5	.817	.086	10.5
10	47	1470	178	12.1	1719	151	8.8	.855	.071	8.2
11	44	1531	198	12.9	1772	157	8.9	.863	.073	8.4
12	37	1684	191	11.4	1877	148	7.9	.897	.066	7.4
13	34	1786	264	14.8	1906	176	9.2	.936	.102	10.9
14	28	2070	312	15.1	2040	156	7.7	1.012	.110	10.9
15	43	2311	299	12.9	2148	149	6.9	1.074	.106	9.8
16	30	2672	400	15.0	2273	182	8.0	1.172	.120	10.2
17	35	2754	372	13.5	2212	173	7.8	1.242	.113	9.1
18	30	2948	363	12.3	2314	160	6.9	1.272	.118	9.3
19	16	3161	258	8.2	2430	156	6.4	1.301	.077	5.9
FEMALES										
6	11	943	107	11.4	1350	179	13.2	.702	.069	9.9
7	20	1004	121	12.0	1442	119	8.3	.695	.042	6.1
8	15	1125	165	14.6	1494	141	9.4	.751	.062	8.3
9	22	1215	137	11.3	1581	149	9.4	.769	.059	7.6
10	24	1181	203	17.2	1548	164	10.6	.760	.095	12.5
11	20	1368	247	18.0	1662	174	10.5	.820	.095	11.6
12	13	1533	238	15.5	1738	199	11.4	.881	.079	8.9
13	15	1661	280	16.9	1841	187	10.2	.900	.094	10.4
14	14	1818	154	8.5	1885	93	4.9	.964	.061	6.3
15	24	1896	174	9.2	1861	118	6.3	1.019	.074	7.3
16	10	1898	164	8.6	1908	176	9.2	.998	.081	8.1
17	18	1948	265	13.6	1877	151	8.0	1.037	.098	9.4
18	6	2102	292	13.9	1902	169	8.9	1.107	.140	12.6
19	3	1940	236	12.2	1870	87	4.7	1.036	.093	9.0

TABLE 9: Absorptiometric Meausrements on the Midshaft of the Humerus in Male and Female Children by Year

COO-1422-143

THE BONE MINERAL CONTENT AND PHYSICAL STRENGTH OF AVASCULARIZED FEMORAL HEADS: AN EXPERIMENTAL STUDY ON ADULT RABBITS

Experimental Results

by

Robert M. Witt
Department of Radiology

INTRODUCTION

This report describes the methods, procedures, and the results of the experiment to induce avascular necrosis in the femoral heads of adult, male rabbits by ligation of the femoral neck. This report is necessarily incomplete since the operative procedure was not successful, and the experiment was terminated. The purpose of the experiment and the proposed procedures have already been described and will not be repeated here (Witt, 1972). The report does describe in detail the actual methods and examinations made and gives a critical discussion of previous experiments in light of the author's own results.

EXPERIMENTAL ANIMALS AND SURGICAL PROCEDURE

The experimental animals were adult New Zealand white male rabbits. They were housed and fed in the Animal Care facilities of the University of Wisconsin Medical School. The animals, which were numbered sequentially, were kept in individual cages. A total of 12 rabbits were obtained for the experiment. Two died of unknown causes within 24 hours after they arrived at Animal Care, and ten rabbits had surgery. Altogether, 12 operations were performed since two rabbits were operated on twice. No rabbits died under anesthesia.

Surgery was performed under aseptic conditions in the operating rooms of the Department of Experimental Surgery. The anesthetic was a 6% solution of pentobarbital sodium (60 mg/ml) which was injected into the lateral ear vein. The dosage was about 20 mg per kilogram body weight and was often supplemented by another 6 mg during the operation.

The surgical procedure used was described by Rokkanen (1962) and was briefly described in the proposed experiment (Witt, 1972). The right hip was the experimental one and the left hip, which received a sham operation, served as the control. For the first 8 operations, #0 silk was used as the ligature. Surgical steel wire 0.635 mm in diameter was used as the ligature for the last four operations.

Each rabbit received an intramuscular injection of 0.25 ml of penicillin and steromycin postoperatively. No apparent infections were observed in any of the hips.

METHODS OF EXAMINATION

The animals were killed by a lethal dose of pentobarbital sodium.

At necropsy both femurs were excised and visual observations were made of both hip joints. The femurs were fixed and stored intact in 10% buffered neutral formalin.

For most of the animals two radiographs were taken, one immediately after the operation and the other immediately after sacrifice. Some of the animals had additional radiographs taken at intermediate times to determine if the experimental hips exhibited evidence of avascular necrosis. For the radiographs a postero-anterior exposure was made on Kodak RP-14 film in a non-screened cassette at a focal spot-to-film distance of about 2 meters. The tube was set for small focal spot and operated at 66 KVP and 100 mA and an exposure time of 1.5 seconds. The exposed film was developed in a Kodak automatic processor. Radiographs were also taken of the excised femurs. The films were principally examined to note any changes in the optical density of the femoral heads. In addition, other items were noted such as the presence of dislocations, location of the wire ligatures, and any changes in the contour of the femoral head.

Bone mineral content (BMC) determinations were made using the photon absorptiometric technique. Area bone mineral scans were made of the entire femoral head and neck, and linear bone mineral scans were made at sites located 50% and 75% of the total length measured proximally.

The area bone mineral scans of the femoral head and neck were made by performing sequential linear scans perpendicular to the line bisecting the femoral head. The scans began at the proximal end of the femoral head and ended when scan path entered the femoral shaft. The linear scan speed was 1.2 mm/sec, and the increment between scans was 0.5 mm. The source to detector distance was approximately 90 mm and the source and detector apertures were 0.51 mm and 3.2 mm, respectively. The bone mineral scans were analyzed with an analog system which provides an immediate direct readout of the BMC and bone width (Mazess et al, 1972). The bone mineral content of the femoral heads was calculated by summing all the linear scans from the second scan which indicated the presence of bone mineral to the scan 4 mm beyond this initial scan for a total of 8 scans. This summing procedure insured the inclusion of nearly the same portion of the femoral heads for all animals. The results of the scans of the femoral shaft are averages of 5 linear scans at each side. The bone mineral content of the control and experimental hips were compared by taking the ratio of the experimental to the control. To attempt to compensate for possible size differences between the rabbits, and for possible bone mineral loss due to disuse in the experimental side, the ratio of bone mineral content of the femoral head was normalized to the bone mineral content of the femoral shaft at both sites.

Since these operations were intended to test the ability to produce bone necrosis, no physical tests were performed on the specimens.

Femoral heads and necks were removed from both femurs of each rabbit as specimens for histological studies. Each femoral head and neck piece was bisected in the frontal plane and one half was sent to the Department of Pathology Laboratory for preparation of the histological sections. The Pathology Lab prepared standard decalcified bone sections stained with hematoxylin and eosin. The specimens were embedded such that the sectioning began at the plane of cleavage.

The histological sections were examined for signs of degeneration and regeneration of the bone tissue and the articular cartilage. In particular, the bone tissue was examined for the presence of empty lacunae indicating possible regions of necrosis, and cocooning of the trabeculae indicating the formation of new bone. The bone marrow was examined for the presence and extent of the vascularization, and for the presence of granulation tissue. The examination of the articular cartilage included an assessment of the surface smoothness and the thickness of the layer.

The results of the macroscopic, roentgenologic, bone mineral content, and microscopic examinations were listed in Table 1.

RESULTS

Not all the different examinations were made for each rabbit; hence, some data are missing. Macroscopic examinations were made for all ten rabbits when the femurs were removed. Radiographs were taken for all rabbits except No. 4. In vivo radiographs of rabbit No. 1 were unsatisfactory. Bone mineral scans were made of all femur pairs except Nos. 3, 4 and 5. Histological sections of both femoral heads were prepared for all rabbits except Nos. 1, 3, 4 and 5.

Macroscopic

Excessive synovial fluid in the joint capsule was observed in rabbits 2, 3, 4 and 7 and large amounts of pericapsular scar tissue were observed in rabbits 2, 4, 923 and 000 making it difficult to remove the femurs. In rabbits 1 and 4 the operated hips were dislocated. In rabbits 4 and 7 the ligamentum teres was intact. In rabbits 5, 6L and 8L the ligatures were not about the femoral neck, but had been placed below the minor trochanter. In most all rabbits soft tissue was present between the ligatures and the femoral necks and the ligatures appeared embedded in the soft tissue. It was particularly difficult to separate the silk ligatures from the scar tissue to determine if they were next to the bone. When the tissue was removed from the wire ligatures about the femoral necks of rabbits 923 and 000, it was apparent that these ligatures had not been tied against the bones. In fact, the loop formed could pass over the femoral head.

Radiographic

No increase in the radiographic density was observed in any of the experimental femoral heads when compared to the controls. In three rabbits examined 31, 32 and 42 days after the operation there was an apparent decrease in the optical density of the femoral heads on the operated side noted on the *in vitro* films. No other changes were noted.

Bone Mineral Content

The BMC of the experimental femoral head was less than that of the control for 3 rabbits.which were examined 32 days, 32 days and 42 days after surgery. The decrease in the BMC normalized to the BMC of the mid-shaft of the femur ranged from 16 percent to 29 percent. The BMC of the experimental femoral head was greater than the BMC of the control head for only one rabbit examined 31 days after the operation. The increase in the BMC normalized to the BMC of the mid-shaft site was 13 percent. The BMC remain unchanged for another rabbit also examined 31 days after the operation. Since both hips received operations in rabbits Nos. 6 and 8, a comparison of their BMC would not be meaningful.

Microscopic

In the specimens obtained from rabbits Nos. 6R, 7 and 923 regions of empty osteocyte lacunae were observed. In the specimens from rabbits Nos. 7 and 8L the articular cartilage appeared thinner than the control side. In one specimen from rabbit No. 8L the marrow appeared very cellular. In all specimens the epiphyseal line was absent indicating that the animals had mature skeletons. No changes were observed in any of the other specimens.

DISCUSSION OF RESULTS

The original review of the literature describing procedures to interfere with the blood supply to the head and neck of the femur in rabbits, indicated that of all the various procedures tried, the procedure of capsulotomy with division of the ligamentum teres and placing a tight ligature about the neck of the femur was the most successful in producing necrosis in the bone tissue in both immature and mature rabbits (Miltner and Hu, 1933, Rokkanen, 1962, Rosingh and James, 1969, Rosingh, et al., 1969). In particular, in a large experiment that compared six different surgical techniques to interfere with the hip joint of mature rabbits, Rokkanen (1962) produced the highest number of animals with evidence of necrosis in the femoral heads with this surgical technique. Since mature rabbits were used, this experiment seemed to show that ligation of the femoral neck was the best procedure to follow to induce avascular necrosis of the femoral head.

Our negative results indicate that this surgical procedure may not be very successful in producing avascular necrosis of the femoral heads. Of twelve hip operations only six resulted in a stable hip joint with the ligature placed about the femoral neck. The macroscopic, radiologic, photon absorptiometric and histologic observations of the specimens from these six successful procedures did not unequivocally indicate that necrosis was produced. In only three of these specimens were spotty regions of cancellous bone with empty lacunae noticed, and in only one of these specimens was thinning of the articular cartilage also observed. In fact none of the histological sections showed any evidence of a repair reaction such as the presence of granulation tissue or new bone formation. Based on observations made at necropsy, tight ligation of the arteries supplying the femoral head may never have been achieved

and the pressure atrophy described by Rokkanen (1962) was never present to disrupt the blood supply and produce bone necrosis. At surgery the ligatures were tied tightly. However, the large amount of soft tissue present between the bone and the ligature may have prevented the application of sufficient pressure to stop the blood flow. Henard and Calandruccio (1970) have indicated that the blood supply would have to be interrupted for about 12 hours to produce avascular necrosis.

A more critical review of Rokkanen's results may also indicate that this procedure may not be as successful in adult rabbits as originally estimated. If one excludes from his results all specimens taken before 3 weeks after the operation, which is the usual time necessary to first observe bone necrosis in the histological sections, all specimens which were dislocated, and all specimens which still had epiphyses, only 12 specimens remain. Of these twelve specimens, 8 had evidence of bone necrosis. If one further restricts the criteria and include only those specimens which have at least one other indication of tissue necrosis such as degeneration of the cartilage or the presence of granulation tissue in the marrow spaces, then only 6 of the specimens showed evidence of tissue necrosis.

Therefore, the results of the present study and a more critical review of Rokkanen's results suggests that possibly at most 50 percent of the surgical procedures of tight ligation of the femoral neck may successfully produce necrosis of the femoral head in adult rabbits. Should another experiment be attempted to produce necrosis in the femoral heads while at the same time maintaining a stable, functioning hip joint many more animals may be needed or a new procedure to interfere with the blood supply to the head and neck of the femur may be necessary.

There was one result of the experiment which tended to confirm existing observations. The BMC of the excised femoral heads could be measured and there existed some correspondence between the optical density of the in vitro radiographs and the BMC. In the three rabbits in which the femoral heads of the experimental side appeared to be less dense than the control, the ratio of the BMC of the femoral heads in each case was also less than one, Table 1. The observed decrease in optical density represented a minimum of a 10 percent decrease in BMC. For the one rabbit which had a 7 percent increase in BMC in the femoral head of the operated hip, no difference was observed in the radiograph. Thus, investigators who have made qualitative estimates in changes in the BMC in the femoral heads of rabbits from in vitro radiographs, only may have been able to detect changes greater than about 10 percent (Bobechko and Harris, 1960). No changes were observed in the in vivo radiographs for the same rabbits, which represented a maximum change of 19 percent in the BMC. Thus investigators who have estimated changes in BMC from in vivo radiographs were probably detecting changes of at least 20 percent (Rokkanen, 1962, Rosingh et al., 1969).

ACKNOWLEDGMENTS

Drs. P. Salamon and J. Jurist of the Division of Orthopedic Surgery performed the operations and assisted in the examination of the radiographs and the histological sections. The staff of Experimental Surgery assisted in the preparing of the animals for surgery and administered the post-operative medication. The experiment was supported in part by NASA Fund 144-8228 and the author was supported by NASA Grant Y-NGR-50-002-051.

Table 1 - Examination results of 12 operations to interfere with the blood supply to the head and neck of the femur in adult rabbits to produce bone necrosis.

Rabbit No.	Experimental Hip	Ligature	Days After Operation	Macroscopic Observations					Radiographic Observations		Bone Mineral Content Measurements			Microscopic Observations			
				Fluid In Joint	Adhesions	Dislocation	Lig. Teres Reattached	Ligature About F. Neck	Increase density of femoral head	Decrease density of femoral head	BMC Ratio of Femoral Head, Exp/Control	BMC Ratio Normalized to Midshaft BMC	BMC Ratio Normalized to BMC of 75% Site	Thin Articular Cartilage	Regeneration: Granulation Tissue New Bone	Regions of Bone with Empty Lacunae	Epiphysis
1	R	S	32			X		X			0.54	0.71	0.73	No Specimen			
2	R	S	32	X	X			X		X	0.81	0.84	0.91				
3	R	S	23	X				X			No Scans			No Specimen			
4	R	S	23	X	X	X	X	X	No X-ray		No Scans			No Specimen			
5	R	S	85								No Scans			No Specimen			
6	R	S	154					X								X	
7	R	S	42	X			X	X		X	0.78	0.76	0.73	X		X	
8	R	S	154					X									
6	L	W	39							X							
8	L	W	39											X	?		
923	R	W	31		X			X		X	0.90	0.99	0.96			X	
000	R	W	31		X			X			1.07	1.13	1.13				

References

Bobechko, W.P., and Harris, W.R. (1960), The radiographic density of avascular bone. J. Bone Joint Surg. 42B: 626-632.

Henard, D.C., and Calandruccio, R.A. (1970), Experimental Production of Roentgenographic and Histological Changes in the Capital Femoral Epiphysis Following Abduction, Extension, and Internal Rotation of the Hip, 16th Annual Meeting of the Orthopaedic Research Society, January 16 and 17, 1970, Chicago, Illinois.

Mazess, R.B., Cameron, J.R., and Miller, H. (1972), Direct Readout of Bone Mineral Content Using Radionuclide Absorptiometry. Int. J. of Applied Rad. and Isotopes 23: 471-479.

Miltner, L.J., and Hu, C.H. (1933), Osteochondritis of head of femur; experimental study. Arch. Surg. (Chicago) 27: 645-657.

Rokkanen, P., (1962), Role of surgical interventions of the hip joint in the aetiology of aseptic necrosis of the femoral head. Acta Orthop. Scand. Suppl. 58: 1-107.

Rosingh, G.E., and James, J., (1969), Early phases of avascular necrosis of the femoral head in rabbits. J. Bone Joint Surg. 51B: 165-174.

Rosingh, G.E., Steendijk, R., and Van den Hooff, A., (1969), Consequences of avascular necrosis of the femoral head in rabbits. A histological and radiological study. J. Bone Joint Surg. 51B: 551-562.

Witt, R.M., (1972), The bone mineral content and physical strength of avascularized femoral heads. An experimental study on adult rabbits. A proposed experiment. USAEC Report COO-1422-125.

COO-1422-144

MEASUREMENTS ON CLINICAL STANDARD USING DIRECT READOUT SYSTEM

Howard Gollup
Department of Radiology
University of Wisconsin
Madison, Wisconsin

For routine clinical and field use the operation of the analog direct readout system is evaluated, and the calibration adjusted, using a standard consisting of three annuli filled with a saturated dipotassium hydrogen phosphate solution. (Witt, Mazess, and Cameron, 1970). The absorption of this solution approximates that of bone, and the bone mineral content values from scans of this phantom cover the range of bone mineral from forearm to finger bones.

Scans have been made on the dipotassium hydrogen phophate standards over a 33 month period using a direct readout device in our clinical laboratories. During this period twelve different ^{125}I sources were used. Generally, measurements of all three annuli were made each day. Often measurements of the middle-sized annulus (or occasionally the large-sized annulus) were made after each patient was scanned, and for this reason there are more measurements for these annuli. The means and coefficients of variation over the 33 month period are given in Table 1. There was little systematic change over the 33 month period even though eleven or twelve sources were used. For source 70 the width calibration was incorrect and this gave somewhat deviant values at the beginning of this period. The coefficient of variation for bone mineral was between 1-2% for all annuli; highest for the small annulus and lowest for the large annulus. The coefficient of variation for bone width was one-half to two-thirds that for mineral

content. Part of this long-term variation appeared simply to reflect the uncertainties in the last digit of the digital panel meter(±0.01), and this could not be remedied. Differences among sources were not large, and were within the range of experimental error; however, for the first six sources, it was necessary to insure that the tin filtration on these sources was identical since the manufacturer(AECL) supplied the sources with filters of varying thickness. This was not necessary for the next five sources. However, the coefficients of variation were much higher with these sources from Norland Instruments.

	Source	Small n	Small Min (g/cm)	Small Width (cm)	Medium n	Medium Min (g/cm)	Medium Width (cm)	Large n	Large Min (g/cm)	Large Width (cm)
Means	70	-	-	-	51	.606	1.260	-	-	-
	97	37	.358	.651	92	.602	1.290	37	1.282	1.593
	116	33	.356	.646	107	.598	1.296	33	1.284	1.592
	132	16	.369	.648	54	.608	1.291	16	1.303	1.589
	153	58	.367	.652	226	.608	1.299	58	1.294	1.594
	173	76	.366	.654	302	.605	1.297	76	1.289	1.594
	232	44	.364	.652	106	.604	1.300	44	1.292	1.597
	130	40	.369	.652	106	.613	1.298	40	1.307	1.595
	145	31	.368	.656	66	.608	1.305	31	1.294	1.606
	180	63	.366	.652	108	.607	1.305	63	1.291	1.606
	217	76	.377	.658	115	.619	1.298	97	1.294	1.595
	261	22	.369	.654	32	.610	1.293	24	1.276	1.590
	All	496	.367	.653	1365	.607	1.296	519	1.292	1.596
CV (%)	70	-	-	-	51	1.25	1.44	-	-	-
	97	37	1.92	1.32	92	1.16	1.16	37	0.90	0.46
	116	33	1.56	0.89	107	1.06	0.59	33	0.81	0.37
	132	16	2.02	0.56	54	1.01	0.60	16	0.89	0.31
	153	58	1.03	0.82	226	0.97	0.54	58	0.74	0.48
	173	76	1.25	0.64	302	1.06	0.47	76	0.88	0.40
	232	44	1.54	0.91	106	0.99	0.47	44	1.15	0.40
	130	40	1.83	1.21	106	1.10	0.66	40	0.61	0.53
	145	31	1.45	1.15	66	1.27	0.71	31	0.86	0.83
	180	63	2.02	1.97	108	1.77	1.16	63	1.64	0.89
	217	76	2.21	2.18	115	1.96	0.95	97	1.42	0.97
	261	22	1.86	1.19	32	1.37	0.55	24	0.97	0.80
	All	496	2.27	1.14	1365	1.50	0.99	519	1.23	0.75
Among Sources		11	1.54	0.51	12	0.88	0.38*	11	0.69	0.35

* N=11

Table 1. Means and coefficients of variation for multiple scans of a three-chambered standard with twelve different ^{125}I sources over a 33-month period in a clinical laboratory. The additional scans for the medium and large-size chambers include scans made on the standard after each patient was measured.

DETECTORS SUITABLE FOR BODY COMPOSITION MEASUREMENTS WITH THE PHOTON ABSORPTIOMETRY TECHNIQUE

by

R. M. Witt
Department of Radiology
University of Wisconsin

Introduction

During the past year we continued our search for compact radiation detectors that are suitable for the photon absorptiometry technique for the determination of bone mineral content, soft tissue content, and soft tissue composition. Last year we reported some nominal specifications for photomultiplier tubes, PMT, to be suitable as a scintillation counter and compared two small PMT (1). This year we report the test results for two small, ruggedized photomultiplier tubes, both which are suitable as scintillator counters and meet space flight specifications. One PMT was received on loan from EMR Photoelectric Division (2) and was the one tested. The other PMT was purchased from RCA, but was received too late for complete test results to be included in this report. We also made preliminary contacts with H. L. Malm from the Neutron and Solid State Physics Branch of the Atomic Energy of Canada Limited to acquire and test a mercuric iodide, HgI_2, crystal as a conduction type detector to determine if it also would be a suitable detector for photon absorptiometry.

Method

For all the tests the multiplier tubes were coupled with DC-200 silicone oil to a 3 mm thick x 1 cm diameter NaI(Tl) scintillation detector with a .001 inch aluminum entrance window (3) and were tested as a scintillation counter system. The various tests made of the counter system were the following: count rate loss; count rate stability; time stability; noise spectrum; and photopeak resolution.

The count rate loss was tested by measuring the deadtime with the fastest nuclear counting system available in the laboratory. The deadtime was measured by reducing the count rate from high values to low values by attenuating a photon source incident upon the detector. The count loss, and consequently the deadtime, were estimated from a linear extrapolation to the zeroth attenuator on a plot of the logrithm of the count rate versus the number of attenuators.

The noise spectrum and the photopeak resolution were measured from the NaI spectrums with and without a photon source. The resolution, R, of the photopeak was defined in the usual manner, R = Full Width at Half Maximum/Pulse Height (4).

The count rate stability and the time stability are tests of the short term gain shifts and the longterm gain shifts, respectively. Both the count rate stability test and the time stability test were performed as specified in the RCA PMT Mannual (5). The count rate stability can be expressed as a percentage gain shift, G,

$$G = (|p_1 - p_2|/p_1) \times 100$$

where, p_1 is the pulse-height position for a count rate of 10,000 counts per second and p_2 is the pulse-height position for a count rate of 1,000 counts per second. The time stability or drift rate can be expressed as the mean gain deviation, MGD, of the hourly pulse-height position measurements. MGD can be calculated from the following equation,

$$MGD = \sum_{i=1}^{n} (p - p_i)/n \times 100/p$$

where p is the mean pulse-height, p_i is the pulse-height for the i-th measurement, and n is the total number of measurements.

Results

The one PMT tested was an EMR model 541N-01-14 multiplier tube. Its electrical and mechanical specifications appear in Table 1. When operated as a scintillation detector, this multiplier tube had a photopeak resolution for ^{125}I (28 keV) of about 43 percent. The phototube was operated at 2250 Volts and the window setting of the pulse-height analyzer was about 10 keV. For these settings the noise spectrum cut-off of the total system occurred at about 20 keV. This phototube was able to count pulses at a frequency rate of 70 kHz from a radionuclide source with no apparent count loss. Both the count rate stability expressed in terms of percentage gain shift, and the time stability expressed as the percentage mean gain deviations were less than one percent, and are within the nominal values specified in the RCA Mannual (5).

The RCA PMT purchased is a developmental type Model C31016F. Its electrical and mechanical specifications also appear in Table 1. For testing it was coupled to the same scintillation detector as the EMR multiplier tube. The preliminary results indicate that the tube has sufficient gain and low noise characteristics to resolve ^{125}I (28 keV) photopeak.

Conclusions

Our tests indicate that the EMR Model 54IN multiplier tube is a suitable scintillation detector for a space flight version of the photon absorptiometry apparatus. The completion of the tests of the RCA tube should also demonstrate that it would also be a suitable detector for that apparatus. Although these small, ruggedized PMTs when coupled to a NaI(Tl) scintillator crystal are suitable detectors for the photon absorptiometry apparatus, the size and weight restrictions may still limit their application to the apparatus designed for space flight. The HgI_2 detector which we shall receive on loan from AECL is mounted in a crystal can 2 cm x 2 cm x 8 mm thick (6) and is not much larger than the mounted NaI(Tl) crystal alone. Moreover,

a conduction type detector such as HgI_2 directly outputs a voltage pulse and does not need the multiplier tube and its associated electronics to provide this same voltage pulse. We intend to test this HgI_2 detector to determine if it is a suitable detector for the photon absorptiometry system.

Acknowledgements

I would like to express our thanks to Robert L. Wisner from EMR Regional Office in Englewood, Colorado, for loaning us the ERM multiplier tube for testing.

References

1. Witt, R. M. and Mazess, R. B. Comparison of Compact Scintillation Detectors for Bone Mineral Content Measurements, USAEC Report COO-1422-119, 1972.

2. EMR Photoelectric Division, Princeton, New Jersey, 08540.

3. Harshaw Chemical Company, Solon, Ohio, 44139, Type MI0HE3M.

4. Hine, G. J. Sodium Iodide Scintillators. In Instrumentation in Nuclear Medicine, G. J. Hine, ed., Vol. 1, p. 95, Academic Press, New York, 1966.

5. RCA Photomultiplier Manual, Technical Series PT-61, RCA Corporation, Harrison, New Jersey, 1970.

6. Malm, H. L. Atomic Energy of Canada Limited, Chalk River Nuclear Laboratories, Chalk River, Ontario, private communication.

TABLE 1: CHARACTERISTICS OF TWO PHOTOMULTIPLIER TUBES SUITABLE FOR SPACE FLIGHT

ELECTRICAL CHARACTERISTICS:	MIN	TYPICAL	MAX	MIN	TYPICAL	MAX	UNITS
Cathode Sensitivity							
Luminous		54.0×10^{-6}		47×10^{-6}	67×10^{-6}		A/lm
Radiant	0.059	0.071			0.079[1]		A/W
Quantum Efficiency	18.0[2]	21.5[2]			24[1]		%
Current Amplification		10^5 at 2280V	2620V		4.5×10^5		
		10^6 at 2950V	3400V				
Anode Dark Current		2.5×10^{-11}	1×10^{-10}		5×10^{-10}	1×10^{-9}	A
Operating Voltage, anode to cathode			3600			1500	V
Operating Current		recommended	1.0			20	A
PHYSICAL CHARACTERISTICS:							
Maximum Length		11			8.9		cm, potted
Maximum Diameter		3.5			3.4		cm, potted
Maximum Cathode Diameter		2.5			1.90 Minimum		cm
Cathode Type		bi-alkali			CsKSb		
Window Material		2056 glass			7056 glass		
Number of Dynodes		14V			10C		
ENVIRONMENTAL:							
Temperature		-55 to +150			-100 to +85		^{o}C
Shock		100g, 11msec			75 $\pm$ 7g, 11 $\pm$ 1msec		
Vibration		30g, 20 to 3,000Hz			20.7g, 50 to 2,000Hz		

Notes: 1. at 400 nm
2. at 410 nm

A COMPACT SCANNER FOR MEASUREMENT OF BONE MINERAL CONTENT AND SOFT-TISSUE COMPOSITION

by

D.A. Hennies, R.B. Mazess and C.R. Wilson

A lightweight mechanical scanner is under construction as a prototype for measurement of bone mineral content and soft-tissue composition in space flight. The scanner is also for use in clinical and field studies. An 18 cm travel is planned, longer than that of a previous scanner (1). The longer travel allows scans across the entire forearm and upper arm, so soft-tissue composition in addition to bone mineral content may be determined.

To conserve space in storage, the arm supporting the source is designed to slide close to the square aluminum tubing supporting the detector. A sliding arm will be used, rather than a folding arm as in the previous scanner, to increase the rigidity of the lengthened source arm. The storage dimensions of the scanner will be approximately 40x24x8 cm. The estimated weight of the scanner is 5 kilograms.

Ball-bearing rollers support the source-detector yoke. A rack gear attached to the detector support arm is driven by a gear on the motor shaft. A lucite scanning table will be supported as indicated in Figure 1, an isometric drawing of the scanner.

REFERENCE

1. R.B. Mazess and Y. Towllati, A Compact Scanner for Measurement of Bone Mineral, USAEC Report COO-1422-120 (1972).

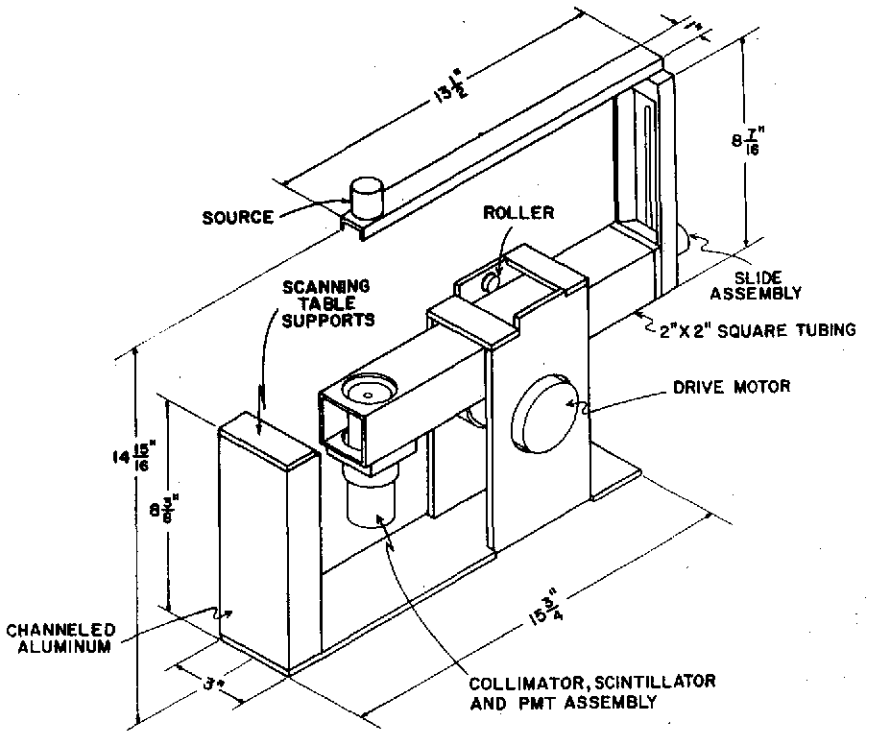

Figure 1.

DIRECT READOUT OF BONE MINERAL CONTENT WITH DICHROMATIC ABSORPTIOMETRY

By

W. C. Kan, C. R. Wilson, R. M. Witt and R. B. Mazess
Department of Radiology
University of Wisconsin Medical Center
Madison, Wisconsin

An analog system has been constructed to calculate the bone mineral mass and bone width from the transmission of two photon beams with different energies such as ^{153}Gd (43 keV and 100 keV) or ^{125}I and ^{241}Am (28 keV and 60 keV). The major advantage of using a dichromatic attenuation technique to measure bone mineral content, BMC, over the technique of using a monoenergetic photon beam is that it does not require the bone to be covered with a constant thickness of soft tissue.

The transmission of the two monoenergetic photon beams through a bone and soft tissue system can be expressed as:

$$I(A) = I_o^*(A) \exp\left(-\mu_{BM(A)} M_{BM} - \mu_{ST(A)} M_{ST}\right) \quad (1)$$

$$I(B) = I_o^*(B) \exp\left(-\mu_{BM(B)} M_{BM} - \mu_{ST(B)} M_{ST}\right) \quad (2)$$

$I_o^*(A)$ = The unattenuated intensity at energy A

$I_o^*(B)$ = The unattenuated intensity at energy B

$I(A)$ = The attenuated intensity at energy A

$I(B)$ = The attenuated intensity at energy B

$\mu_{BM(A)}$ = Mass attenuation coefficient of bone mineral at energy A (cm^2/gm)

$\mu_{ST(A)}$ = Mass attenuation coefficient of soft tissue at energy A (cm^2/gm)

M_{BM} = Mass per unit area of bone mineral (gm/cm^2)

M_{ST} = Mass per unit area of soft tissue (gm/cm^2)

These equestions can be solved, with point bone mineral mass, M_{BM}, and point soft tissue mass, M_{ST}, expressed as,

$$M_{BM} = K_S \left[\mu_S \log I(B) - \log I(A)\right] - \left[\mu_S \log I_o^*(B) - \log I_o^*(A)\right] \quad (3)$$

$$M_{ST} = K_B \left[-\mu_B \log I(B) + \log I(A)\right] - \left[-\mu_B \log I_o^*(B) + \log I_o^*(A)\right] \quad (4)$$

where

$$\frac{\ln(10)\ \mu_{ST(B)}}{\mu_{BM(A)}\mu_{ST(B)} - \mu_{BM(B)}\mu_{ST(A)}} = K_S \qquad \frac{\mu_{ST(A)}}{\mu_{ST(B)}} = \mu_S$$

$$\frac{\ln(10)\ \mu_{BM(B)}}{\mu_{BM(A)}\mu_{ST(B)} - \mu_{BM(B)}\mu_{ST(A)}} = K_B \qquad \frac{\mu_{BM(A)}}{\mu_{BM(B)}} = \mu_B$$

As in the earlier single photon direct readout unit (1) the integration of M_{BM} with respect to distance across the bone yields the direct readout of bone mineral content per unit length of bone (g/cm); simultaneously, integration of a fixed current source indicates the bone width.

The dichromatic analog system functions similarly to the single photon system and uses the output of a basic nuclear counting system (omitted from Figure 1) such as NaI(TL) scintillation detector, photomultiplier tube, amplifiers, two single channel analyzers, two scalers with buffers, timer and the control system. This permits collection of digital data from the pulse height analyzer channels, and storing them periodically in the scaler buffers.

The digital data collection system has been previously described (2). In the former data collection system the contents of the scaler buffers are recorded on magnetic tape. The tape is subsequently processed by a computer which calculates the bone mineral content and the bone width.

In the new analog system (Figure 1), the digital contents of the scaler buffers are converted to analog voltage signals. These signals are then simulated as equation (3) to compute M_{BM} in an analog manner at each point during the scan.

The digital to analog converter (D/A), converts the digital signals from the scaler buffers to analog signals. Since a portion of the counts in the lower energy channel is due to Compton interactions of the higher energy photon in the scintillator and the surrounding materials, a correction factor must be subtracted from the lower channel voltage. This fraction depends upon the photon energy, the window setting, the crystal size, and

the source-detector geometry. An estimate of this correction factor can be found by attenuating the beam until nearly all the counts in the lower channel are due to the "spill-over" from the upper energy photons. For the ^{153}Gd source, the correction factor, f, was found to be approximately 10% of the upper energy channel counts. The corrected voltage for channel B becomes (B-fA), Fig. 1.

After the spill-over correction, the two logarithmic amplifiers take the logarithm of the analog signals from both channels. Channel B is multiplied by coefficient (μ_S in BMC equations) and subtracted from channel A by a low drift linear differential amplifier. The resulting analog signal is $[\mu \log I(B) - \log I(A)]$.

Prior to entering the bone, $M_{BM} = 0$ and $\mu \log I(B) - \log I(A) = \mu \log I_o^*(B) - \log I_o^*(A)$. The value of $\mu \log I_o^*(B) - \log I_o^*(A)$ is set and stored as a constant D.C. voltage. Presently this value is adjusted manually with a potentiometric setting to establish a base line reference, and is shown in the block diagram as the "Base Line Adjustment". A circuit which automatically sets this level will be designed and constructed to replace the manual adjustment.

As the beam moves from the soft tissue region into the bone the quantity, $[\mu \log (B) - \log I(A)] - [\mu \log I_o^*(B) - \log I_o^*(A)]$ is no longer equal to zero. The comparator stage, which consists of a differential amplifier and a relay, automatically detects the edge of the bone. When the above quantity deviates from zero by a preset value, the comparator activates the relay. The closing of the relay contacts begins the integration of the output from the differential amplifier. When the beam leaves the other edge of the bone, the comparator causes the relay to open and terminates the integration. The opening and closing of the relay also starts the integration of a constant current source which gives a measure of the bone width.

After integration across the bone is completed, the voltages of the two integrators can be displayed in the digital panel meter as a direct readout of BMC and bone width. A simple resistive divider network provides the multiplication factor K as indicated earlier in the bone mass, M_{BM}, equation (3).

Preliminary tests of the analog system were performed by scanning an upper arm standard. The arm standard is composed of 2.24 cm diameter aluminum tube which simulates the bone and is embedded in a methyl

methacrylate block with round edges and flat sides over the aluminum tube. The approximate dimensions are 5.6 x 7.05 x 8 $(cm)^3$. The scans were made with a 22 mCi ^{153}Gd source at a scan speed of 1.2 mm/sec and with detector collimation 6.4 mm in diameter. The point bone mineral expression $[\mu \log I(B) - \log I(A)] - [\mu \log I_o^*(B) - \log I_o^*(A)]$ from the output of the differential amplifier were plotted by an x-y plotter, Fig. 2. The step nature of the plot is related to the scaler buffers which receive the contents of the scaler at the end of each timer interval and maintain the same contents during next timer interval. The average value for six consecutive scans of the arm standard was 6.27 (arbitrary units) with standard deviation of 0.09 , coefficient of variation 1.45%.

As previously stated one advantage of dichromatic attenuation technique is that it does not require the bone to be covered with a constant thickness of soft tissue. When no bone is present, M_{BM} is simply zero and independent of the amount of soft tissue cover. To show this independence, a 5 cm thick methyl methacrylate block was scanned in air and the point value for bone mineral mass were recorded with the x-y recorder along the scan path (Fig. 3). The base line level differs little when scanning from air into the methyl methacrylate and then back into air. However, the fluctuations of point bone mineral values were larger when the beam is traveling through the plastic block than the air because of the increased variation due to the decrease in counting statistics.

The analog system described was a breadboard model. An engineering model of this system is now being constructed. The results of the dual channel direct analog system with the dual channel digital system will be evaluated during the coming year. System sensitivity, reproducibility and long term stability will also be examined.

REFERENCES

1. Mazess, R.B., Cameron, J.R. and Miller, H. (in press). Direct Readout of Bone Mineral Content Using Radionuclide Absorptiometry, International Journal of Applied Radiation and Isotopes 23: 471, 1972.

2. Judy, P.F., Ort, M.G., Kianian, K. and Mazess, R.B. Developments in the Dichromatic Attenuation Technique for the Determination of Bone Mineral Content In Vivo, USAEC Report COO-1422-97 (1971).

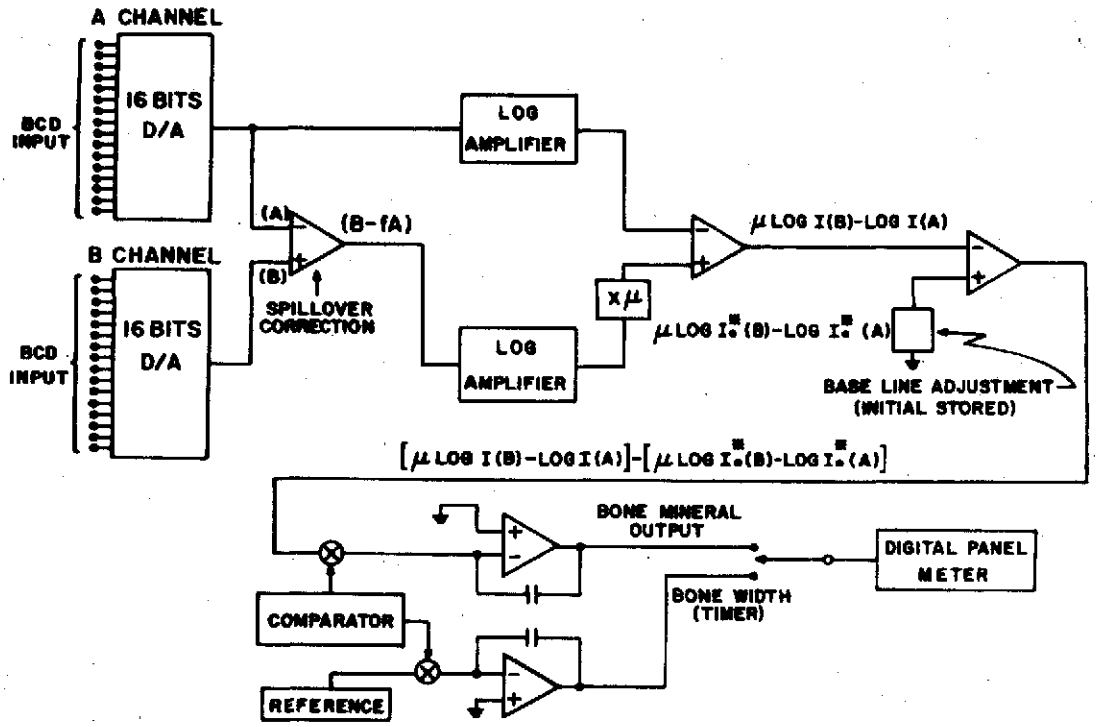

Figure 1 Dichromatic analog system

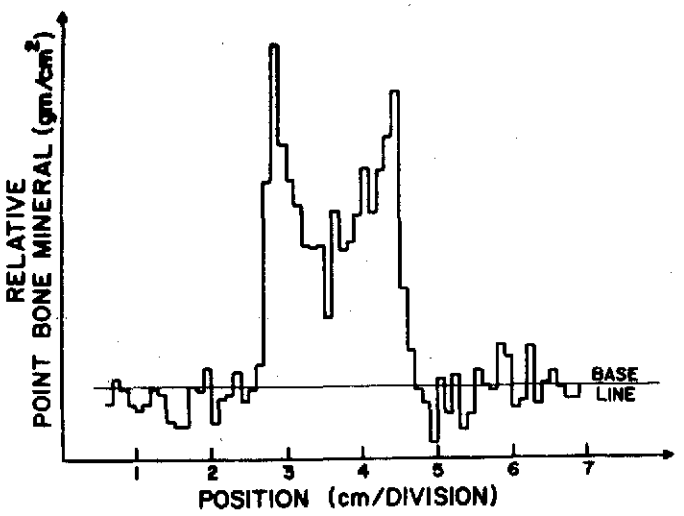

Figure 2 Point bone mineral mass versus scan position across arm standard.

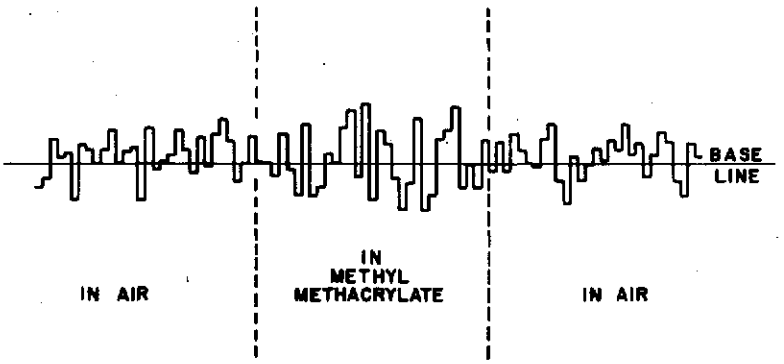

Figure 3 Point bone mineral mass versus scan position across 5 cm block of methyl methacrylate.

COO-1422-148

ABSORPTIOMETRY USING ^{125}I AND ^{241}Am TO DETERMINE TISSUE COMPOSITION IN VIVO

by

Norbert J. Pelc
Department of Radiology
University of Wisconsin Medical Center
Madison, Wisconsin

I. Introduction

The dichromatic attenuation technique can be used to study bone mineral soft tissue and fat-lean mixtures.[1-4] Other investigators have used ^{153}Gd and ^{109}Cd as dual photon sources.[1-4] This study was made to check the feasability of using ^{125}I and ^{241}Am in a dual source holder as a dichromatic photon source.

II. Dual Source Holder

Brass holders to contain commercially available sealed point sources of ^{125}I and ^{241}Am were made. Ideally, when using the dichromatic attenuation technique, both beams should be simultaneously attenuated by the same tissue mass. In a dual source with two radionuclides, however, the sources must be physically separated. When designing the source holder several source-detector geometries existed which would allow the detection of photons from each source which have been attenuated simultaneously by the same tissue mass. The holder could have been designed so that the beams would cross at the target. This source arrangement would require a large detector collimator, thus allowing the detection of more scattered radiation than for the case of good geometry. The source holder could be constructed so that the beams cross at the detector, thus minimizing the size of the collimation necessary and scattered radiation detected. However, the beams would sample different tissue masses. Moreover, the angle between the source capsules would be extremely small and difficult to machine accurately. It was decided that the sources should lie side by side as close together as possible so that each would be attenuated by almost the same tissue mass.

Two such holders were made. In the first holder the two sources were loaded from the top, with the sources, as well as a .002 in. tin filter, held in place by a lucite plug (Fig. 1). An improved source holder has been constructed in which the sources are rear loaded and held in place by a

spring loaded screw. This eliminated the possibility of the sources falling out accidentally. A rubber O-ring set into the face of the holder allows the holder to be firmly fixed into the scanner (Fig. 2).

III. Iodine Escape Peak Correction

When the ^{125}I and ^{241}Am sources are simultaneously detected by a NaI(Tl) scintillator, the iodine escape peak, which occurs at 31 keV, overlaps the ^{125}I photopeak (Fig. 3). When the 60 keV photon from the ^{241}Am source interacts with the NaI(Tl) crystal, it undergoes a fluorescent interaction with the iodine atoms in NaI. The iodine escape peak is due to the escape of some of the K fluorescent x-rays from the crystal.[5] For transmission measurements, the photopeaks of the two sources must be separated and the number of escape peak events in the ^{125}I channel must be subtracted from the total counts in that channel.

To determine the escape peak's contribution to the lower channel, the dual source was attenuated with copper foils until nearly all of the ^{125}I photons were attenuated. When the ^{125}I photons are almost totally attenuated the counts in the ^{125}I channel are only due to the escape peak events and are proportional to the number of counts in the ^{241}Am channel, i.e. Escape Peak Counts = k x Counts in ^{241}Am channel, where k is a constant of proportionality. The constant k was estimated by extrapolating the attenuation curves for the ^{241}Am channel and the counts due to escape peak events in the ^{125}I channel to zero attenuators and taking the ratio of these initial count rates (Fig. 4). The constant k was estimated at four different window settings of the ^{125}I and ^{241}Am channels (Table 1). The escape peak correction factor is characteristic of source-detector geometry and must be determined for each system at the window settings desired. With the constant, k, determined, the corrected count rate in the ^{125}I channel can be estimated from the following relationship, Correct count rate ^{125}I channel = Measured count rate ^{125}I channel - k x Measured count rate ^{241}Am channel.

An attenuation measurement was made to determine the accuracy of the escape peak correction. The mass attenuation coefficients for water for ^{125}I and ^{241}Am were simultaneously measured using the dual channel system. This was done for the same four window settings used to estimate the constant k. The corrected lower channel counts were used to calculate the attenuation coefficient for ^{125}I. The values ranged from .3981 cm^2/gm to .3985 cm^2/gm and were about 5% lower than the tabulated value.[6] The value for the ^{241}Am

attenuation coefficient was consistently .1914 cm^2/gm, which is also about 5% lower than the tabulated value (Table 1). However, the ratio of the attenuation coefficients for the two energies differed by only about 1% from the ratio of the tabulated values (Table 1), indicating that the escape peak correction is accurate. The error in the absolute value for the attenuation coefficient is probably systematic and may be due to source-detector geometry. For these attenuation measurements the detector collimation was large (6 mm) allowing more scattered radiation to be detected which would cause the measured attenuation coefficients to be lower than tabulated ones.

IV. Fortran Program for Data Analysis

A Fortran program was written to process the data from the dual source scans. A typical linear scan starts in air, traverses the arm, and ends in air. The two radionuclide sources are aligned with the scanner so that a line joining the sources is colinear with the scan direction. The program first detects the edge of the object scanned and determines which channel (i.e. source) is leading and by how many data points, and then shifts the data arrays so that they represent transmitted counts through the same tissue mass. Each scan is divided into three regions: 1) the section from the beginning of the arm to the first edge of the first bone; 2) the section from the first edge of the first bone to the second edge of the last bone; and 3) the section from the last edge of the last bone to the end of the arm. In regions one and three where no bone is present, R, the total mass of soft tissue, the amount of fat and lean tissue, and the percent fat relative to the total soft tissue are calculated from equations (A.2)* (A.3), and (A.4). In region two the program calculates soft tissue mass using (A.3) and bone mineral using (A.5). Total soft tissue and total bone mineral are then computed.

V. Study of Upper Arm Phantom

To determine the precision of scanning with the dual source, various measurements were made on an upper arm phantom consisting of an aluminum tube embedded in a piece of lucite. Since tissue composition can vary significantly from sites only a few millimeters apart, [3] it is important for the two sources to be attenuated by the same tissue mass. An experiment to check the precision of aligning the data arrays of air to air scans was conducted. Scans of the standard were made with the sources in two different

* All equations are in Appendix A.

configurations. The line joining the sources was either 1) colinear or 2) perpendicular to the direction of the scan path. In configuration 1) the beams pass through the same tissue but at different times. In configuration 2) the beams pass through the phantom at the same time, but are attenuated by different tissue masses displaced by about 2 mm (the separation of the sources).

For actual subjects, the first configuration, where the sources are attenuated by the same tissue mass but at different times is desirable if the data points can be shifted so that the count rates from each photon source represent those which have been transmitted by the same tissue mass.

The first study of the standard was done to check the precision of aligning the data arrays. The data was processed by an earlier version of the above program. For this version of the program, the number of data points to shift the data arrays was part of the data input. Both total soft tissue mass and total bone mineral were calculated using equation (A.3). The coefficient of variation for the total soft tissue was $\pm$ 0.86% when the ^{125}I source lead the ^{241}Am and $\pm$ 0.98% when the sources were side by side. The coefficient of variation for the total bone mineral were $\pm$ 4.7% when ^{125}I source was leading and $\pm$ 5.0% when the sources were side by side. The coefficients of variation were large for the total bone mineral measurement because the ^{125}I count rate was extremely low (25 counts/sec) in the bone portion of the upper arm phantom, thus increasing the variation due to counting statistics. With a more active ^{125}I source the errors in the bone mineral content should decrease.

These scans of the upper arm phantom showed that the data arrays can be shifted reproducibly to correct for the physical separation of two sources and that for symmetric objects there is no difference between the results for the two scanning configurations.

The second study of the standard was done to determine the day-to-day precision of the total system, the same upper arm standard was scanned 7 different times over a period of 3 days. The standard deviation for total soft tissue mass for a single day was $\pm$ 0.5% while the deviation for all the scans was $\pm$ 0.7%.

Table 1: Results of correction for the iodine escape peak for four window settings.

	WINDOW SETTINGS		WATER ATTENUATION COEFFICIENTS (cm^2/gm)			
	LOWER CHANNEL	UPPER CHANNEL	k	^{125}I	^{241}Am	Ratio
1 LLD	21.9 keV	49.3 keV	.0981	.3985	.1914	2.082
1 ΔE	12.3 keV	27.4 keV				
2 LLD	17.8 keV	49.3 keV	.1235	.3985	.1914	2.082
2 ΔE	21.9 keV	27.4 keV				
3 LLD	21.9 keV	50.7 keV	.0997	.3982	.1914	2.080
3 ΔE	12.3 keV	21.9 keV				
4 LLD	17.8 keV	50.7 keV	.1256	.3981	.1914	2.080
4 ΔE	21.9 keV	21.9 keV				

The ratio of the tabulated attenuation coefficients for ^{125}I and ^{241}Am is 2.053.

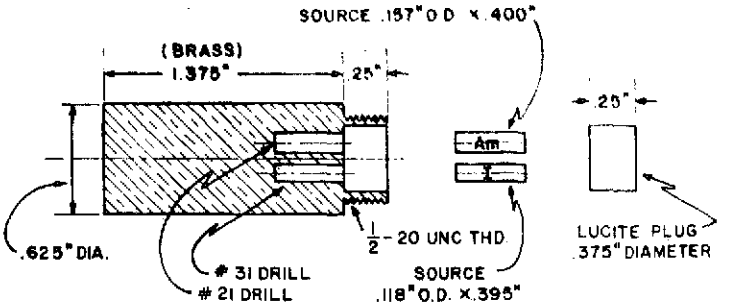

DUAL SOURCE HOLDER

Figure 1: First dual source holder

DUAL SOURCE ASSEMBLY, MATERIAL BRASS

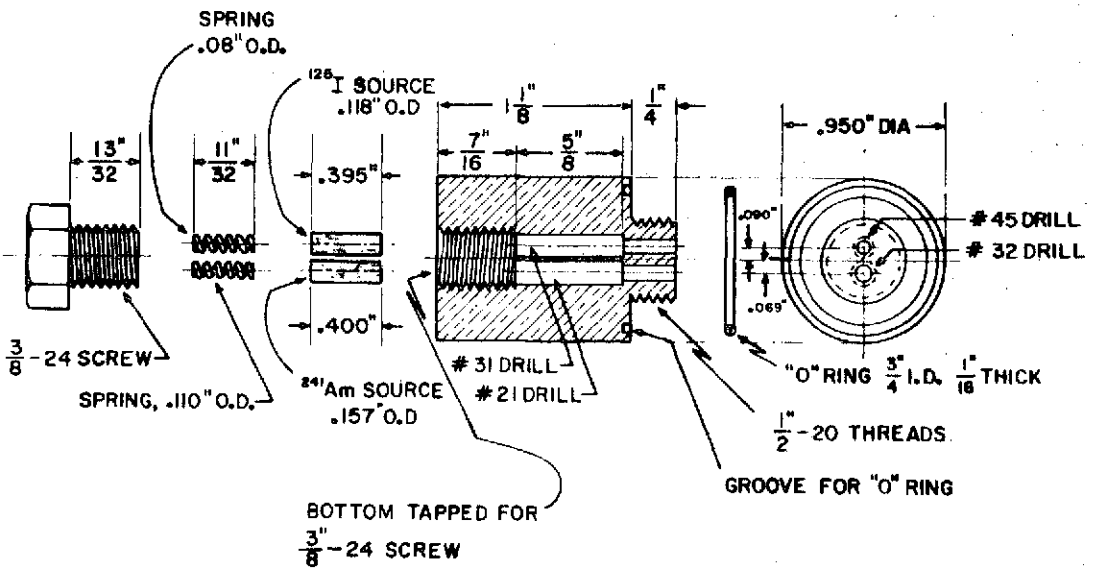

Figure 2: Improved dual source holder

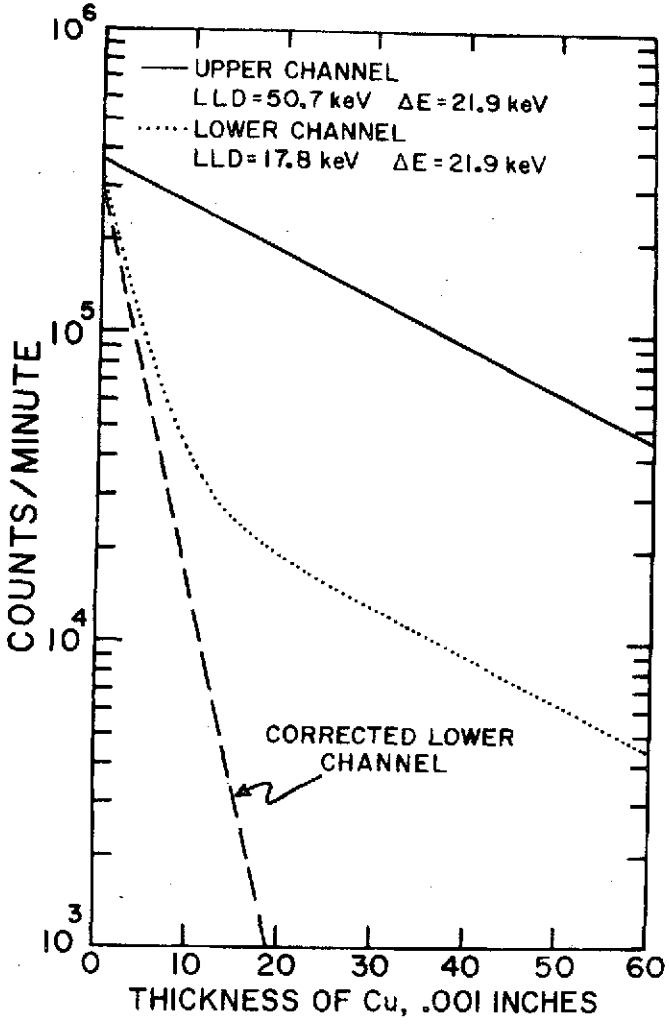

Figure 4: Transmitted intensity as a function of thickness of Cu attenuator for upper and lower channels using the dual photon system, and lower channel corrected for the iodine escape peak.

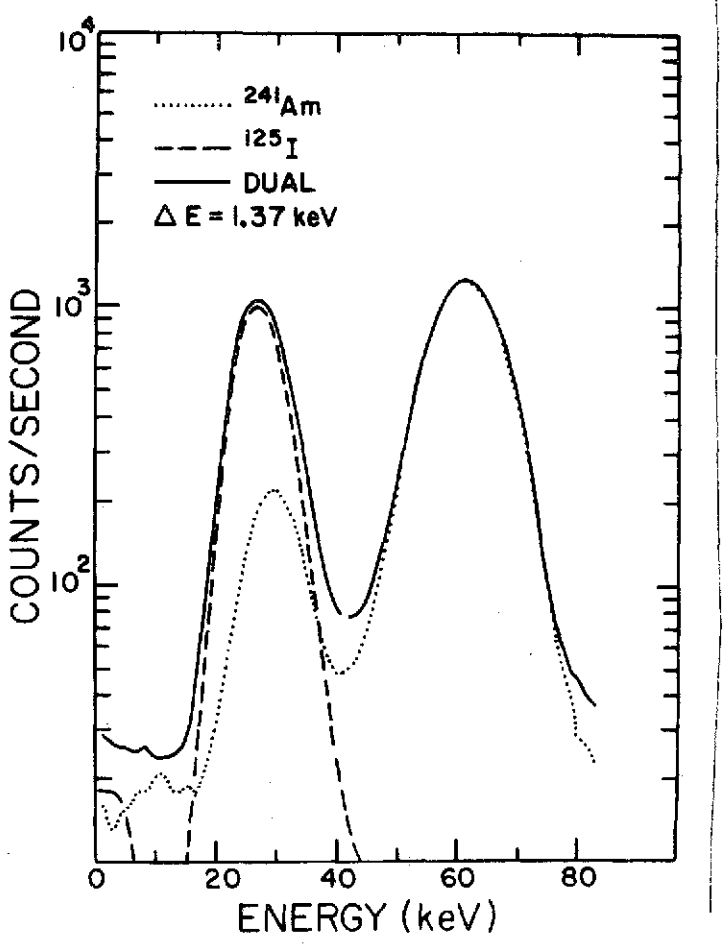

Figure 3: Pulse height spectrum for ^{241}Am, ^{125}I and dual source.

References

1. Mazess, R. B., Cameron, J. R. and Sorenson, J. A.; Determining Body Composition by Radiation Absorption Spectrometry; Nature, Vol 228, No. 5273, pp. 771-772, Nov. 21, 1970.

2. Judy, P. F., Ort, M. G., Kianian, K. and Mazess, R. B.; Developments in the Dichromatic Attenuation Technique for the Determination of Bone Mineral Content In Vivo; USAEC Progress Report COO-1422-97 (1971).

3. Judy, P. F.; A Dichromatic Attenuation Technique for the In Vivo Determination of Bone Mineral Content; University of Wisconsin (1971).

4. Preuss, L. E. and Schmonsees, W.; ^{109}Cd for Compositional Analysis of Soft Tissue; International Journal of Applied Radiation and Isotopes, Vol. 23, pp. 9-12 (1972).

5. Hine, G. J.; Sodium Iodide Scintillators; Instrumentation in Nuclear Medicine, G. J. Hine (ed), Academic Press Inc., New York (1967), pp. 95-117.

6. Hubbell, J. H.; Photon Cross Sections, Attenuation Coefficients, and Energy Absorption Coefficients from 10 keV to 100 GeV; National Bureau of Standards, U.S. Department of Commerce, NSRDS-NBS 29, Washington, D.C. (1969).

APPENDIX

Let:

I_{01} = Unattenuated intensity in channel 1

I_{02} = Unattenuated intensity in channel 2

I_1 = Transmitted intensity in channel 1

I_2 = Transmitted intensity in channel 2

m_f, m_l, m_s, m_b = gm/cm^2 of fat, lean, soft tissue, and bone mineral, respectively

μ_{f1}, μ_{f2}, μ_{l1}, μ_{l2}, μ_{s1}, μ_{s2}, μ_{b1}, μ_{b2} = mass absorption coefficient in cm^2/gm

For fat-lean mixtures, the transmission equation for two photons can be written as:

$$\ln (I_{01}/I_1) = \mu_{f1}m_f + \mu_{l1}m_l$$

$$\ln (I_{02}/I_2) = \mu_{f2}m_f + \mu_{l2}m_l \qquad \text{(A.1)}$$

Solving (A.1)

$$m_l = \frac{\mu_{f2}}{\mu_{l1}\mu_{f2} - \mu_{l2}\mu_{f1}} \ln (I_{01}/I_1) - \frac{\mu_{f1}}{\mu_{l1}\mu_{f2} - \mu_{l2}\mu_{f1}} \ln (I_{02}/I_2)$$

$$m_f = \frac{-\mu_{l2}}{\mu_{l1}\mu_{f2} - \mu_{l2}\mu_{f1}} \ln (I_{01}/I_1) + \frac{\mu_{l1}}{\mu_{l1}\mu_{f2} - \mu_{l2}\mu_{f1}} \ln (I_{02}/I_2) \qquad \text{(A.2)}$$

Similarly, for bone mineral-soft tissue mixtures,

$$m_b = \frac{\mu_{s2}}{\mu_{b1}\mu_{s2} - \mu_{s1}\mu_{b2}} \ln (I_{01}/I_1) - \frac{\mu_{s1}}{\mu_{b1}\mu_{s2} - \mu_{s1}\mu_{b2}} \ln (I_{02}/I_2)$$

$$m_s = \frac{-\mu_{b2}}{\mu_{b1}\mu_{s2} - \mu_{s1}\mu_{b2}} \ln (I_{01}/I_1) + \frac{\mu_{b1}}{\mu_{b1}\mu_{s2} - \mu_{s1}\mu_{b2}} \ln (I_{02}/I_2) \qquad \text{(A.3)}$$

If $m_b = 0$, i.e., no bone is present, then from (A.3)

$$\mu_{s2} \ln (I_{01}/I_1) - \mu_{s1} \ln (I_{02}/I_2) = 0 \qquad \text{so that,}$$

$$R = \frac{\mu_{s1}}{\mu_{s2}} = \ln (I_{01}/I_1) \,/\, \ln (I_{02}/I_2) \tag{A.4}$$

Also, from (A.3)

$$m_b (\mu_{b1}\mu_{s2} - \mu_{b2}\mu_{s1}) = \mu_{s2} \ln (I_{01}/I_1) - \mu_{s1} \ln (I_{02}/I_2)$$

Dividing by μ_{s2}

$$m_b = \left[\frac{1}{\mu_{b1} - R\,\mu_{b2}}\right] \left[\ln (I_{01}/I_1) - R \ln (I_{02}/I_2)\right] \tag{A.5}$$

BONE MINERAL CONTENT OF NORTH ALASKAN ESKIMOS

Richard B. Mazess and Warren E. Mather
Department of Radiology
University of Wisconsin Medical Center
Madison, Wisconsin 53706

Direct photon absorptiometry was used to measure the bone mineral content of Eskimo natives of the north coast of Alaska during the summers of 1968 to 1970. Preliminary analysis of this data has been reported (Mazess, 1970; Mather and Mazess, 1971, 1972).

METHODS

Direct photon absorptiometry as developed at the University of Wisconsin was used to determine the bone mineral content (Cameron and Sorenson, 1963; Sorenson and Cameron, 1967; Cameron, 1970). This method has been shown to provide precise and accurate (around 2% error) measurements (Cameron et al, 1968; Mazess et al, 1964, 1970). Moreover an absorptiometric scan at a particular site on the long bones is highly correlated ($r>0.9$) not only to the local mineral content but to the total bone weight and skeletal weight (Mazess, 1971; Horsman et al, 1970) and to total body calcium (Chestnut et al, 1973). Measurements were made with a portable system allowing immediate digital readout of bone mineral content and bone width (Mazess et al, 1972). Calibration of absorptiometric scans using an ^{125}I source (28 keV) was made with various standards including the three-chamber bone phantom of saturated dipotassium hydrogen phosphate solution (Witt et al, 1970).

Measurements of the mid-humerus and the radius and ulna (one-third of the distance up from the distal end) were made on Wainwright Eskimos in 1968 and 1969. In 1970 measurements of the radius and ulna shaft, and also the distal radius and ulna (2-cm from the end) were made in Pt. Hope and Barrow. In all cases an average of about 4 determinations was taken at each of the

scan sites on each subject. The coefficient of variation at each site was 2 to 4%, decreasing with larger bone size and smaller in adults than children. In all, 413 subjects were measured, of which 217 were children (age 5 to 19), 89 were adults (age 20-49), and 107 were elderly (over 50 years). Sixty-three of the Wainwright subjects were measured in 2 successive years, and average values were taken for these cases. For the 20 adults that had measurements in both years the correlations between the measurements were 0.94 to 0.98 for bone mineral and 0.90 to 0.93 for bone width. T-tests were done to examine differences among the villages, but most of the few significant differences were due to the highly variable bone width at the distal ulna site. Consequently the data were merged.

RESULTS

The heights and weights of the Alaskan Eskimos are given in Table 1. U.S. Whites (Mazess and Cameron, 1973; McCammon, 1970) are taller and heavier than Alaskan Eskimo males, and taller though not heavier than Eskimo females. Eskimos are, in short, about 5% smaller than Whites. Tables 2, 3, 4, 5, and 6 outline the bone mineral measurements of the Eskimos, and give their values as a percentage of U.S. white normative standards (Mazess and Cameron, 1973) where there is sufficient data available on Whites.

Eskimo bone widths were generally similar to those of Whites for most sex-age combinations except for the distal radius site where the adult Eskimos had a markedly larger bone width. Bone mineral content (BMC) was about 5 to 10% lower in Eskimo children than in Whites, but this was in part a reflection of their slightly smaller body and bone size; the Eskimo children were lower in the bone mineral-width ratio (BMC/W) by less than 5%. In young adults (20-39 years) the BMC and BMC/W were about the same as in Whites, but from age 40 on, a relative deficit of bone was evident in Eskimos. This deficit amounted to about 10 to 15% in both males and females.

DISCUSSION AND CONCLUSIONS

North Alaskan Eskimos appeared to have a relatively normal bone mineral status compared to U.S. Whites during the periods of growth and early adulthood. However, in both sexes there appeared to be an early and large loss of bone with aging, so that the older Eskimos had 10 to 15% less bone than comparable Whites. Probably the best comparison can be made at the radius midshaft site, for which the greatest amount of data is available, and here, as elsewhere, the deficit of bone mineral appeared to increase with age. During the fourth decade of life the deficit in Eskimos was about 10%, during the fifth decade it amounted to about 15%, and by the sixth decade it was almost 20%. Apparently a continuous process accompanies aging in both Eskimo males and females which accelerates and exacerbates the aging bone loss evident in so many other populations (Mazess and Cameron, 1973; Garn et al, 1967; Dequeker, 1972; Johnston et al, 1968; Smith et al, 1972). In White females there is a plateau of bone loss during the seventh decade with the rate of loss changing from the 9.5% per decade evident between 45 and 75 years to about 4.5% per decade (Mazess and Cameron, 1973). Thus White females plateau at about the bone mineral value (680 mg/cm) which discriminates between normals and osteoportics at risk of fracture (Smith and Cameron, 1973). Eskimo women reached this state of extreme demineralization during the sixth rather than the seventh decade of life, but in Eskimos there was no plateau of bone loss and demineralization continued to even greater levels. Sixty percent of Eskimo women over age sixty would be classified in the population at risk of fracture, and by age 70 virtually all Eskimo women were in this class.

These findings amplify and substantiate our previous results (Mazess, 1970) on Alaskan Eskimos and similar findings were described in a preliminary report on Canadian Eskimos (Mather and Mazess, 1972). Studies on the bones of a

modern Eskimo archeological population, the Sadlermiut Eskimo from Southampton Island at the northern border of Hudson Bay, have indicated that the Sadlermiut had normal bone composition and that the densities of bone sections and whole bones were comparable to those of U.S. Whites, however, the older group of Sadlermiut both male and female had about 10 to 15% lower bone weights and densities than the young adults (Mazess, 1966; Mazess and Jones, 1972). This is a striking concordance with the present results. Interestingly the studies of Merbs (1969) and Merbs and Wilson (1960) on the pathology of the Sadlermiut skeletons has indicated that there was a very high incidence of compression fractures. Recent investigations (Merbs and Mazess, unpublished data) have shown that bone density was correlated with compression fractures in this population. It may well be that the extensive bone loss in contemporary Eskimos will also be correlated with bone pathology including fractures and tooth loss.

The reasons for the rapid and large decline of bone in the Alaskan Eskimos is not apparent from the present data and the numerous factors implicated in aging bone loss evident in other populations may also be operative on the Eskimos (Barzel, 1970; Garn, 1970; Harris and Heaney, 1969). One obvious explanation would be the differing diet of Eskimos and the possible effects of such a diet on elderly persons.

The nutritional status of Canadian Eskimos (Davies and Hanson, 1965; Rabinovitch, 1936), and Alaskan Eskimos (Heller, 1965) has been examined. In Wainwright it has been assessed by Sauberlich et al (1972), who found anemia and marginal intakes of vitamin B_6 in children but the nutritional state was otherwise unremarkable. There is little doubt that Eskimos have a high protein diet and possibly low calcium intake which may affect calcium homeostasis and bone. Rats fed a high meat diet develop rarified bones

(Hammond and Storey, 1970) and vegetarians are known to have higher bone mineral contents during old age than omnivores (Ellis et al, 1972). It has long been known that acidosis results in increased calcium excretion and dissolution of bone (Lemann et al, 1966, 1967; Barzel, 1969; Barzel and Jowsey, 1969). On the other hand high phosphorus diets with high phosphorus-calcium ratios may increase calcium excretion and bone loss both through secondary hyperparathyroidism and even through other as yet unspecified mechanisms (Draper et al, 1972; Krishnarao and Draper, 1972; Anderson and Draper, 1972). In humans, however, the effects of phosphate seems to differ from the effects on the rat and phosphates have relatively little effect (Farquharson et al, 1931a, 1931b). and in fact phosphates are used in treatment of osteoporosis. In contrast, high protein intake, even when the acid effect is buffered or when the phosphorus is maintained constant, does increase calcium loss primarily through increased calcium excretion (Johnson et al, 1970;Walker and Linksweiler, 1972). Also vitamin D could be a factor in bone loss (Exton-Smith et al, 1966) though it is unlikely that the Eskimos are so little exposed to sunlight that they could not produce sufficient amounts for storage over the sunless winter, and there is ample supply in the animal fats, including seal oil, consumed by Eskimos. Consequently with a marginal calcium intake, the high protein diet may well be related to the high bone loss of elderly Eskimos, especially if the renal handling of an acid load should be less than adequate with advanced age. The mechanisms and consequences of this great bone loss warrant further examination, both to elucidate the particular case of the Eskimos and to throw light on the common problem of aging bone loss in other populations.

ACKNOWLEDGEMENTS

Supported by NASA-Y-NGR-50-002-051 and AEC-(11-1)-1422. Doctors Fred Milan, Steve Babcock, and John R. Cameron aided substantially. The study was part of the investigation of Circumpolar Populations, Human Adaptability Section of the International Biological Program.

REFERENCES

Anderson, G.H. and H.H. Draper 1972. Effect of dietary phosphorus on calcium metabolism in intact and parathyroidectomized adult rats. J. Nutr. 102: 1123 - 1132.

Barzel, U.S. 1969. The effect of excessive acid feeding on bone. Calc. Tiss. Res. 4: 94 - 100.

Barzel, U.S. (ed) 1970. Osteoporosis. Grune and Stratton, N.Y.

Barzel, U.S. and J. Jowsey 1969. The effects of chronic acid and alkali administration on bone turnover in adult rats. Clin. Sci. 36: 517 - 524.

Cameron, J.R. (ed) 1970. Proceedings of the Bone Measurement Conference. U.S. AEC Conf. 700515, CFSTI, Springfield, Va.

Cameron, J.R. and J.A. Sorenson 1963. Measurement of bone mineral in vivo: an improved method. Science 143: 230-232.

Cameron, J.R., R.B. Mazess, and J.A. Sorenson, 1968. Precision and accuracy of bone mineral determination by the direct photon absorptiometric method. Invest. Radiol. 3: 141 - 150.

Chestnut, C.B. III, E. Manske, D. Baylink, and W.B. Nelp 1973. Correlation of total body calcium (bone mass) and regional bone mass. Clin. Res.21: 200.

Davies, L.E.C. and S. Hanson 1965. The Eskimos of the Northwest passage: a survey of dietary composition and various blood and metabolic measurements. Canad. Med. Assoc. J. 92: 205 - 216.

Dequeker, J. 1972. Bone Loss in Normal and Pathological Condition. Leuven Univ. Press, Belgium.

Draper, H.H., T.L. Sie and J.G. Bergan 1972. Osteoporosis in aging rats induced by high phosphorus diets. J. Nutr. 102: 1133 - 1142.

Ellis, F.R., S. Holesh, and J.W. Ellis 1972. Incidence of osteoporosis in vegetarians and omnivores. Am. J. Clin. Nutr. 25: 555 - 558.

Exton-Smith, A.N., H.M. Hodkinson, and B.R. Stanton 1966. Nutrition and metabolic bone disease in old age. Lancet (Nov.): 999 - 1001.

Farquharson, R.F., W.T. Salter, D.W. Tibbets and J.C. Aub 1931a. Studies of calcium and phosphorus metabolism. XII. The effect of the ingestion of acid-producing substances. J. Clin. Invest. 10: 221 - 249.

Farquharson, R.F., W.T. Salter and J.C. Aub, 1931b. Studies of calcium and phosphorus metabolism. XIII. The effects of ingetstion of phosphates on the excretion of calcium. J. Clin. Invest. 10: 251 - 269.

Garn, S.M. 1970. The Earlier Gain and the Later Loss of Cortical Bone. C.C. Thomas, Springfield.

Garn, S.M., C.G. Rohmann and B. Wagner 1967. Bone loss as a general phenomenon in man. Fed. Proc. 26: 1729 - 1736.

Harris, W.H. and R.P. Heaney 1969. Skeletal renewal and metabolic bone disease. New Eng. J. Med. 280: 193 -202, 253 - 259, and 303 - 311.

Hammond, R.H. and E. Storey 1970. Measurement of growth and resoption of bone in rats fed mead diet. Calc. Tiss. Res. 4: 291-304.

Heller, C.A. 1965. The diet of some Alaskan Eskimos and Indians. J. Am. Dietetic Assoc. 45: 425 - 428.

Horsman, A., L. Bulusu, H.B. Bentley and B.E.C. Nordin 1970. Internal relationships between skeletal parameters in twenty-three male skeletons: In: J.R. Cameron (ed) Proc. Bone Measurement Conference. U.S. Atomic Energy Comm. Conf. 700515; U.S. Dept. of Commerce, Springfield, Va. pp. 365 - 382.

Johnson, N.E., E.N. Alcantaram and H. Linksweiler 1970. Effect of level of protein intake on urinary and fecal calcium and calcium retention in young adult males. J. Nutr. 100: 1425.

Johnston, C.C., D.M. Smith,P.L. Yu and W. P. Deiss Jr. 1968. In vivo measurement of bone mass in the radius. Metabolism. 17: 1140 - 1153.

Krishnarao and H.H. Draper 1972. Influence of dietary phosphate on bone resorption in senescent mice. J. Nutr. 102: 1143 - 1146.

Lemann, J. Jr., J.R. Litzow and E.J. Lennon 1966. The effects of chronic acid loads in normal man: Further evidence for the participation of bone mineral in the defense against chronic metabolic adidosis. J. Clin. Invest. 45: 1608 - 1614.

Lemann, J. Jr., J.R. Litzow, E.J. Lennon, and D.A. Kelley 1967. Studies of the mechanism by which chronic metabolic acidosis augments urinary calcium excretion in man. J. Clin. Invest. 46: 1318 - 1328.

Mather, W.E. and R. B. Mazess 1971. Bone mineral content of the Eskimos of Point Hope and Barrow: Preliminary report. Ann. Prog. Report Bone Mineral Lab. AEC # COO-1422-103.

Mather, W. and R.B. Mazess 1972. Bone mineral content of Eskimos in Alaska and Canada: Preliminary Report. Annual Progress Report Bone Mineral Lab. AEC # COO-1422-123.

Mazess, R.B. 1966. Bone density in Sadlermiut Eskimo. Human Biol. 38: 42 - 49.

Mazess, R.B. 1970. Bone mineral content in Wainwright Eskimo: Preliminary report. Arctic Anthropology 7: 114 - 117.

Mazess, R.B. 1971. Estimation of bone and skeletal weight by direct photon absorptiometry Invest. Radiol. 6: 52 - 60.

Mazess, R.B. and J.R. Cameron 1973. Bone mineral content in normal subjects. Annual Progress Report Bone Mineral Lab. AEC # COO-1422-142.

Mazess, R.B. and R. Jones 1972. Weight and density of Sadlermiut Eskimo long bones. Human Biology. 44: 537 - 548.

Mazess, R.B., J. R. Cameron and H. Miller 1972. Direct readout of bone mineral content using radionuclide absorptiometry. Intern. J. Appl. Rad. Isot. 23: 471 - 479.

Mazess, R.B., J.R. Cameron, R. O'Connor, and D. Knutzen 1964. Accuracy of bone mineral measurement. Science. 145: 388 - 389.

Mazess, R.B., J.R. Cameron and J.A. Sorenson 1970. A comparison of radiological methods for determining bone mineral content. In: G.D. Whedon and J.R. Cameron (eds) Progress in Methods of Bone Mineral Measurement (pp. 455 - 479), U.S. Dept. Health, Educ. and Welfare, Supt. of Documents, Washington, D.C.

McCammon, R.W. 1970. Human Growth and Development. C.C. Thomas, Springfield.

Merbs, C.F. 1969. Patterns of Activity-Induced Pathology in a Canadian Eskimo Isolate. Ph.D. Thesis in Anthropology, Univ. of Wisc.

Merbs, C.F. and W.H. Wilson 1960. Anomalies and pathologies of the Sadlermiut Eskimo vertebral column. National Museum of Canada Bull. 180, Contrib. Anthrop. 1960, Part 1: ;54 - 180.

Rabinowitch, I.M. 1936. Clinical and other observations on Canadian Eskimos in the Eastern Arctic. Canad. Med. Assoc. J. 34: 487 - 501.

Sauberlich, H.E., W. Goad, Y.F. Herman, F. Milan, and P. Jamison 1972. Biochemical assessment of the nutritional status of the Eskimos of Wainwright, Alaska. Am. J. Clin. Nutr. 25: 437 - 445.

Smith, E. and J.R. Cameron, 1973. A proposed quantitative definition of osteoporosis. (submitted)

Smith, D.M., C.C. Johnston and P.L. Yu 1972. In vivo measurement of bone mass. J. A. M. A. 219: 325 - 329.

Sorenson, J.A. and J.R. Cameron 1967. A reliable in vivo measurement of bone mineral content. J. Bone Jt. Surg. 49-A: 481 - 497.

Walker, R.M. and H.M. Linksweiler 1972. Calcium retention in the adult human male as affected by protein intake. J. Nutr. 102: 1297 - 1302.

Witt, R.M., R.B. Mazess, and J.R. Cameron. Standardization of bone mineral measurements. In: J.R. Cameron (ed) Proc. Bone Measurement Conference, U.S. AEC Conf. 700515, CFSTI Springfield, Va.

			HEIGHT (cm)				WEIGHT (kg)			
MALES	AGE	N	X	SD	CV	%	X	SD	CV	%
	5-7	23	116.9	5.3	4.6	93.2	23.3	2.8	12.1	93.9
	8-9	19	129.8	7.5	5.8	94.1	30.4	5.1	16.8	97.3
	10-11	22	140.1	7.4	5.3	95.6	35.2	5.4	15.4	95.6
	12-14	20	151.0	8.9	5.9	94.0	47.5	10.8	22.7	94.8
	15-16	9	162.9	5.6	3.5	92.6	55.1	6.5	11.8	81.6
	17-19	15	171.0	8.5	5.0	94.9	69.7	7.0	10.0	91.5
	20-29	16	168.6	4.7	2.8	94.2	70.0	6.5	9.3	91.7
	30-39	17	167.7	7.1	4.2	93.4	67.4	10.1	15.0	84.5
	40-49	7	166.9	6.8	4.1	94.3	67.9	8.9	13.0	86.2
	50-59	13	166.1	4.0	2.4	93.6	74.6	11.6	15.5	93.8
	60-69	27	163.2	4.8	2.9	93.1	67.7	12.9	19.0	89.2
	70+	13	163.0	4.8	2.9	93.2	69.8	12.6	18.1	94.2
FEMALES	5-7	26	119.5	7.5	6.3	94.4	24.8	5.8	23.4	102.3
	8-9	22	123.0	5.9	4.6	93.9	28.9	3.9	13.7	97.6
	10-11	17	139.7	7.7	5.5	95.5	37.3	8.2	21.9	100.2
	12-14	22	151.8	6.5	4.3	93.3	53.1	11.1	21.6	107.9
	15-16	10	157.4	3.8	2.4	94.6	58.7	6.6	11.3	104.6
	17-19	12	157.6	4.6	2.9	95.3	59.8	5.3	8.8	102.4
	20-29	14	157.1	5.6	3.5	96.0	60.8	12.7	20.9	104.6
	30-39	19	155.1	6.0	3.9	94.0	63.6	14.2	22.3	97.5
	40-49	16	152.3	7.6	5.0	95.0	65.5	15.9	24.2	102.6
	50-59	23	153.3	7.7	5.0	95.2	62.4	11.5	18.5	97.8
	60-69	20	152.8	5.6	3.7	96.0	65.5	15.4	23.6	104.3
	70+	11	141.3	10.2	7.2	89.3	48.6	10.7	22.0	77.6

Table 1: Morphology of Alaskan Eskimo children and adults. The Eskimo values as a percent of white values are given.

			MINERAL (mg/cm)				WIDTH (m x 10^{-5})				M/W			
MALES	AGE	N	X	SD	CV	%	X	SD	CV	%	X	SD	CD	%
	5-7	23	462	73	15.9	92.9	1006	203	20.2	102.0	.466	.061	13.0	92.8
	8-9	19	536	71	13.3	92.6	1005	117	11.6	96.1	.533	.045	8.6	96.4
	10-11	22	626	90	14.4	93.7	1086	93	8.5	96.3	.574	.060	10.5	96.9
	12-14	20	760	138	18.1	93.1	1189	137	11.5	94.7	.636	.060	9.4	98.1
	15-16	9	926	87	9.4	84.5	1293	87	6.7	103.0	.715	.050	7.0	94.1
	17-19	15	1163	130	11.8	94.2	1411	95	6.7	97.8	.823	.059	7.1	98.4
	20-29	16	1273	155	12.2	97.4	1497	157	10.5	101.4	.852	.088	10.4	96.3
	30-39	17	1200	117	9.7	90.8	1458	110	7.6	98.6	.823	.066	8.0	91.9
	40-49	7	1171	91	7.8	89.8	1514	128	8.4	101.9	.774	.061	7.8	87.9
	50-59	13	1125	96	8.5	85.7	1508	119	7.9	101.3	.748	.072	9.6	85.0
	60-69	27	1017	160	15.7	82.9	1499	160	10.6	95.5	.680	.100	14.7	86.1
	70+	13	1058	103	9.7	84.2	1530	148	9.6	98.5	.693	.063	9.1	85.4
FEMALES	5-7	26	437	72	16.4	101.8	922	151	16.4	101.2	.475	.056	11.9	97.5
	8-9	22	483	53	11.0	92.3	929	121	12.4	97.3	.497	.054	11.0	90.7
	10-11	17	558	70	12.6	92.1	958	104	10.9	92.6	.582	.040	6.9	99.6
	12-14	22	762	129	16.9	96.7	1115	135	12.1	95.9	.681	.078	11.4	100.4
	15-16	10	848	50	5.8	97.0	1184	103	8.7	98.7	.718	.045	6.3	98.5
	17-19	12	878	100	11.4	95.7	1192	154	12.9	97.5	.738	.049	6.6	98.4
	20-29	14	889	108	12.1	93.4	1166	144	12.3	94.8	.764	.055	7.2	98.7
	30-39	19	928	127	13.7	92.8	1262	168	13.3	96.8	.736	.059	8.0	95.7
	40-49	16	883	124	14.1	90.4	1273	125	10.0	98.1	.693	.066	9.5	90.8
	50-59	23	782	140	17.8	88.4	1282	118	9.2	102.4	.609	.081	13.4	86.3
	60-69	20	685	112	16.4	89.1	1278	144	11.3	101.5	.536	.072	13.5	87.9
	70+	11	507	131	25.9	70.2	1264	78	6.2	100.7	.399	.090	22.5	69.4

Table 2: Bone mineral measurements of the shaft of the radius of Alaskan Eskimo children and adults. The Eskimo values as a percent of white values are given.

			MINERAL (mg/cm)				WIDTH (m x 10^{-5})				M/W			
MALES	AGE	N	X	SD	CV	%	X	SD	CV	%	X	SD	CV	%
	5-7	23	402	71	17.5	99.5	906	129	14.3	105.8	.443	.041	9.4	93.8
	8-9	19	456	84	18.4	95.6	928	149	16.1	99.8	.490	.050	10.2	95.3
	10-11	22	543	94	17.3	98.0	1012	107	10.6	105.2	.535	.064	12.0	92.7
	12-14	20	661	111	16.7	100.3	1062	114	10.7	102.7	.618	.058	9.3	97.3
	15-16	9	817	62	7.6	89.0	1162	95	8.2	96.7	.706	.073	10.4	92.4
	17-19	15	1005	126	12.6	97.2	1167	70	6.0	92.6	.859	.085	9.8	103.9
	20-29	16	1060	119	11.3	--	1205	90	7.4	--	.877	.069	7.8	--
	30-39	17	1067	135	12.7	--	1189	81	6.8	--	.895	.083	9.3	--
	40-49	7	1032	85	8.2	--	1223	84	6.9	--	.844	.053	6.3	--
	50-59	13	1066	132	12.4	--	1308	102	7.8	--	.815	.072	8.8	--
	60-69	27	930	181	19.5	--	1235	136	11.0	--	.751	.111	14.7	--
	70+	13	946	125	13.2	--	1251	82	6.6	--	.755	.075	9.9	--
FEMALES	5-7	26	371	63	16.7	100.8	826	80	9.7	103.1	.455	.055	12.0	98.9
	8-9	22	412	58	14.0	92.0	865	94	10.9	100.6	.477	.053	11.2	90.8
	10-11	17	480	60	12.6	95.4	862	117	13.6	94.8	.558	.046	8.2	101.8
	12-14	22	642	117	18.2	--	958	107	11.1	--	.669	.093	13.9	--
	15-16	10	752	45	6.0	--	1043	69	6.6	--	.721	.045	6.3	--
	17-19	12	767	98	12.8	--	1011	95	9.4	--	.759	.070	9.2	--
	20-29	14	793	65	8.2	94.0	980	87	8.9	91.2	.810	.057	7.1	102.4
	30-39	19	815	88	10.7	93.9	1024	102	9.9	92.4	.797	.076	9.5	100.4
	40-49	16	811	90	11.2	93.4	1106	118	10.6	99.8	.734	.058	8.0	92.4
	50-59	23	712	148	20.8	88.5	1096	112	10.2	99.2	.646	.093	14.4	88.7
	60-69	20	647	105	16.3	92.2	1110	129	11.6	100.0	.585	.093	15.9	93.6
	70+	11	462	133	28.9	75.4	1037	109	16.5	94.0	.442	.106	23.9	78.6

Table 3: Bone mineral measurements of the shaft of the ulna of Alaskan Eskimo children and adults. The Eskimo values as a percent of white values are given.

			MINERAL (mg/cm)				WIDTH (m x 10^{-5})				M/W			
MALES	AGE	N	X	SD	CV	%	X	SD	CV	%	X	SD	CV	%
	5-7	9	974	147	15.1	90.4	1384	115	8.3	95.2	.701	.082	11.8	94.5
	8-9	10	1138	153	13.4	88.2	1535	125	8.1	96.5	.737	.056	7.6	90.8
	10-11	8	1432	168	11.7	95.5	1699	117	6.9	97.4	.840	.059	7.0	97.8
	12-14	7	1773	256	14.4	97.5	1883	90	4.8	97.7	.937	.116	12.4	99.4
	15-16	3	1982	276	13.9	80.6	1987	46	2.3	90.3	.995	.122	12.3	89.3
	17-19	8	2518	316	12.5	86.6	2110	81	3.8	92.0	1.191	.133	11.1	94.1
	20-29	12	2760	327	11.8	99.8	2157	160	7.4	93.6	1.279	.122	9.5	106.6
	30-39	10	2840	393	13.8	103.9	2256	140	6.2	98.1	1.254	.125	10.0	105.5
	40-49	4	2748	349	12.7	100.6	2145	126	5.9	92.6	1.279	.143	11.1	108.3
	50-59	3	2763	233	8.4	99.4	2213	193	8.7	94.4	1.259	.196	15.6	105.9
	60-69	9	2336	472	20.2	90.6	2228	92	4.1	96.9	1.047	.201	19.2	93.3
	70+	--	--	--	--	--	--	--	--	--	--	--	--	--
FEMALES	5-7	12	917	146	16.0	93.5	1309	112	8.5	92.4	.696	.069	10.0	100.2
	8-9	9	1015	137	13.5	86.6	1433	92	6.4	93.0	.706	.090	12.8	92.9
	10-11	9	1106	154	13.9	87.6	1519	63	4.2	95.0	.727	.099	13.6	92.5
	12-14	14	1635	278	17.0	97.2	1771	169	9.6	97.0	.920	.116	12.6	100.1
	15-16	5	1898	167	8.8	100.1	1812	151	8.3	96.6	1.045	.054	5.2	103.5
	17-19	4	1724	226	13.1	87.0	1852	123	6.6	98.4	.929	.099	10.7	88.5
	20-29	6	1820	215	11.8	86.7	1817	93	5.1	91.4	.988	.067	6.8	93.6
	30-39	9	2001	257	12.9	94.5	1902	191	10.0	96.6	1.052	.104	9.8	89.9
	40-49	4	1911	206	10.8	91.8	1917	67	3.5	95.2	.993	.075	7.6	92.1
	50-59	4	1570	184	11.7	86.7	1845	130	7.1	95.1	.855	.137	16.1	90.7
	60-69	--	--	--	--	--	--	--	--	--	--	--	--	--
	70+	--	--	--	--	--	--	--	--	--	--	--	--	--

Table 4: Bone mineral measurements of the midshaft of the humerus of Alaskan Eskimo children and adults. The Eskimo values as a percent of white values are given.

			MINERAL (mg/cm)				WIDTH (m x 10^{-5})				M/W			
MALES	AGE	N	X	SD	CV	%	X	SD	CV	%	X	SD	CV	%
	5-7	14	478	86	18.0	--	1464	194	13.2	--	.326	.043	13.1	--
	8-9	9	554	80	14.5	--	1592	269	16.9	--	.349	.019	15.4	--
	10-11	14	608	80	13.2	--	1740	164	9.4	--	.349	.039	11.1	--
	12-14	13	769	207	26.9	--	1917	489	25.5	--	.407	.072	17.6	--
	15-16	6	1007	225	22.3	--	2459	501	20.4	--	.409	.033	8.0	--
	17-19	7	1397	248	17.7	--	2701	391	14.5	--	.517	.068	13.1	--
	20-29	4	1568	179	11.4	113.1	3020	391	13.0	128.9	.523	.069	13.2	87.2
	30-39	7	1433	185	12.9	108.8	2702	221	8.2	118.3	.530	.058	11.0	90.1
	40-49	3	1308	238	18.2	100.8	3300	171	5.2	152.6	.395	.062	15.7	65.0
	50-59	19	935	218	23.3	70.3	2382	362	15.2	108.2	.397	.097	24.4	64.6
	60-69	18	1052	209	19.9	88.3	2712	335	12.3	114.8	.394	.098	24.8	76.3
	70-81	10	1029	190	18.4	86.7	2535	396	15.6	108.8	.410	.075	18.2	76.5
FEMALES	5-7	14	423	67	15.8	--	1305	180	13.8	--	.326	.048	14.8	--
	8-9	13	438	80	18.2	--	1442	271	18.8	--	.307	.044	14.5	--
	10-11	8	539	83	15.4	--	1561	297	19.1	--	.357	.087	24.3	--
	12-14	8	712	185	25.9	--	2014	346	17.2	--	.352	.058	16.5	--
	15-16	5	881	182	20.6	--	2352	90	3.8	--	.373	.066	17.7	--
	17-19	8	969	153	15.8	--	2121	513	24.2	--	.473	.092	19.5	--
	20-29	8	1080	191	17.7	109.7	2435	480	19.7	131.1	.449	.060	13.4	83.3
	30-39	10	964	163	16.9	100.9	2404	423	17.6	147.0	.468	.079	16.9	83.0
	40-49	12	1042	162	15.6	111.7	2364	256	10.8	121.0	.444	.069	15.6	89.1
	50-59	10	1213	255	21.0	136.9	2847	348	12.2	153.5	.428	.090	21.0	88.8
	60-69	18	696	161	23.2	93.8	2256	368	16.3	118.6	.315	.088	27.9	78.3
	70-82	11	472	146	30.9	65.7	1830	457	24.9	100.5	.263	.084	31.9	65.9

Table 5: Bone mineral measurements of the distal radius of Alaskan Eskimo children and adults. The Eskimo values as a percent of white values are given.

			MINERAL (mg/cm)				WIDTH (m x 10^{-5})				M/W			
MALES	AGE	N	X	SD	CV	%	X	SD	CV	%	X	SD	CV	%
	5-7	14	271	54	19.9	--	876	103	11.8	--	.311	.055	17.6	--
	8-9	9	305	57	18.7	--	915	181	19.7	--	.336	.033	9.9	--
	10-11	14	330	49	14.9	--	945	108	11.5	--	.351	.050	14.5	--
	12-14	13	415	87	21.1	--	1045	220	21.1	--	.400	.066	16.6	--
	15-16	6	520	82	15.8	--	1191	147	12.3	--	.436	.044	10.2	--
	17-19	7	712	142	20.0	--	1319	273	20.7	--	.544	.078	14.3	--
	20-29	4	847	103	12.1	--	1423	241	17.0	--	.598	.034	5.7	--
	30-39	7	1432	185	13.0	--	1140	116	10.2	--	.630	.046	7.3	--
	40-49	4	699	54	7.7	--	1285	110	8.5	--	.545	.038	6.9	--
	50-59	10	656	125	19.1	--	1242	126	10.2	--	.532	.110	20.6	--
	60-69	18	563	118	20.9	--	1196	136	11.4	--	.472	.086	18.3	--
	70-81	10	514	81	15.7	--	1133	159	14.1	--	.455	.053	11.6	--
FEMALES	5-7	14	234	35	15.0	--	776	88	11.4	--	.303	.048	15.8	--
	8-9	13	236	35	14.7	--	831	114	13.7	--	.287	.046	16.2	--
	10-11	8	307	64	20.9	--	876	87	10.0	--	.355	.092	26.1	--
	12-14	8	368	71	19.4	--	1057	149	14.1	--	.348	.052	14.9	--
	15-16	5	465	91	19.6	--	1171	211	18.1	--	.406	.098	24.2	--
	17-19	8	503	76	15.1	--	1091	251	23.0	--	.476	.095	20.0	--
	20-29	8	528	98	18.7	103.3	1089	207	19.0	109.0	.494	.099	20.0	96.7
	30-39	10	483	70	14.6	96.7	1042	125	12.0	103.3	.468	.079	16.9	92.3
	40-49	12	503	118	23.4		1052	118	11.2		.479	.099	20.6	
	50-59	19	470	102	21.7	103.9	1098	129	11.8	113.1	.427	.071	16.6	91.0
	60-69	18	333	75	22.6	91.5	1012	130	12.9	101.2	.332	.079	23.9	90.7
	70-81	11	220	74	33.8	66.7	889	259	29.1	85.6	.254	.066	26.3	79.9

Table 6: Bone mineral measurements of the distal ulna of Eskimo children and adults. The Eskimo values as a percent of white values are given.

THE BONE MINERAL AND SOFT TISSUE COMPOSITION OF THE SIEMENS-REISS REFERENCE STEP WEDGES

(A PRELIMINARY REPORT, AUGUST 6, 1973)

by

R. H. Jurisch, R. M. Witt and J. R. Cameron

Departments of Radiology and Physics
University of Wisconsin
Madison, Wisconsin

Four epoxy resin step wedges containing different concentrations of hydroxyapatite, HA, were constructed by Siemens and were sent to our laboratory by Dr. Reiss for measurement. These step wedges represent a reference system for the determination of the mineral content in the skeleton. This report represents the preliminary results of our evaluation of these reference step wedges and should not be interpreted as final estimates for the bone mineral and soft tissue composition of these step wedges. The "bone mineral content", BMC, and the "soft tissue content", STC, of these four step wedges were determined by the dichromatic attenuation technique. The apparatus and the method of measurement were the same as those used by Judy (1971). The photon sources were ^{125}I (28 keV) and ^{241}Am (60 keV). The diameter of the collimating aperature on the detector was 6.4 mm and was chosen to minimize repositioning error which may be due to local spacial variations in the composition of the step wedge. A total of 250,000 counts were collected for each point measurement. All count rates were corrected for count loss errors from experimentally estimated dead times of the counting system. The dead times were 4.2 μsec for the Differential Mode, of the pulse height analyzer, PHA, used to count ^{125}I, and 3.6 μsec for the Integral Mode of the PHA used to count ^{241}Am.

The BMC and STC were calculated from modified forms of the dual photon equations, and were expressed as follows:

$$m_{BM} = \frac{1}{\mu_{BM1} - A\,\mu_{BM2}} \left[\log(I_{01}/I_1) - A\log(I_{02}/I_2) \right]$$

$$m_{ST} = \frac{1}{\mu_{ST2}(u_{BM1} - A\mu_{BM2})} \left[-\mu_{BM2}\log(I_{01}/I_1) + \mu_{BM1}\log(I_{02}/I_2) \right]$$

where,

m = distance of matter traversed expressed in mass per unit area

μ = mass attenuation coefficient

I_0 = unattenuated intensity

I = transmitted intensity

$A = \mu_{ST1}/\mu_{ST2}$, ratio of the mass attenuation coefficients for the soft tissue component for the two energies.

The subscript 1 refers to ^{125}I as the photon source and the subscript 2 refers to ^{241}Am as the photon source.

The mass attenuation coefficients for bone mineral, which was assumed to be HA, were obtained from a tabulation of mass attenuation coefficients for various compounds (Judy, 1970). The values for μ_{BM1} and μ_{BM2} were 2.59 cm^2/g and 0.408 cm^2/g, respectively. The value for A was calculated by setting the equation for BMC to zero for Wedge I, which has zero concentration of HA. The value chosen for A was 1.505 and represented an average of the A values for two of the steps which gave the best overall agreement with the assigned HA values for all four wedges. To calculate the STC, the mass attenuation coefficient of the epoxy must be determined independently for ^{241}Am. This mass attenuation coefficient of the epoxy resin was determined by measuring its half-value layer with Wedge I and was 0.1982 cm^2/g.

The measured and assigned values for BMC were tabulated and compared, Table 1. The expected BMC values were those supplied with the wedges. The measured and assigned values for the soft tissue content were also tabulated, Table 2. Only the expected values for the soft tissue content for Wedge I are given and these values were estimated from its dimensions and measured density of 1.16 g/cm^3.

For almost all of the steps of the four wedges, the difference between the measured and assigned values for BMC was less than one percent. Differences larger than 1 percent were observed for steps in Wedge II. These differences are dependent upon the value chosen for A. The values measured for A as well as all the detected count rates were dependent upon the count loss correction. Because the measured dead times for the detection system were large ($\sim$4 μsec) and were dependent upon the incident count rates, the count loss corrections probably represent the largest inaccuracies in these measurements. Sufficient data exist to make better estimates of the dead times of the counting system. With more accurate estimates of the count loss

corrections, a better estimate of the value of the constant A can be made which then will be independent of the assumption that the measured results agree with the assigned BMC values.

A second systematic error which appeared in these dichromatic measurements of BMC with ^{125}I and ^{241}Am is the decrease in the measured BMC for large values of BMC. This decrease in BMC is due to hardening of the ^{125}I beam (Sandrik and Judy, 1973). An independent set of single photon measurements of the BMC were made with the ^{125}I photon source filtered with approximately 0.051 mm of tin. The estimated decrease in the BMC for step 5 of Wedge IV was approximately 2.5 percent and approximately agreed with the 1.6 percent decrease in BMC of this step when measured with the dichromatic technique. Therefore, even if a more accurate estimate were obtained for the count rate correction, for large values of BMC, the measured BMC values still would be less than the assigned BMC for the thicker steps in the wedges.

References

1. Judy, P. R. A Dichromatic Attenuation Technique for the In Vivo Determination of Bone Mineral Content. Ph.D. Thesis, University of Wisconsin, Madison, Wisconsin, 1971.

2. Judy, P. R. Private Communication. 1970.

3. Sandrik, J. M. and Judy, P. F. Effects of the Polyenergetic Character of the Spectrum of ^{125}I on the Measurement of Bone Mineral Content. Invest. Radiol. 8, No. 3:143, 1973.

Table 1, Bone Mineral Content, g/cm^2

	Step 1			Step 2			Step 3			Step 4			Step 5		
Wedge	Measured BMC	Assigned BMC	Ratio	Measured BMC	Assigned BMC	Ratio	Measured BMC	Assigned BMC	Ratio	Measured BMC	Assigned BMC	Ratio	Measured BMC	Assigned BMC	Ratio
I	-.005	0.0	-	-.002	0.0	-	.000	0.0	-	.000	0.0	-	.005	0.0	-
II	.063	.051	1.25	.108	.102	1.07	.154	.152	1.01	.210	.203	1.04	.272	.254	1.08
III	.198	.198	1.00	.397	.395	1.01	.593	.592	1.00	.800	.790	1.01	.990	.988	1.00
IV	.366	.381	0.96	.753	.762	0.99	1.134	1.144	0.99	1.507	1.525	0.99	1.861	1.906	0.98

Table 1: The measured and assigned values of Bone Mineral Content in units of g/cm^2 and the ratio of the measured to the assigned values of BMC of the Siemens-Reiss Reference Step Wedges.

Table 2, Soft Tissue Content, g/cm^2

Step	Wedge I Measured STC	Wedge I Assigned STC	Wedge I Ratio	Wedge II Measured STC	Wedge III Measured STC	Wedge IV Measured STC
1	.611	.581	1.05	.635	.680	.627
2	1.184	1.162	1.02	1.254	1.202	1.085
3	1.767	1.743	1.01	1.825	1.734	1.545
4	2.338	2.323	1.01	2.359	2.161	1.975
5	2.900	2.904	1.00	2.900	2.661	2.406

COO-1422-151

The Expected Precision of Dual-Photon-Absorptiometry for Fat-Lean Composition

by

James Hanson
Department of Radiology
University of Wisconsin Medical Center
Madison, Wisconsin

Introduction

A dual photon absorptiometry technique has been applied to bone mineral and soft tissue determinations (Judy '71, Roos '70) and fat and lean tissue determinations (Mazess '70, '72, Preuss '72, Sorenson '64). A mathematical analysis was performed to determine 1) the optimum pair of photon energies and 2) the expected precision of the determination of the fat fraction of a fat and lean system using a dual photon absorptiometry technique.

The attenuation of two photons of energies E_1 and E_2, by a fat and lean system, is

$$I_1 = I_{0,1} \exp -(\mu_{Fat,1} m_{FaT} + \mu_{Lean,1} m_{Lean}) \quad (1a)$$

$$I_2 = I_{0,2} \exp -(\mu_{Fat,2} m_{FaT} + \mu_{Lean,2} m_{Lean}) \quad (1b)$$

where $I_{0,1}$ and $I_{0,2}$ are the unattenuated intensities and I_1 and I_2 are the transmitted intensities at energies E_1 and E_2 respectively, $\mu_{fat,1}$, $\mu_{fat,2}$ and $\mu_{lean,1}$, $\mu_{lean,2}$ are the attenuation coefficients for fat and leat at the energies E_1 and E_2 and m_{fat} and m_{lean} are the mass of matter (g/cm^2) traversed by the photon beam. If the attenuation coefficients are known, equations 1a and 1b can be used to calculate the mass, in units of g/cm^2, of each component.

As shown by Sorenson '64 and Preuss '72, a ratio, R, can be determined solely from the intensities (expressed by a ratio) as follows,

$$R = \frac{\ln \frac{I_{0,1}}{I_1}}{\ln \frac{I_{0,2}}{I_2}} = \frac{\mu_{Fat,1} m_{FaT} + \mu_{Lean,1} m_{Lean}}{\mu_{Fat,2} m_{FaT} + \mu_{Lean,2} m_{Lean}} . \quad (2)$$

Defining y, the fraction of fat as

$$y \equiv \frac{m_{FaT}}{m_{FaT} + m_{Lean}} \quad (3)$$

we can rewrite equation 2 as

$$R = \frac{(\mu_{Fat,1} - \mu_{Lean,1})y + \mu_{Lean,1}}{(\mu_{Fat,2} - \mu_{Lean,2})y + \mu_{Lean,2}} . \quad (4)$$

At energies greater than approximately 50 kev, for materials of low atomic number ($Z \sim 8$), the attenuation process is primarily Compton interactions, which are only dependent on the electron densities of the materials. Since the electron densities are nearly equal for all materials, for these higher photon energies, the attenuation coefficient of fat tissue will approximately equal the attenuation coefficient of lean tissue. If the photon energy E_2 is picked such that $\mu_{fat,2} \approx \mu_{lean,2}$, then equation 4 becomes

$$R = \frac{(\mu_{Fat,1} - \mu_{Lean,1})y + \mu_{Lean,1}}{\mu_{Lean,2}} \quad (5)$$

which gives a linear relation between R, the measured value, and the fraction of fat.

In order to determine the sensitivity of the measured R value on the fraction of fat, we take the derivative of R with respect to y, which gives

$$\frac{dR}{dy} = \frac{\mu_{Fat,1} - \mu_{Lean,1}}{\mu_{Lean,2}} \quad (6)$$

This expresses the rate of change of the measured R value as a function of the fraction of fat. By picking the photon energy E_1 to give the largest absolute value of the numerator the derivative will be maximized. The greater the difference in attenuation coefficients of fat and lean for E_1, the more sensitive the measured R value will be to the fraction of fat.

Photon energies which give maximum differences in attenuation coefficients are in the range of 15 to 35 kev where the photoelectric effect dominates. The lower limit of the energy E_1, is determined by the fact that as the difference in attenuation coefficients increases, the value of the attenuation coefficients also increases, which will cause a reduction of the transmitted beam with an increase in error due to counting statistics. Above 35 kev, R becomes very insensitive to the actual fraction of fat present because of the small difference in the attenuation coefficients for fat and lean tissue.

The sensitivity of R to the actual percent fat can be increased by picking photon energy E_2 to give the smallest value possible for the denominator of equation 6. Since the attenuation coefficients decrease with increasing energy, the denominator will be minimized for a large photon energy.

Standard Deviation of Fraction of Fat as a Function of Energy Pairs

The optimum pair of photon energies to determine the total mass of fat can be choosen from an examination of the standard deviation of the mass of fat measured as a function of the photon energy pair.

In the general case of $x = f(u,v)$ the propagation of errors in terms of the variance becomes

$$\sigma_x^2 = \left(\frac{\partial x}{\partial u}\right)^2 \sigma_u^2 + \left(\frac{\partial x}{\partial v}\right)^2 \sigma_v^2 \qquad (7)$$

where u and v are uncorrelated parameters. (Bevington '69). From equation 1 the variance of R becomes

$$\sigma_R^2 = \left(\frac{\partial R}{\partial I_{o,1}}\right)^2 \sigma_{I_{o,1}}^2 + \left(\frac{\partial R}{\partial I_1}\right)^2 \sigma_{I_1}^2 + \left(\frac{\partial R}{\partial I_{o,2}}\right)^2 \sigma_{I_{o,2}}^2 + \left(\frac{\partial R}{\partial I_2}\right)^2 \sigma_{I_2}^2 \qquad (8)$$

where $\sigma_{I_{o,1}}^2 = I_{o,1}$; $\sigma_{I_1}^2 = I_1$; $\sigma_{I_{o,2}}^2 = I_{o,2}$; $\sigma_{I_2}^2 = I_2$

due to Poisson statistics. Solving equation 8 in terms of the attenuation coefficients gives

$$\sigma_R^2 = \frac{1}{I_{o,1} T^2}\left[\left(1 + \exp(D)\right) + K\left(\frac{D}{T}\right)^2\left(1 + \exp(T)\right)\right] \qquad (9)$$

where K is the ratio of $I_{0,1}$ to $I_{0,2}$ and

$$D = \mu_{Fat,1}\, m_{Fat} + \mu_{Lean,1}\, m_{Lean}$$

$$T = \mu_{Fat,2}\, m_{Fat} + \mu_{Lean,2}\, m_{Lean}$$

Using equation 5 to express the fractional composition of fat, y, as

$$y = \frac{R - \frac{\mu_{Lean,1}}{\mu_{Lean,2}}}{\frac{\mu_{Fat,1}}{\mu_{Lean,2}} - \frac{\mu_{Lean,1}}{\mu_{Lean,2}}} \qquad (10)$$

and following the form of equation 7 gives

$$\sigma_g^2 = \left(\frac{\partial g}{\partial R}\right)^2 \sigma_R^2 \tag{11}$$

$$\sigma_g^2 = \left(\frac{1}{\frac{\mu_{Fat,1}}{\mu_{Lean,2}} - \frac{\mu_{Lean,1}}{\mu_{Lean,2}}}\right)^2 \sigma_R^2 \tag{12}$$

where σ_R^2 is the result of equation 9. Now the estimate of the standard deviation of the fraction of fat is

$$\text{Standard deviation} = \sqrt{\sigma_g^2} \quad . \tag{13}$$

This expresses the estimate of the standard deviation as a function of attenuating coefficients, and the initial intensities $I_{0,1}$ and $I_{0,2}$.

A computer program was written to calculate equation 13 for energy pairs between 10 and 100 kev in increments of 1.0 kev. Total initial counts were set at 10^6 for both energies and the total soft tissue was 5.0 g/cm^2 with 15% fat composition. Figure 1 shows a graph of the calculated standard deviation of the fraction of fat versus the high photon energy for a family of curves representing the lower photon energy. As the lower energy decreased from 100 to 20 kev, the standard deviation decreased. A decrease in the lower energy is accompanied with an increase in the difference between the attenuation coefficients of fat and lean tissue which increases the sensitivity of R. Below 20 kev, the standard deviation increased. This is due to the fact that the attenuation becomes so large that the transmitted beam is substantially reduced, which causes an increase in the standard deviation due to Poisson statistics. As the higher photon energy increases, the standard deviation in the fat mass decreases. However, at energies above 70 kev, the rate of decrease is less than for energies below 70 kev. This leveling off is due to the slow rate of change of attenuation coefficients in the region.

The results of Figure 1 can be used to determine the usefulness of certain radionuclides in determining the fat-lean ratio of a system. Figure 2 shows the standard deviation of the fraction of fat versus the lower photon energy for two common higher photon energies. The higher energies are represented by the energies of the ^{125}I and ^{241}Am combination and ^{109}Cd. The low sensitivity of the standard deviation to an increase in

the higher energy is shown by the upward displacement of the 60 kev curve with respect to the 88 kev curve. The high dependency of the variation of the lower energy is shown by the rapid decrease in variation as the lower energy decreases to 20 kev.

The effect of the amount of total soft tissue present on picking the optimum photon energy pair was determined from a calculation of the standard deviation of the fraction of fat for a system of 15% fat with the total soft tissue varying from 2 to 20 g/cm^2. The higher energy, E_2, was set at 90 kev and the optimum lower photon energy, E_1, was found for different amounts of total soft tissue. The lower photon energy was the variable rather than the higher photon energy, since the standard deviation is more sensitive to changes in E_1. Figure 3 shows the results of the calculation. The optimum lower photon energy increases as the total soft tissue increases. At low photon energies the sensitivity of R to the actual fraction of fat present is due to the wide spread of the attenuation coefficients for fat and lean tissue. An increase in the photon energy decreases this spread, and also causes the transmitted intensities to increase, which lowers the error due to counting statistics. As total soft tissue increases the transmitted intensities decrease, which makes a higher photon energy more optimal than low energy photon.

Choosing a Radionuclide Source

The precision of the dual photon technique to analyze a fat and lean system depends on having two monochromatic photons; one with a low energy which will maximize the difference in attenuation between fat and lean tissue and the other, an energy high enough such that $\mu_{fat,2} \approx \mu_{lean,2}$. Other important characteristics in choosing a radionuclide source are a long half-life, availability, cost, and the possibility of two suitable photons from a single radionuclide. Previous investigators (Sorenson '64, Mazess '70, '71, Preuss '72) have used ^{125}I and ^{241}Am as a dual source or ^{109}Cd. ^{125}I, with a half-life of 60.2 days, and ^{241}Am, with a half-life of 458 years, are readily available at reasonable cost. ^{109}Cd, though not as readily available as ^{125}I and ^{241}Am, has the advantages of a wider spread of energies, two suitable photons from the single source and a long half-life (453 days).

The polyenergetic characteristics of most radionuclides makes it necessary to use a filtration technique. The polyenergetic nature of ^{125}I is increased when combined with ^{241}Am into a dual source with simultaneous counting in both upper and lower channels, due to the presence of a 26.3 kev gamma from ^{241}Am. Table 1 shows the effect of filtration. For the case of ^{125}I and ^{241}Am a 2 mil tin filter with K_{ab} 29.2 kev, and for ^{109}Cd a 4 mil palladium filter with K_{ab} 24.35 kev was used in calculating

the values in Table 1 with reductions in original K-alpha intensities by a factor of 1.79 and 4.75 respectively. The ratio of K-alpha/K-beta for the unfiltered and filtered sources was, in the case of ^{125}I, 4.6/1.0, and 13.1/1.0 respectively, and 5.0/1.0 and 1122.4/1.0 for the ^{109}Cd source.

The 26.3 kev gamma ^{241}Am occurs 5% of the time and contributes to the counts in the lower energy channel. The contribution of the 26.3 kev gamma to the polyenergetic characteristics of the lower energy is dependent on the relative source activities of ^{125}I to the ^{241}Am which was taken to be 1.66 for the calculations in Table 1. Table 2 shows the attenuation coefficients used in calculating the R values for 100% fat and 100% lean and the range of R shown in Table 3.

Expected Precision Using $^{125}I/^{241}Am$ and ^{109}Cd for Determination of Fat Fraction

The estimate of the variation in the fraction of fat measured is expressed by equation 13. Assuming the attenuation coefficients and the total soft tissue mass and composition to be accurately known, then the effect of different initial intensities can be calculated using equation 13. This calculation was done for an unfiltered and filtered dual source of the ^{125}I and ^{241}Am combination and an unfiltered ^{109}Cd source. For ^{109}Cd the relative unfiltered initial intensities of the ratio K-alpha/K-beta/87.7 kev was 25.5/5.5/1.0 and for the filtered case 5.57/.006/1.0. The ratio of $I_{0,1}/I_{0,2}$ for ^{109}Cd unfiltered and filtered was 25/1 and 5/1 respectively. The total soft tissue was assumed constant at 10 g/cm^2 with a composition of 15% fat. Figures 4 and 5 show the standard deviation of the fraction of fat as a function of total initial counts. For the case of an unfiltered ^{125}I and ^{241}Am dual source with initial counts at both energies of 10^6, the standard deviation would be approximately 0.010 for a fat fraction of 0.15 while for a filtered ^{109}Cd source the standard deviation would be approximately 0.014. This precision is acceptable for assessing inter-individual differences of fat fraction as in diagnosis.

The effect of increasing total soft tissue on the precision of the determination of fraction of fat was calculated using equation 13. The initial counts in the lower energy was fixed at 10^6 with a 15% fat composition and an increasing total soft tissue from 2 to 10 g/cm^2 (Figures 6 and 7). The assumed known attenuation coefficients used in these calculations are the ones shown in Table 3. The determination of the fraction of fat can be considered as the difference of large values (the attenuated intensities) which will have a small difference for small values of total soft tissue.

This small difference will have a larger uncertainty than the case of a larger total soft tissue mass where the difference is also larger. For larger values of total soft tissue the standard deviation starts to increase due to the reduction of the transmitted intensities which increases the error due to Poisson statistics.

In developing a model to express the expected precision for the determination of the fraction of fat consideration was not taken of the effects of hardening or finite beam size. The photon energies used for the calculations were assumed monoenergetic and equal to a weighted average based on their relative intensities. The use of unfiltered and filtered sources takes into consideration the shift of the range of effective energies which increased the range of the R value making it more sensitive to the actual fraction of fat. This is what caused the downward shifts of the filtered curves relative to the unfiltered curves in Figures 4, 5, 6, and 7.

References

1. Bevington, P. R., 1984. Data Reduction and Error Analysis for the Physical Sciences. McGraw Hill Book Company, New York.

2. Judy, P. R., 1970. A Dichromatic Attenuation Technique for the In Vivo Determination of Bone Mineral Content. Ph.D. Thesis, University of Wisconsin, Madison, Wisconsin.

3. Mazess, R. B., Cameron, J. R. and Sorenson, J. A., 1970. Determining body composition by radiation absorption spectrometry. Nature, 228: 771-772.

4. Mazess, R. B., 1972. Prediction of body composition from absorptiometric limb scans. USAEC Progress Report COO-1422-122.

5. Preuss, L. E. and Schmonsees, W., 1972. ^{109}Cd for compositional analysis of soft tissue. Int. J. Appl. Radiation Isotopes, 23:9-12.

6. Roos, B., Rosengren, B. and Skoldborn, H., 1970. Determination of Bone Mineral Content in Lumbar Vertebrae by a Double Gamma-Ray Technique. In Proceedings of Bone Mineral Conference, Cameron (Ed.), USAEC Division of Technical Information, Oak Ridge, Tenn., CONF-700515, p. 243.

7. Sorenson, J. A. and Cameron, J. R., 1964. Body composition determination by differential absorption of monochromatic x-rays. In Symp. Low-Energy X- and Gamma Sources and Applications, Technology Research Institute, Chicago, AEC Report ORNL-11C-5:277-289.

Table 1

Source	lower photon energies (kev)	unfiltered relative intensities	weighted average of lower energies	filtered relative intensities	weighted average of filtered lower energies	higher photon energy (Kev)
	Te K x-rays			2 mils Sn		
^{125}I & ^{241}Am	K_1 27.471	.495		.572		Am's γ at 59.51
	K_2 27.200	.247		.283		
	K_1 30.993	.133	28.236	.051	27.714	
	K_2 31.698	.128		.012		
	γ_I 35.0	.047		.027		
	γ_{Am} 26.35	.048		.053		
	Ag K x-rays			4 mils of Pd		
^{109}Cd	K_1 22.16	.552		.663		Cd's γ at 87.7
	K_2 21.99	.282		.336		
	K_1 24.9	.138	22.58	.00067	22.103	
	K_2 25.5	.028		.00022		

Table 2

Weighted Attenuation Coefficients

Sources	unfiltered		filtered	
	Fat Tissue (triglyceride)	Lean Tissue (muscle)	Fat Tissue (triglyceride)	Lean Tissue (muscle)
^{125}I ^{241}Am				
lower energy	.3058	.4202	.3113	.4308
higher energy	.1945	.2050	.1945	.2050
^{109}Cd				
lower energy	.4054	.6263	.4156	.6479
higher energy	.1764	.1778	.1764	.1778

Table 3

Source	R at 100% fat		R at 100% lean		Range of R
	unfiltered	filtered	unfiltered	filtered	
^{125}I & ^{241}Am	1.572	1.600	2.049	2.101	unfiltered .477 filtered .501
^{109}Cd	2.298	2.356	3.522	3.644	unfiltered 1.224 filtered 1.288

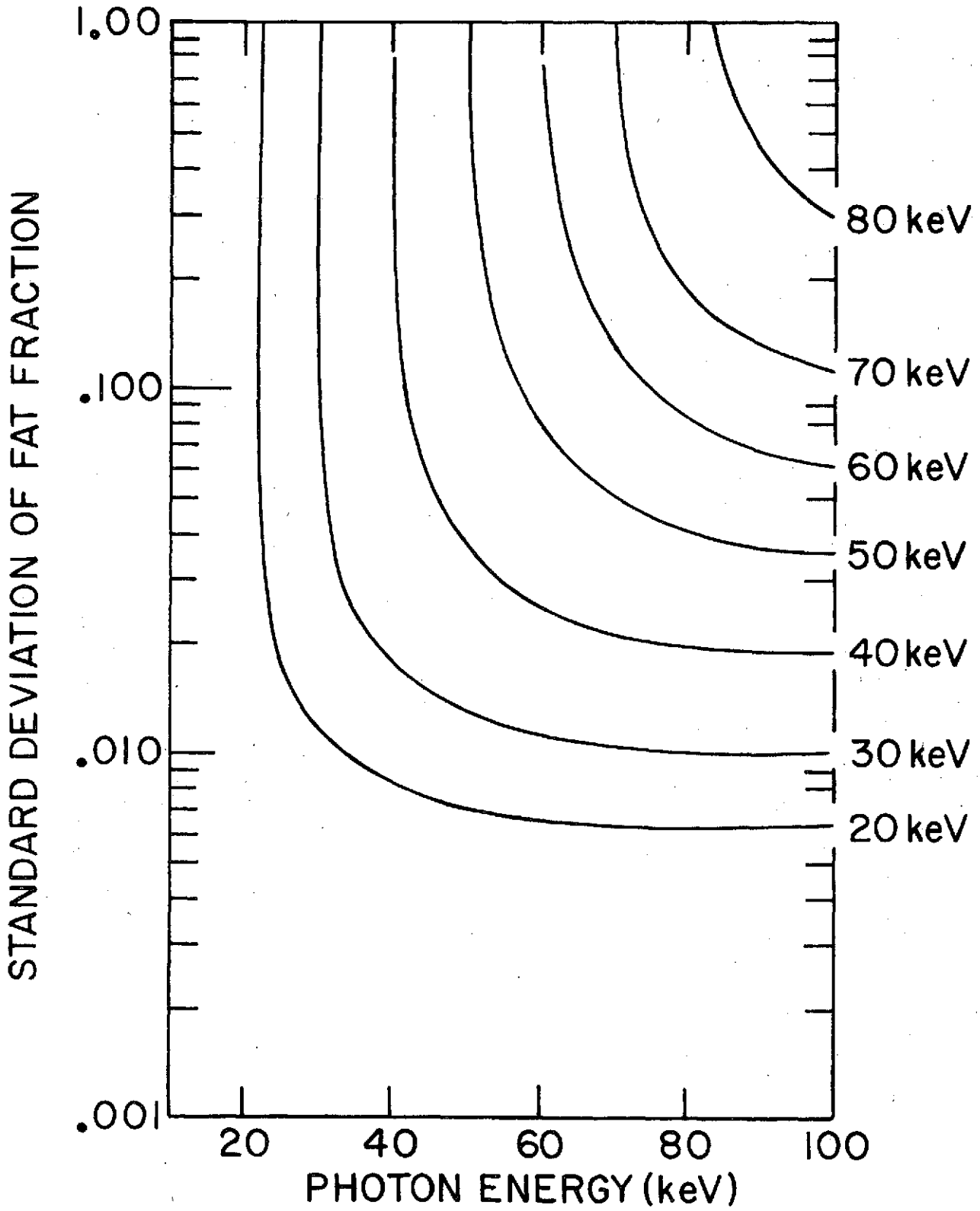

1) The standard deviation of the fraction of fat measured as a function of the pair of photon energies. The unattenuated intensities were assumed constant and equal, and the total soft tissue was 5.0 g/cm^2 with a 15% fat composition.

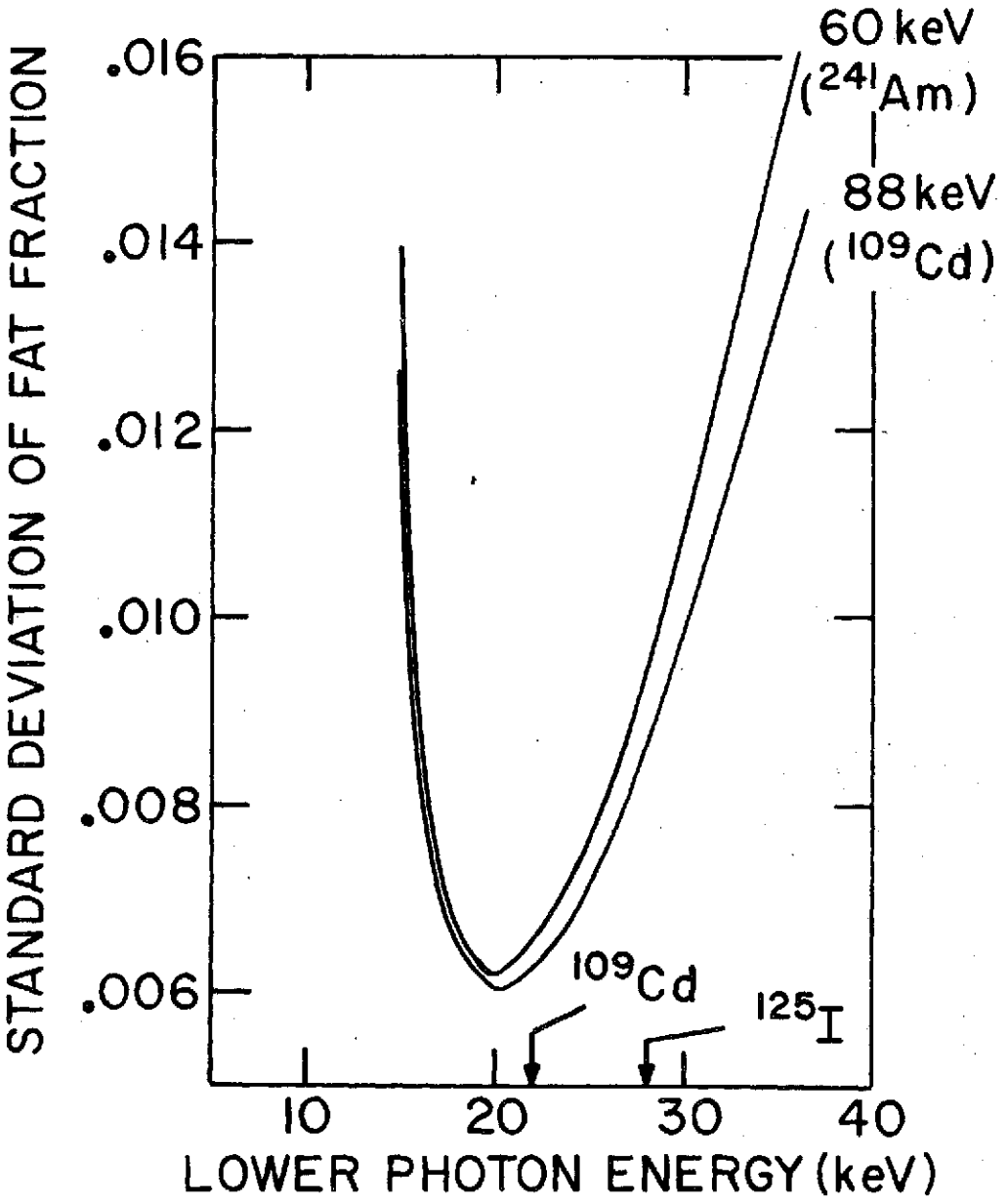

2) The standard deviation of the fraction of fat measured as a function of the lower photon energy for a higher energy of 88 kev and 60 kev. The 88 kev corresponds to the gamma from ^{109}Cd and the 60 kev is the gamma from ^{241}Am. The lower energies associated with these are the 22 kev Ag K x-rays from ^{109}Cd and the 29 kev Te K x-rays from the ^{125}I. The unattenuated intensities were assumed constant and equal and the total soft tissue was 5.0 g/cm^2 with a 15% fat composition.

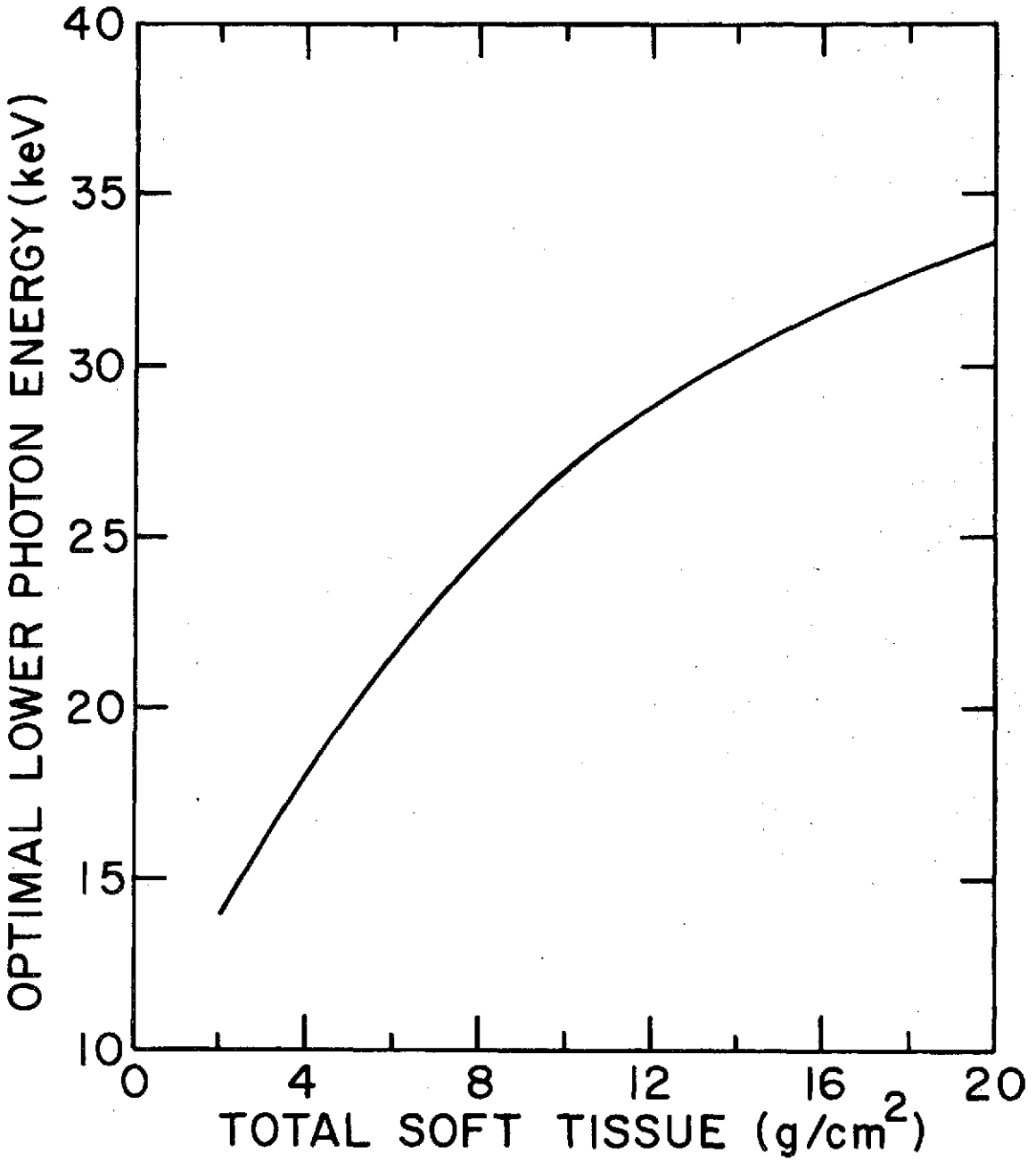

3) Optimal lower photon energy as a function of increasing total soft tissue from 2 to 20 g/cm^2 with a 15% fat composition. The higher photon energy was assumed constant at 90 kev.

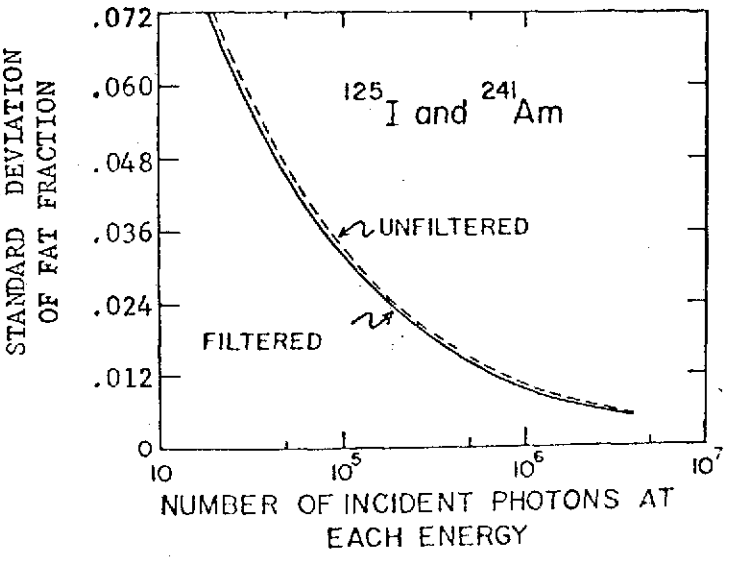

4) Standard deviation of fraction of fat as a function of the initial counts at either energy for the ^{125}I and ^{241}Am dual source. The total soft tissue was assumed constant at 10 g/cm^2 with a percent fat of 15.

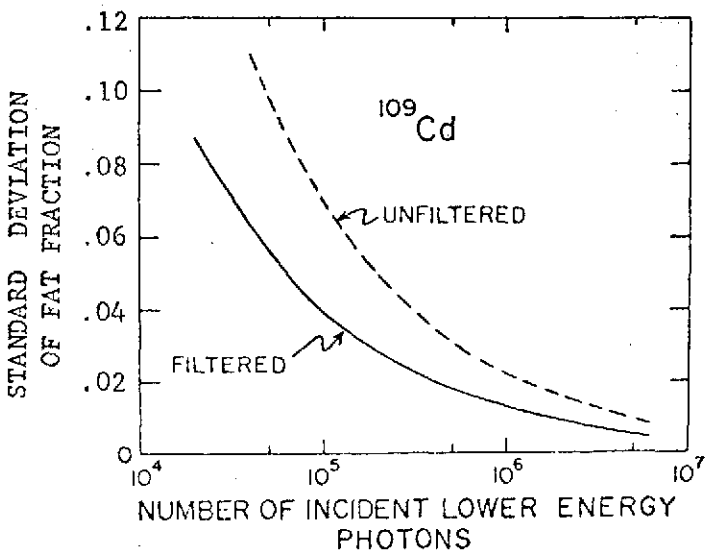

5) Standard deviation of fraction of fat as a function of the initial lower energy for ^{109}Cd. The total soft tissue was assumed constant at 10 g/cm^2 with a percent fat of 15.

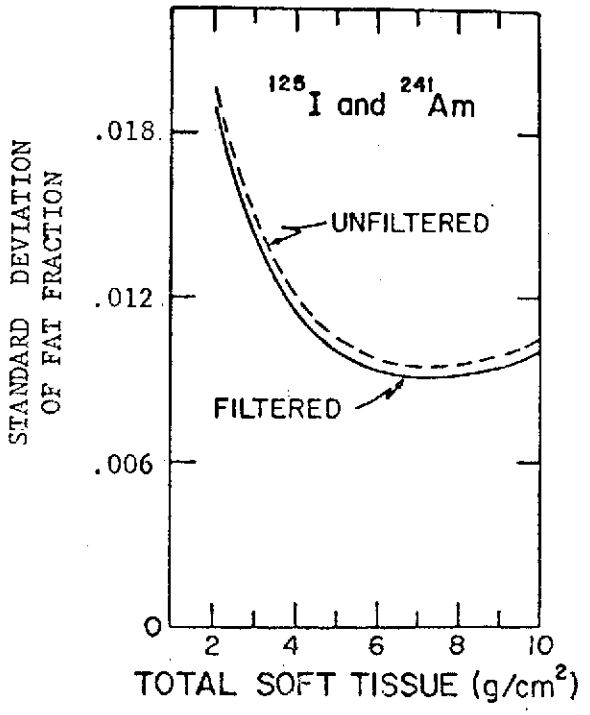

6) Standard deviation of fraction of fat as a function of increasing total soft tissue from 2 to 10 g/cm^2 with a 15% fat composition for the dual source of ^{125}I and ^{241}Am. The initial counts at both energies was assumed constant at 10^6.

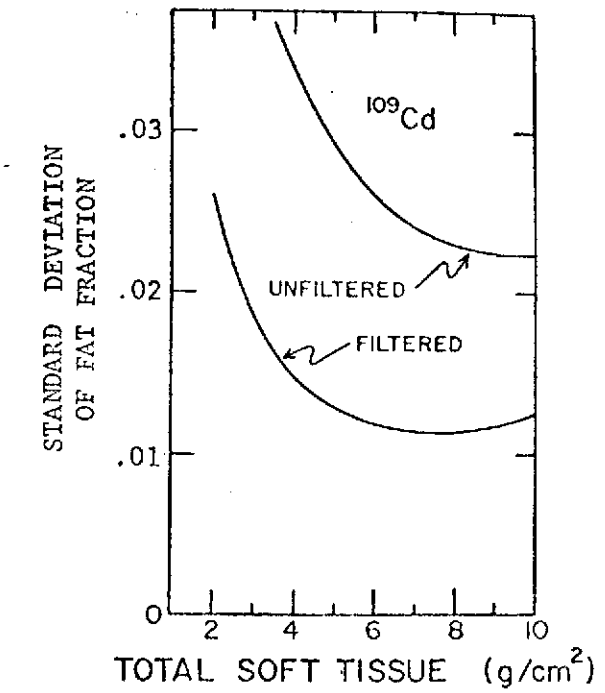

7) Standard deviation of fraction of fat as a function of increasing total soft tissue from 2 to 10 g/cm^2 with a 15% fat composition for ^{109}Cd. The initial counts at the lower energy was assumed constant at 10^6.

COO-1422-152

VIDEO-ROENTGEN ABSORPTIOMETRY FOR THE MEASUREMENT OF BONE MINERAL MASS *

C. R. Wilson and J. R. Cameron
Medical Physics and Engineering Center
Department of Radiology, University of Wisconsin
Madison, Wisconsin

E. L. Ritman, R. E. Sturm and R. A. Robb
Mayo Clinic, Rochester, Minnesota

Abstract

The feasibility of performing absorptiometry measurements using a televised image intensified fluoroscopic system has been examined. The system consists of an x-ray generator, image intensifier, TV camera and A/D converter under computer control for digitizing the video signal. Preliminary experiments in vitro have been performed to evaluate the system's potential for determining in vivo the mass of bone mineral in the axial skeleton. All measurements were made in 20 cm of water using small field sizes of about 5 x 10 cm. Phantoms of bone equivalent material representing vertebral bodies with different amounts of bone mineral were measured. The correlation coefficient between the actual and measured mass was 0.99 and the standard error of estimate of the regression was less than 2%. The day-to-day precision in the measurement was about 3% and the agreement between measurements taken three months apart was within 3%.

Introduction

Osteoporosis is characterized by an absolute loss of bone leading to a failure of the skeleton to provide adequate structural function throughout life. The most serious loss of bone and consequently strength occurs in the femoral neck and spine, particularly in women over 60 years of age. The loss of bone from these areas manifests itself in an increased incidence of femoral neck fractures and vertebral collapse with age. A direct measurement in vivo of the mass of bone present in the femoral neck and spine would be useful in epidemiologic and therapeutic studies of osteoporosis. Of those in vivo techniques which might be considered, such as x-ray photon absorptiometry, biopsy, morphology, and neutron acrivation of calcium, x-ray photon absorptiometry is the most practical and desirable from the standpoint of precision and minimal inconvenience to the patient.

A series of preliminary measurements aimed at determining the feasibility of using an image intensified fluoroscopic system for measurement of bone mineral mass of the vertebra and femoral neck were performed. These studies were performed at Mayo Clinic. The system employed in this study was designed by Wood (1964) and Strum (1971) and others at Mayo Clinic for dynamic studies of the cardiovascular system. Others (Silverman-1971, 1972; and Heintzen-1971) have also been active in the development of this type of system for the measurement of ventricular volume, pulmonary ventilation, etc. These

* Presented at the Annual A.A.P.M. Meeting, 1973, San Diego.

techniques are generally referred to as videodensitometry or fluoro-densitometry. For purposes of bone mineral mass measurements we prefer the term video roentgen absorptiometry, VRA, since bone mineral mass rather than bone density is measured. Also, this descriptive name may prevent confusion with other x-ray techniques used to measure bone.

The studies were performed on two separate occasions about three months apart and were concerned with three areas; 1) the absorptiometric characteristics of the system, i.e. whether the measured transmission of the x-ray beam as a function of absorber mass follows an exponential relation over the mass range of interest; 2) the precision of the measurement, i.e. what the short and long term variation is in the measured mass; and 3) the accuracy of the measurement, i.e. how well the measured quantity can be related to the actual mass present. All studies were performed in vitro. 20 cm of water and vertebral phantoms, plastic bottles filled with different concentrations of di-potassium hydrogen phosphate solution (Witt-1969), were used to approximate the situation in vivo.

Method

The system is shown in Figure 1. It consists of an x-ray generator, image intensifier, video camera, TV monitor, video recording device and an A/D converter under computer control. The torso phantom is also shown. Briefly the system operates as follows. After the x-ray beam passes through the object it strikes the input of the image intensifier forming an image which is optically coupled to the target of the video camera. This image is scanned off in a raster pattern to generate the video signal. The amplitude of the video signal is proportional to the brightness of the image and therefore the intensity of the x-ray beam at the corresponding point on the input phosphor of the image intensifier. The video signal contains information of the spatial distribution of the transmitted x-ray intensities through the subject. Conversion of the analog video signal to digital data is accomplished by the A/D converter and recorded on magnetic tape for subsequent analysis. A/D conversion could be done either on-line, i.e. with the x-rays on, or from the fluoroscopic images recorded on the video disc recorder.

The procedure generally used in obtaining the measurements was as follows. A fluoroscopic image of the vertebral phantom or absorber was obtained on the monitor. The x-ray beam was then collimated to limit the area of the image intensifier exposed to the beam. All fields were about 4 cm x 8 cm or smaller at the input phosphor with the longer dimension being parallel to the horizontal direction on the video monitor. The beam was limited to reduce the effect on image contrast of light scatter within the image intensifier and x-ray scatter from the subject or object in the beam. A/D conversion was done using a Biomation Model 8100 Transient Recorder under computer control. The number of lines to be digitized, the vertical position of the first line, the portion of the line to the digitized, the rate of conversion and the number of bits in each conversion could be chosen. This system has been described by Robb-1973. The digital data was then recorded on magnetic tape. Typically four or five adjacent lines with only the central portion of the trace, starting and ending outside the x-ray beam,were digitized. Figure 2 is a

plot of the actual digitized portion of a single horizontal trace through oneof the vertebral phantoms. The dotted line represents the baseline. This voltage, in the composite video signal, is greater than zero even when no x-rays are incident on the input phosphor and must be subtracted from each point across the trace to obtain the incident x-ray intensity. This baseline was established by interposing a lead absorber in the x-ray beam and then digitizing a trace passing through this area.

With a monoenergetic photon beam it can be shown that the mass of bone mineral in a constant thickness of tissue is given by equation 1 (Cameron-1963).

$$M_{BM} = \frac{\rho_B}{\mu_B \rho_B - \mu_S \rho_S} \log_e (I_0^* / I) \qquad (1)$$

M_{BM} is the mass of bone per unit area. I_0^* is the beam intensity transmitted through only the soft tissue. I is the transmitted intensity through both the bone and soft tissue. μ_B and μ_S are the mass absorption coefficients (cm^2/g) and ρ_B and ρ_S are the microscopic densities (g/cm^3) of bone and soft tissue respectively. These are constant for monoenergetic photon beams. Thus, M_{BM} is equal to a constant times the $\log_e$ of the ratio of the transmitted intensities. Although monoenergetic photons are not strictly necessary for absorptiometric measurements we found that the system obeyed Lambert-Beer's Law in the mass range of interest (see next section) thus allowing us to use the simple expression above to determine bone mineral mass.

The digitized composite video signal of a horizontal trace through one of the vertebral phantoms is shown in Fig. 2. The difference between the signal and the baseline, I_0^* and I_0, as shown in the figure were used in Equation 1 to calculate the mass of bone per unit area at each point across the trace. By summing each of these contributions across the trace the mass of bone in a slice across the bone can be found. Then by summing the mass per unit length in each trace over the length of the bone the total mass (in grams) of bone mineral in that length can be found. The vertebral phantoms used in this study were uniform along their length; only the mass in a single trace was used. In this study the bone mineral mass is given in arbitrary computer units, corresponding to the sum of the logarithms of the ratio I_0^*/I. These units can be converted to g/cm of bone mineral by a knowledge of the densities and absorption coefficients of soft tissue and bone mineral, or by an experimentally determined calibration.

Results

Absorptiometric Characteristics

The absorptiometric properties of aluminum and di-potassium hydrogen phosphate, DPHP, were measured. The absorbers were placed in 20 cm of water and the tube voltage was 110 kVp. A single horizontal trace across the absorber was digitized and the average voltage above background of all points was taken as the intensity of the transmitted x-rays. Figure 3 is

the semi-log plot of the measured intensity versus the mass per unit area of aluminum. The curve is linear up to about 7 g/cm^2 (~1 inch of aluminum). Figure 4 shows the attenuation of theDPHP absorbers. The curve is linear up to about 1.5 g/cm^2. This amount corresponds to the maximum vertebral mass per unit area which will be encountered in an actual subject in vivo. Although beam hardening is apparent in these curves, it is negligible in the range of interest and in the first approximation, the beam can be considered to be monoenergetic.

Precision

The precision of the VRA technique was estimated by repeat measurements of one of the vertebral phantoms, Table 1. The variation in the calculated mass for five adjacent horizontal lines digitized from a single video field was about 0.2%. The variation in the mass determined from five different fields recorded over a period of about 15 seconds was about 0.4%. Completely independent measurements, i.e. tube voltage and current reset, and phantom repositioned prior to each measurement, taken over a period of one day had a variation of about 3.0%. This was repeated at a different tube voltage and the same variation was found. The agreement between mass determinations of the same phantom made three months apart was within the variation of the measurements made on the same day.

Accuracy

The accuracy of the system was examined by measuring vertebral phantoms of di-potassium hydrogen phosphate, DPHP, solution. A saturated solution of DPHP is nearly radiographically equivalent to compact bone (Witt-1969). At lower concentrations it can be used to simulate cancellous bone. The vertebral phantoms were plastic bottles, all 4.5 cm in diameter, filled with different concentrations of DPHP. The mass per unit length of the phantoms ranged from 0.70-5.5 g/cm. The diameter is about the diameter of the lower lumbar vertebrae and the range of mineral mass, up to 5.5 g/cm, is slightly greater than the mineral mass in vivo. Figure 5 shows a comparison between the measured quantity, $\Sigma \ln I_0^*/I$, and the actual mass per unit length of the phantoms. The correlation coefficient between the parameters is better than 0.99. A linear relation was assumed and standard regression analysis was performed on the data. The standard error of estimate in the mass of the phantom mass from the regression equation is less than 2%. This calibration study was repeated three months later under the same experimental conditions with essentially the same results being found.

In actual subject measurement a varying amount of soft tissue will be encountered overlying the vertebrae. Slight compression of the subject's soft tissue or boluses, i.e. rubber bags filled with water, will be used to achieve the uniform thickness over the bone necessary to meet the condition for Equation 1. The total thickness of each patient will be different and it may be necessary to measure a calibration wedge

in order to provide a standard to which the measured quantity can be referenced. A step wedge of DPHP was used to test the use of a reference standard for calibrating the system for different thicknesses of water (or soft tissue). The wedge and one of the phantoms were measured separately, about one minute apart, in 10, 15 and 20 cm of water. Table 2 gives the measured mass of the phantom referenced to the step wedge. The standard deviation of the mass is within the variation associated with individual measurements in the same thickness of water.

Conclusion

These initial results in vitro are encouraging and indicate the feasibility of employing a computer aided intensified fluoroscopic system to obtain x-ray transmission data suitable for the measurement of bone mineral mass. The x-ray beam, due to the heavy filtration provided by the subject is nearly monochromatic and obeys Lambert-Beer's Law over the range of vertebral mineral mass of interest. The precision, $\simeq 3\%$, is sufficient to follow small changes in bone mineral mass and the measured mass is an accurate estimate, $\simeq 2\%$, of the actual mineral mass.

Table 1. VRA Reprducibility

Conditions	Coef. of Variation	Number
Line-to-line	0.2%	5
Field-to-field	0.4%	5
Day	3.0%	10

Table 2.

Water Thickness (cm)	Bone Mineral Mass (arbitrary units)
10	2.60
15	2.46
20	2.56
	mean = 2.54 ± 0.07

References

1. Cameron, J.R. and Sorenson, J.A. Measurement of Bone Mineral In Vivo: An Improved Method, Science 142: 230-233, 1973.

2. Robb, R.A. and Wood, E.H., Computer Controlled Video Digitization and Video Graphics, To be published, 1973.

3. Silverman, N.R. Videometry of Blood Vessels, Radiol. 101: 597-604, 1971.

4. Silverman, N.R. Clinical Video-densitometry, Am. J. of Roent. 114: 840-848, 1972.

5. Sturm, R.E. and Wood, E.H. Roentgen image-intensified television recording system for dynamic measurements of roentgen density for circulatory studies. Roentgen-Cine-and Videodensitometry. Fundamentals and Applications for Blood Flow and Heart Volume Determination. G. Thieme, Stuttgart, 1971, P.H. Heintzen, ed. pp. 23-44.

6. Witt, R.M. and Cameron, J.R. Bone Standards, USAEC Progress Report COO-1422-42, 1969.

7. Wood, E.H., Sturm, R.E. and Sanders, J.J. Data processing in cardiovascular physiology with particular reference to roentgen videodensitometry, Mayo Clin. Proc. 39: 849-865, 1964.

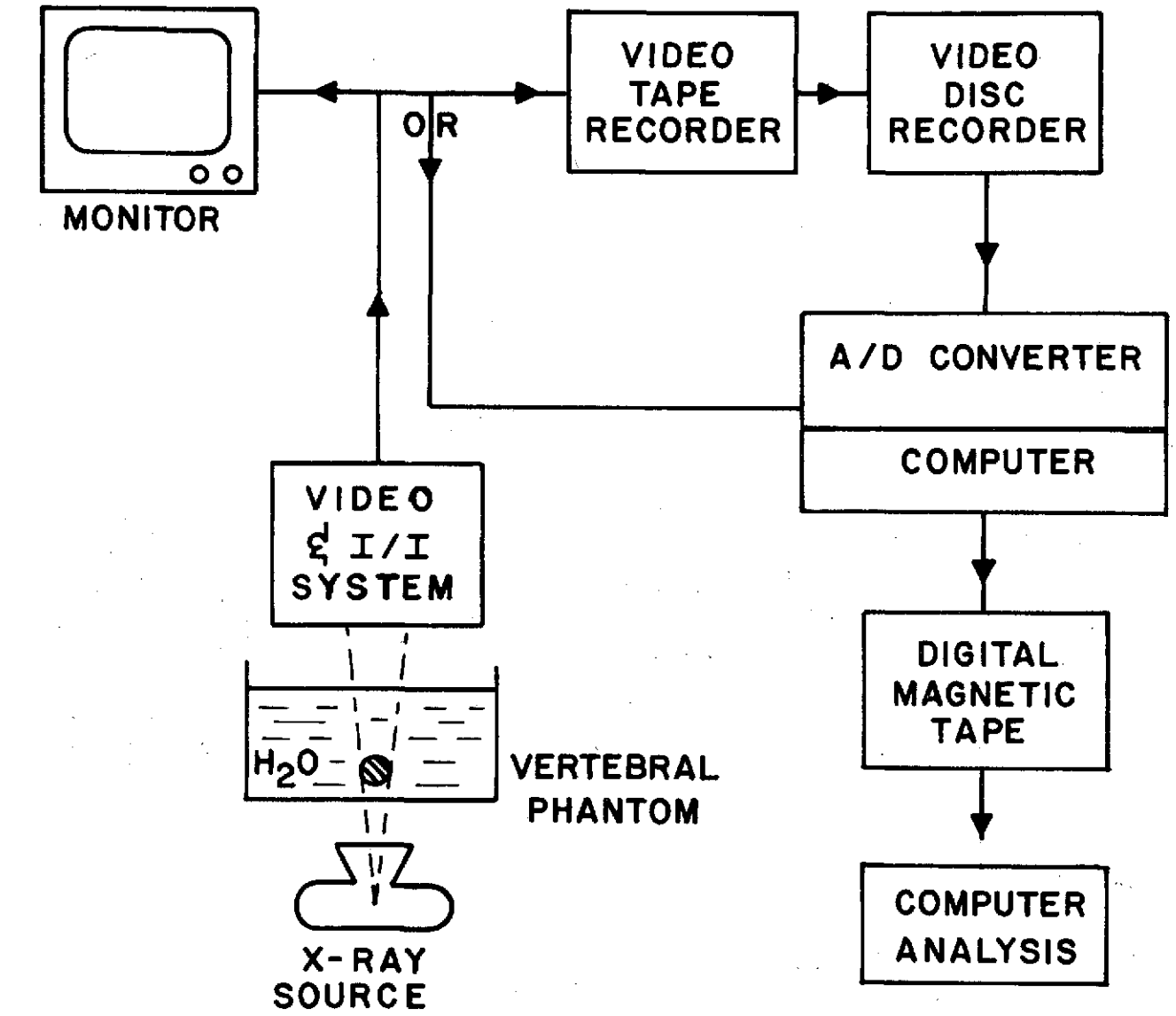

VIDEO ROENTGEN ABSORPTIOMETRY SYSTEM

Figure 1 Block diagram of VRA system.

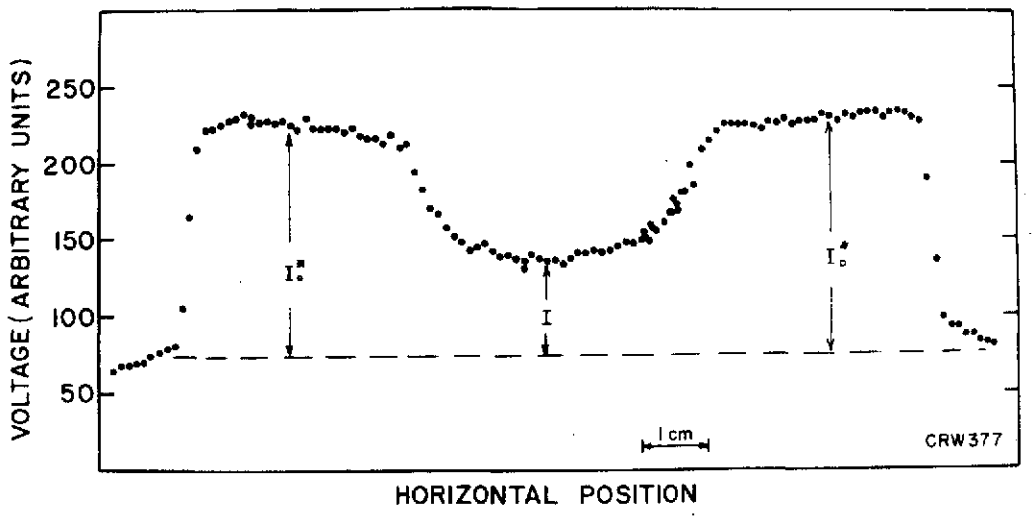

Figure 2 Single digitized horizontal video trace of vertebral phantom in 20 cm of water, 110 kVp, 8 bit conversion.

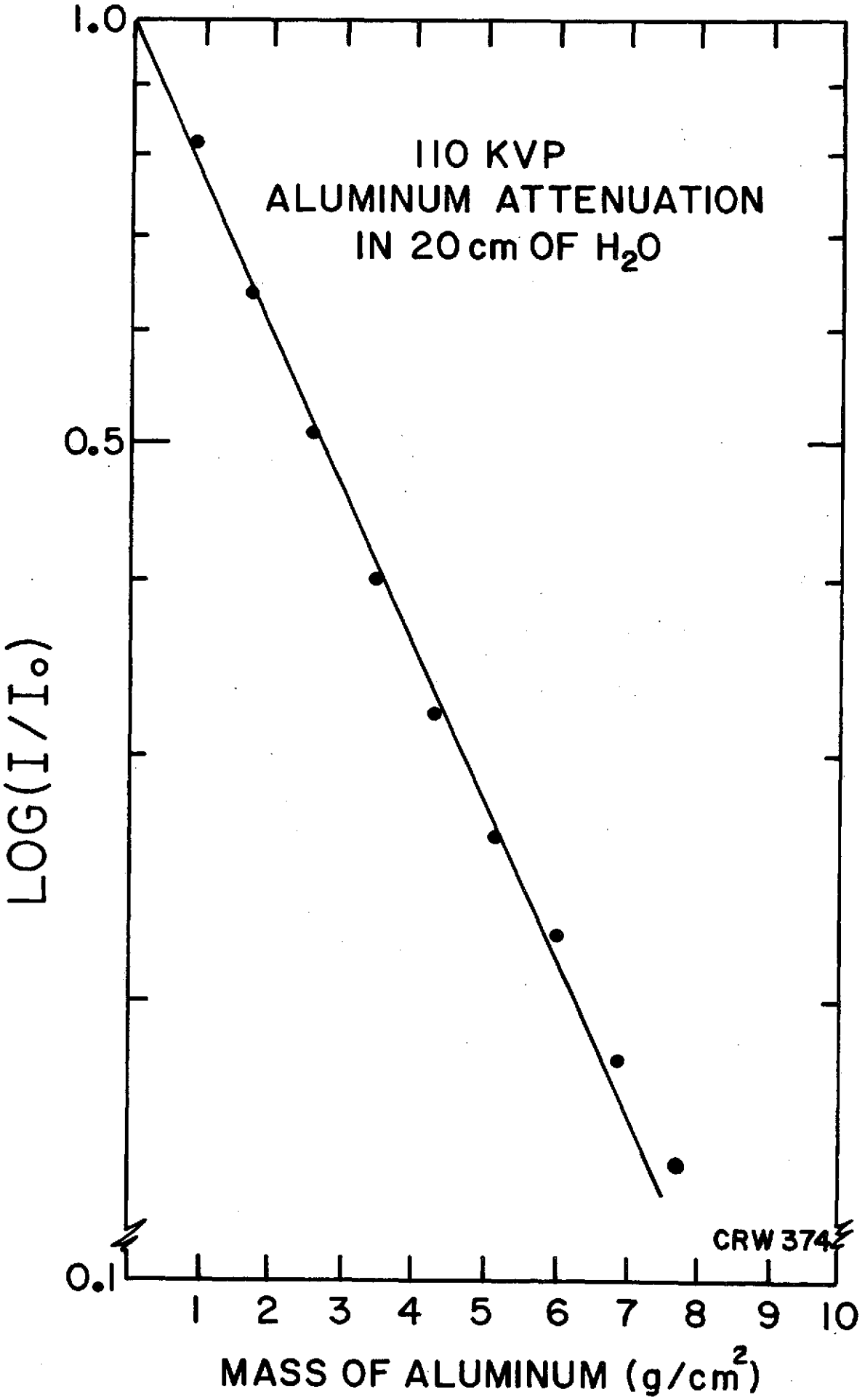

Figure 3 Attenuation of aluminum absorbers measured with the VRA system: aluminum absorbers in 20 cm of water, 110 kVp.

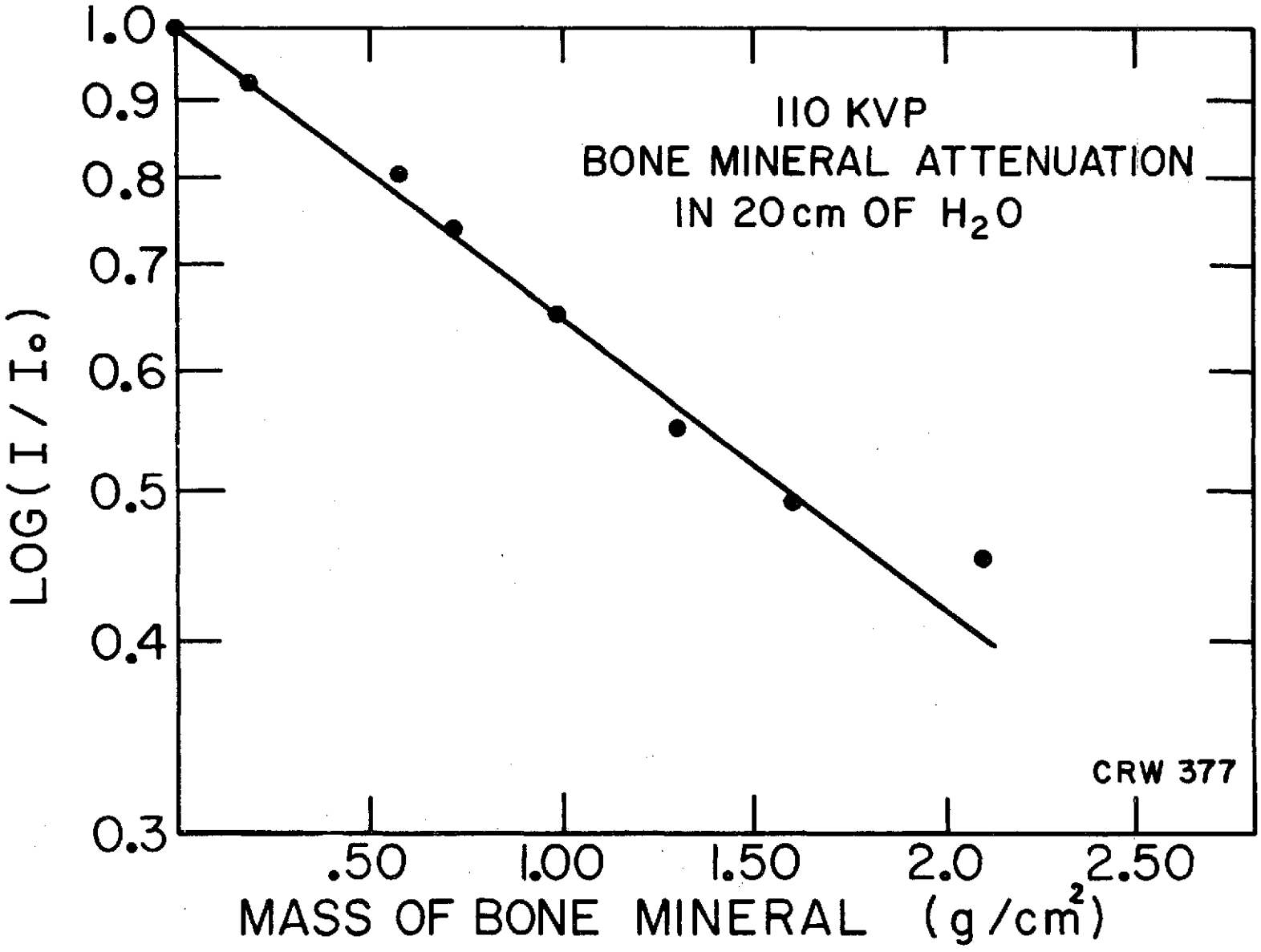

Figure 4 Attenuation of di-potassium hydrogen phosphate absorbers measured with VRA system: DPHP absorbers in 20 cm of water, 110 kVp.

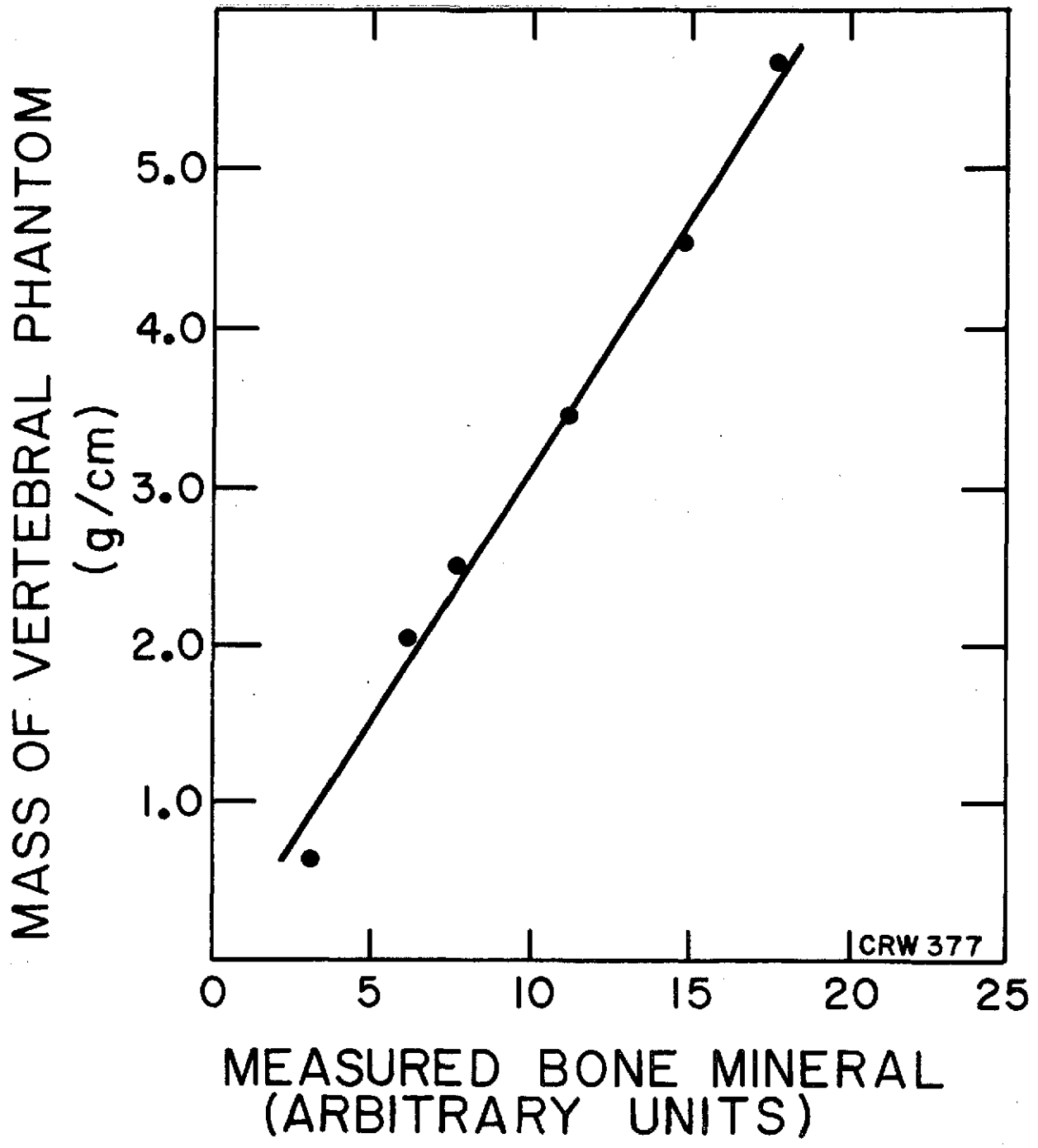

Figure 5 Observed bone mineral mass of vertebral phantoms versus actual mass.

COO-1422-153

EFFECTS OF THE POLYENERGETIC CHARACTER OF THE SPECTRUM OF ^{125}I ON THE MEASUREMENT OF BONE MINERAL CONTENT*

John M. Sandrik, M.S. and Philip F. Judy, Ph.D.

Investigative Radiology 8, No. 3: 143-149, 1973

The effects of the polychromatic nature of the spectrum of ^{125}I on the photon absorptiometric determination of bone mineral content (BMC) have been investigated. Theoretical analysis of the effects was performed assuming exponential attenuation of the individual components of the spectrum. These analyses were in good agreement with, and verified by, experimental results on phantoms. The photon absorptiometric determination of BMC was found to be nonlinearly related to the actual thickness, g/cm^2, of hydroxyapatite. However, a linear relation between these two variables was derived which yielded values of BMC within $\pm 1\%$ of those predicted by the nonlinear relation over a range of 0.6 to 1.5 g/cm^2 of hydroxyapatite. Variations in soft-tissue cover were found to alter the determination of BMC by 0.5 to 1.0% per g/cm^2 of soft tissue, assuming a tin filtration of 51 μm of the ^{125}I source. The effects of tin filtration of the primary beam were investigated for filter thicknesses over the range of 0 to 76 μm of tin. Calculations, verified by measurements on phantoms, indicated that variations in the amount of tin filtration altered the value of BMC by 0.12 to 0.16% per μm of tin. Maintaining a tolerance of ± 2.5 μm on the thickness of tin filtration of ^{125}I sources used in BMC measurements would limit the variation in BMC due to the variation of filter thickness to $\leq 1\%$.

---

* Abstract only; article available upon request.

COO-1422-154

RECTILINEAR AND LINEAR SCANNING IN THE DETERMINATION OF BONE MINERAL CONTENT

J. M. Sandrik, C. R. Wilson, and J. R. Cameron

Two studies have been conducted to compare the precision of rectilinear and linear modes of scanning for the determination of bone mineral content (BMC) by the photon absorptiometric technique (1). Repetitive BMC determinations were made at midshaft and distal sites on the forearms of normal males; five were involved in the midshaft study and eight in the distal study. Each study lasted about two months with the midshaft measurements being made in May-June, 1972, and the distal measurements in June-July, 1973. In repetitive or long-term studies one of the major factors affecting precision, particularly in the clinical situation, is the repositioning of the scan path to the same site on the bone for each measurement (5).

METHOD

The photon absorptiometric measurements of BMC were performed with the nuclear spectroscopy and data acquisition equipment described by Judy et al. (2). The photon source was ^{125}I and the number of photons transmitted was sampled at 0.4 sec intervals. All data were recorded on digital magnetic tape for computer processing. A scanner capable of both linear and rectilinear motions was used with a scanning speed of 2 mm/sec (3,4).

For the midshaft study the measurement site was located one-third the distance from the olecranon to the head of the ulna measured proximally from the ulnar head on the right arm of each subject. A linear BMC determination consisted of ten scans at this site. A rectilinear BMC determination was initiated at a site located 13.6 mm proximal to the site of the linear determination and proceeded distally with scans being made at 2.71 mm intervals. Eleven such scans covered a length of 27.1 mm centered about the site of the linear determination. In this study separate determinations of BMC of the radius and the ulna were made.

BMC measurements in the distal study were performed at a distal forearm site on the left arm of each subject. A linear determination, consisting of 10 scans, was performed at a site located 2 cm, measured proximally, from the ulnar styloid. A rectilinear determination was initiated at the head of the ulna and proceeded proximally with scans being made at 5.38 mm intervals for a total of 10 scans. The total BMC in each scan path was determined without separation into radial and ulnar components.

In both studies five measurement sessions were held for each subject at which time both a linear and a rectilinear determination were made. At

the start of each session the scan sites were located and marked with ink on the skin of the subject's arm. The subject then immersed his arm in a water bath with a depth of 6.5 cm over the scan site. A lucite tray held stationary over this site maintained a constant water level. After the subject was situated as comfortably as possible, the scanner was driven to the site of the first scan; a stylus attached to the detector holder of the scanner was aligned with the appropriate mark on the subject's arm. After the first set of scans of a session the subject's arm was removed from the water bath and then replaced before beginning the second set. The duration of either a linear or a rectilinear determination, from positioning the subject in the water bath to the last scan of a set, was 15 to 20 min.

During the midshaft study the subject's arm was not restrained in any way. However, some subjects noticed that their arms tended to float if they did not consciously restrain them. Consequently, during the distal study light pressure was applied to the hand with a cushioned clamp attached to the scanning table.

On each day that subject measurements were performed, a set of bone standards (7) was also scanned. This was done at least at the beginning and end of each day of scanning. In addition, the standards were scanned before resuming subject measurements if several hours had elapsed since the last measurement session.

RESULTS

A BMC determination was calculated as the mean of the BMC values from the individual scans of a set; this mean value is designated the session mean BMC. The standard deviation and coefficient of variation (CV) of the set of BMC values were also calculated. For each subject the five values of this CV obtained from the five BMC determinations by each scanning mode at each site were averaged to yield the average CV/session given in columns 6, 7, and 8 of Table I. The average CV/session for a linear determination indicates the precision of the BMC value from a single scan. At the radial midshaft site the average CV/session values range from 1.81 to 2.97%. For the ulnar measurements these values were in the range of 2.67 to 4.34%. These larger values for the ulna compared to the radius may be attributable to the subject motion problem mentioned previously.

Subject motion as well as repositioning errors will be expected to produce greater variability in measurements on the ulna than on the radius at this site. Evidence for this is found by examining the values of the average CV/session for the rectilinear scans at the midshaft site. The range of values for the radius, reflecting the variability of the BMC from scans made at eleven different sites along the radius, is 2.86 to 3.86%. This range is not much higher than that obtained for ten scans at the same site on the radius (1.81 to 2.97%). For the ulna the average CV/session for the rectilinear scans is in

the range of 4.05 to 7.80% compared to 2.67 to 4.34% for the linear scans. The mineral distribution of the radial midshaft is fairly uniform, hence the BMC determination at this site is not sensitive to small errors in repositioning or to limited subject motion (5). However, the corresponding site on the ulna shows greater variability of BMC with position and hence the BMC determination is more sensitive to these problems.

The average CV/session for rectilinear scans at the distal site varied from 3.61 to 10.59%; the range for the linear scans was 1.01 to 2.07%. These data indicate that the mineral distribution at this site is highly non-uniform; yet high precision was maintained for individual scans. Considering the data for linear scans at the radial midshaft and the distal forearm, the precision of the BMC determination from a single scan measurement was in the range of 1 to 3% for the subjects in these studies. This level of precision is the same as was obtained in the daily measurements of the bone standards.

The average, standard deviation, and CV of the five session mean BMC values were also calculated. This average is termed the study mean BMC; values are given in columns 3, 4, and 5 of Table I. This CV represents the coefficient of variation of the session mean BMC and therefore the reproducibility of the BMC determination from session-to-session; values are given in columns 9, 10, and 11 of Table I. For the standards 15 to 18 such session mean BMC values had been obtained in each study based on 5 scans of each standard at each session. The CV of the session mean BMC for the standards was in the range of 1 to 3%. Consequently no adjustment of BMC values of the subjects was made in either study; all BMC values are given in arbitrary units.

DISCUSSION

Although rectilinear scanning did not yield higher precision for every session mean BMC, in 15 of 18 determinations the CV of the session mean BMC for rectilinear determinations was lower than that for linear determinations. Furthermore, both the average and the range of the session mean CV's over all subjects for a particular scanning site were smaller for rectilinear determinations than for linear determinations (Table II). The averages of the CV's of the session means for rectilinear determinations were lower than those values for linear determinations by a factor of 1.5 to 2. In no rectilinear determination was the CV of a session mean greater than 3%. These results indicate that the BMC determination at an areal scan site is subject to less variation due to repositioning than at a linear site (5).

Another benefit of rectilinear scanning is that the BMC distribution with position along the bone can be obtained for an individual at the time of the first BMC determination. This distribution can be compared with those obtained in subsequent determinations either to verify repositioning or to ascertain the location of mineral changes. Such a series of distributions of BMC at the distal site for a particular subject is shown in Figure 1. There is evidence in this series that an error in repositioning occurred in the second determination. Minima which occur at positions 2 and 6 in the other four distributions appear at positions 1 and 5 in the second. By shifting the second distribution to the right by one scan interval, about 5 mm, it agrees closely with the other four. This procedure suggests further

improvement in the precision of a BMC determination by using mineral distribution patterns for repositioning in addition to external landmarks (6). However, this technique has not been applied to the results presented in this report.

CONCLUSION

Studies on ten normal males have indicated that rectilinear scanning for the determination of BMC can reduce the coefficient of variation of the mineral values obtained in repetitive measurement sessions by a factor of 1.5 to 2 compared to measurements performed by linear scanning. In addition rectilinear scanning can yield the same level of precision, 2-3%, in a region where the mineral content varies widely with position as in a region of uniform mineral content. Rectilinear scanning also offers the possibility of establishing the BMC distribution as a function of position along the bone of an individual so that in subsequent measurements repositioning can be verified or the location of mineral changes determined.

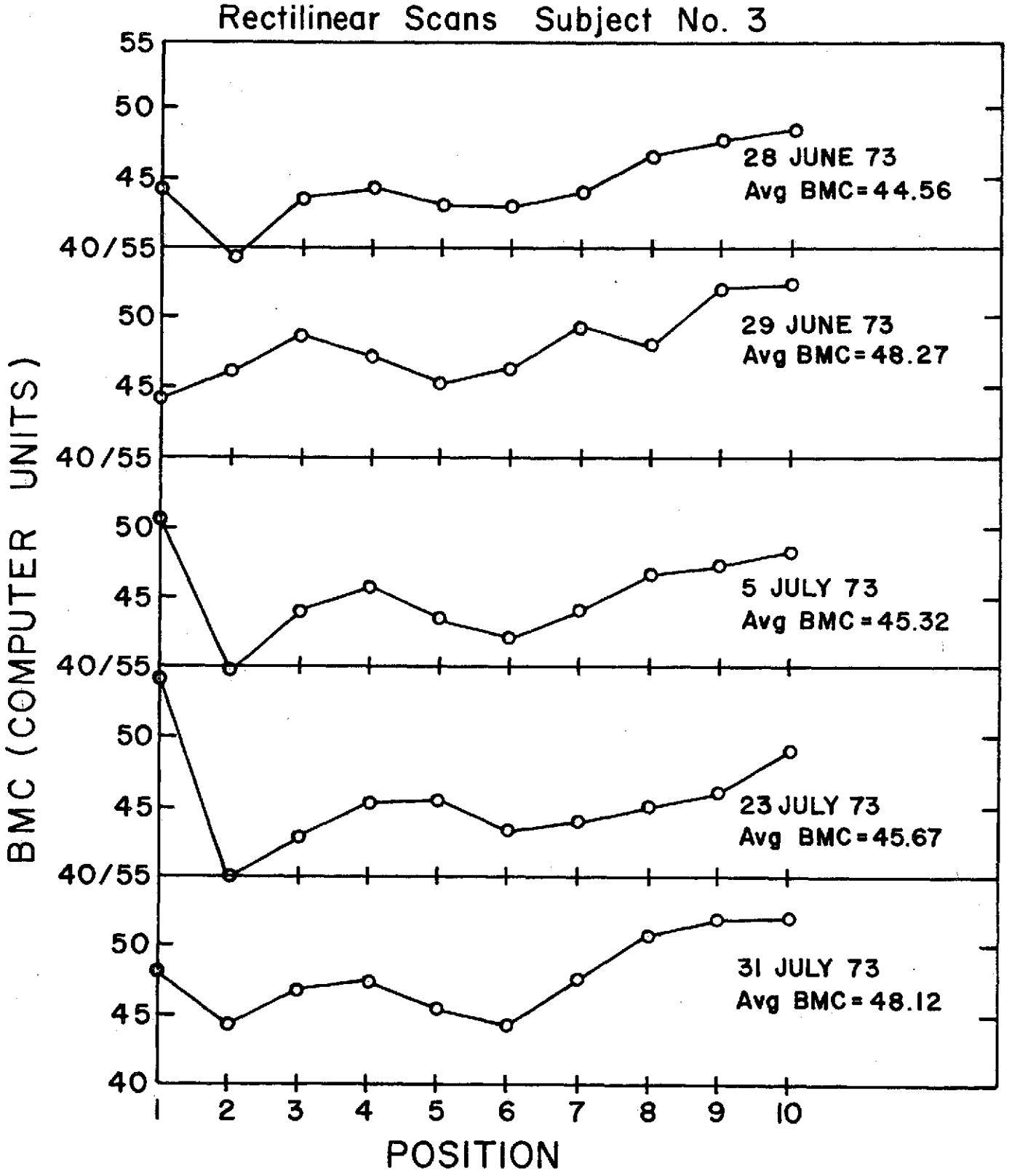

Figure 1. Distribution of BMC as a function of position along the arm for succesive rectilinear scans of a subject. The scanning site is the distal forearm with position 1 being at the ulnar head and succeeding scans proceeding proximally. Intervals between scans are 5.38 mm.

TABLE I

RECTILINEAR AND LINEAR SCAN RESULTS

Subject (1)	Scan Type (2)	Study Mean BMC(arb.units) Midshaft Radius (3)	Midshaft Ulna (4)	Distal Total (5)	Average CV/session (%) Midshaft Radius (6)	Midshaft Ulna (7)	Distal Total (8)	CV of Session Mean BMC(%) Midshaft Radius (9)	Midshaft Ulna (10)	Distal Total (11)
1	Rec	40.75	31.08	56.33	3.28	4.05	9.09	.82	1.31	1.24
	Lin	40.56	30.95	55.48	1.81	3.11	1.52	.91	1.47	1.85
2	Rec	40.24	30.90		3.39	7.80		1.15	2.30	
	Lin	40.61	30.69		2.97	3.68		1.09	2.32	
3	Rec	30.37	25.13	46.39	3.86	7.04	6.63	.95	1.47	3.66
	Lin	30.10	24.95	46.06	2.34	4.34	1.39	1.52	3.93	7.19
4	Rec	42.93	37.24	65.95	2.90	5.67	7.02	.84	1.20	1.96
	Lin	42.31	37.58	62.81	2.25	2.67	1.32	1.83	1.86	2.09
5	Rec	33.42	29.18		2.86	5.13		.23	1.63	
	Lin	33.58	29.65		2.69	3.31		1.93	2.25	
6	Rec			51.33			3.61			.84
	Lin			51.68			1.68			1.10
7	Rec			51.39			5.84			2.64
	Lin			52.00			1.12			1.62
8	Rec			55.65			6.96			1.63
	Lin			53.44			2.07			3.35
9	Rec			63.31			10.59			1.48
	Lin			60.90			1.63			3.85
10	Rec			66.78			5.46			3.00
	Lin			66.50			1.01			1.56

TABLE II

AVERAGES AND RANGES OF CV'S OF SESSION MEANS

Site	Linear Scans Avg. CV (Range)	Rectilinear Scans Avg. CV (Range)
Midshaft Radius	1.46 (0.91 - 1.93)	0.66 (0.23 - 1.15)
Midshaft Ulna	2.57 (1.47 - 3.93)	1.58 (1.20 - 2.30)
Distal Total	2.83 (1.10 - 7.19)	2.04 (0.84 - 3.00)

References

1. Cameron, J. R. and Sorenson, J. A.: Measurement of Bone Mineral in Vivo: An Improved Method, Science 142:230, 1963.

2. Judy, P. F., Ort, M. G., Kianian, K. and Mazess R. B.: Developments in the Dichromatic Attenuation Technique for the Determination of Bone Mineral Content In Vivo. USAEC Report COO-1422-97, 1971.

3. Sandrik, J. M., Mazess, R. B., Vought, C. E., and Cameron, J. R.: Rectilinear Scanner for Determination of Bone Mineral Content. USAEC Report COO-1422-96, 1971.

4. Sandrik, J. M.: Technical Information on a Rectilinear Scanner for Determination of Bone Mineral Content. USAEC Report COO-1422-117, 1972.

5. Sorenson, J. A., and Cameron J. R.: A Reliable In Vivo Measurement of Bone Mineral Content. J. of Bone and Joint Surgery 49-A, No. 3:481, 1967.

6. Vogel, J. M. and Anderson, J. T.: Rectilinear Transmission Scanning of Irregular Bones for Quantification of Mineral Content. J. of Nuclear Medicine 13, No. 1:13, 1972.

7. Witt, R. M., Mazess, R. B., and Cameron, J. R.: Standardization of Bone Mineral Measurements. USAEC Report COO-1422-70, 1970.

Acknowledgement

This work supported in part by NIH Training Grant No. 5-T01-CA-05104-11 and by NASA Grant No. Y-NGR-50-002-051.

COO-1422-155

DETERMINATION OF LUNG TUMOR MASS

BY ROENTGEN VIDEO ABSORPTIOMETRY

J. M. Sandrik, C. R. Wilson and J. R. Cameron
Departments of Radiology and Physics
University of Wisconsin

Initial investigations have been carried out to determine the feasibility of using an x-ray generator, image intensifier, television chain to obtain a quantitative determination of the mass of lung tumors in vivo. The aims of these investigations included estimating the precision of the method and determining the effects on the measurement due to variation of the energy of the x-ray beam and of the position within the television field at which the measurement is made.

EQUIPMENT AND METHOD

The x-ray generator, image intensifier, closed circuit television system, and data handling facilities used were part of the roentgen video-densitometry system at Mayo Clinic. The components of this system have been described in detail (1,2,3,4) and only the general aspects of the equipment used will be discussed here.

The x-ray generator was a fluoroscopic type with maximum ratings of 120 kVp and 10 mA. The x-ray tube had a 0.3 mm focal spot which was located 79 cm below the tabletop. Filtration of the beam was 3 mm Al equivalent.

An image intensifier, located with its input phosphor 42.5 cm above the tabletop, was coupled to a Plumbicon television camera. With this system the fluoroscopic image could be viewed on a TV monitor and portions of the study recorded on videotape as desired.

Measurements were made on a chest phantom consisting of 10 cm of cork, with a bulk density of 0.19 g/cm^3, sandwiched between two slabs of polystyrene each 2.54 cm thick. Eight lucite cylinders with diameters ranging from 3.2 to 25.4 mm in 3.2 mm increments simulated lung tumors. These were located at a depth of 10.5 cm measured from the surface of the phantom facing the focal spot with their axes oriented perpendicular to the x-ray beam axis. In the TV images the cylinder axes were parallel to the TV scan lines.

Studies were performed with x-ray generator potentials of 60, 80, and 100 kVp. All irradiations were done in a narrow beam geometry to minimize the contribution of scattered radiation to the radiologic image. The field size at the position of the cylinders was approximately 2.5 x 3.8 cm^2.

The signals recorded on the videotape were used to estimate the mass per unit length of the cylinders with two data analysis systems. In one case analyses were performed in an analog mode by inputting the videotaped signals to a videodensitometer (2,3). Analyses were also performed digitally by transferring the signals from the tape to a videodisc, digitizing the voltage waveforms, and processing the data with a computer.

QUANTITATION OF MASS/LENGTH: VIDEODENSITOMETER

The voltage waveform representing one line of a TV frame corresponds to the distribution of photon fluence with position in the radiologic image at the location of that line in the image. A series of such waveforms yields the distribution of transmitted fluence over an area. The videodensitometer has a "window" of variable dimensions which can be positioned over the area to be studied as viewed in a TV monitor. The portion of the voltage waveform of a TV line that is within this window is integrated with the integration continuing for all lines within the window. Such integrations are repeated for each successive field at the rate of 60 fields/sec.

To determine the mass of an object in the x-ray beam, the radiologic image is recorded first without and then with the object in the videodensitometer window. If the TV signal voltage at a point without the object in the window is I_o and the voltage at the same point with the object is I, then the mass per unit area at that point, assuming exponential attenuation, is proportional to $\ln(I_o/I)$. The integral of this expression over the area of the object yields a measure of the mass of the object. In these studies each cylinder displaced its volume in the cork so that the total thickness of material in the beam remained constant.

When the videodensitometer is used for this determination, the video signal is first put through a differential amplifier so that the voltage level corresponding to black in the TV image can be subtracted from the transmitted intensity signal. The net signal then goes to a logarithmic amplifier before the integration is performed. The videodensitometer signal from the window area excluding the object represents the integral of $\ln(I_o)$ over this area. This signal is called the white level. When the same window is placed over the object of interest, the integral of $\ln(I)$ is obtained. The difference of these two signals yields the mass estimate. In the studies of the uniform cylinders these results were expressed in terms of mass per unit length of the cylinder.

A rectangular densitometer window was used with the length perpendicular to the cylinder axes and extending beyond the cylinder diameters on both sides. One window size was used for analyzing all eight cylinders. The white level and the densitometric integral of each cylinder were output as traces on a chart recorder. The estimate of mass/length was obtained by measuring the distance between these two traces on the record.

The relations between the densitometric integral and the mass/length for the three x-ray potentials used are shown in Fig. 1. About 3 to 5 sec of fluoroscopic study of each cylinder were taped, corresponding to 200 to 300 TV fields. The points plotted in Fig. 1 represent the average integral for these fields and the error bar indicates the typical range of the determinations, about 0.2 units, as measured from the chart record. Such variations represent the short-term fluctuations of the measurement which may be attributable to inconstancy of the x-ray generator output or instabilities in the electronics of the TV and analysis systems. For cylinders of about 20 mm diameter this error is in the range of 2 to 5% while for cylinders of about 5 mm diameter this error is in the range of 10 to 20%.

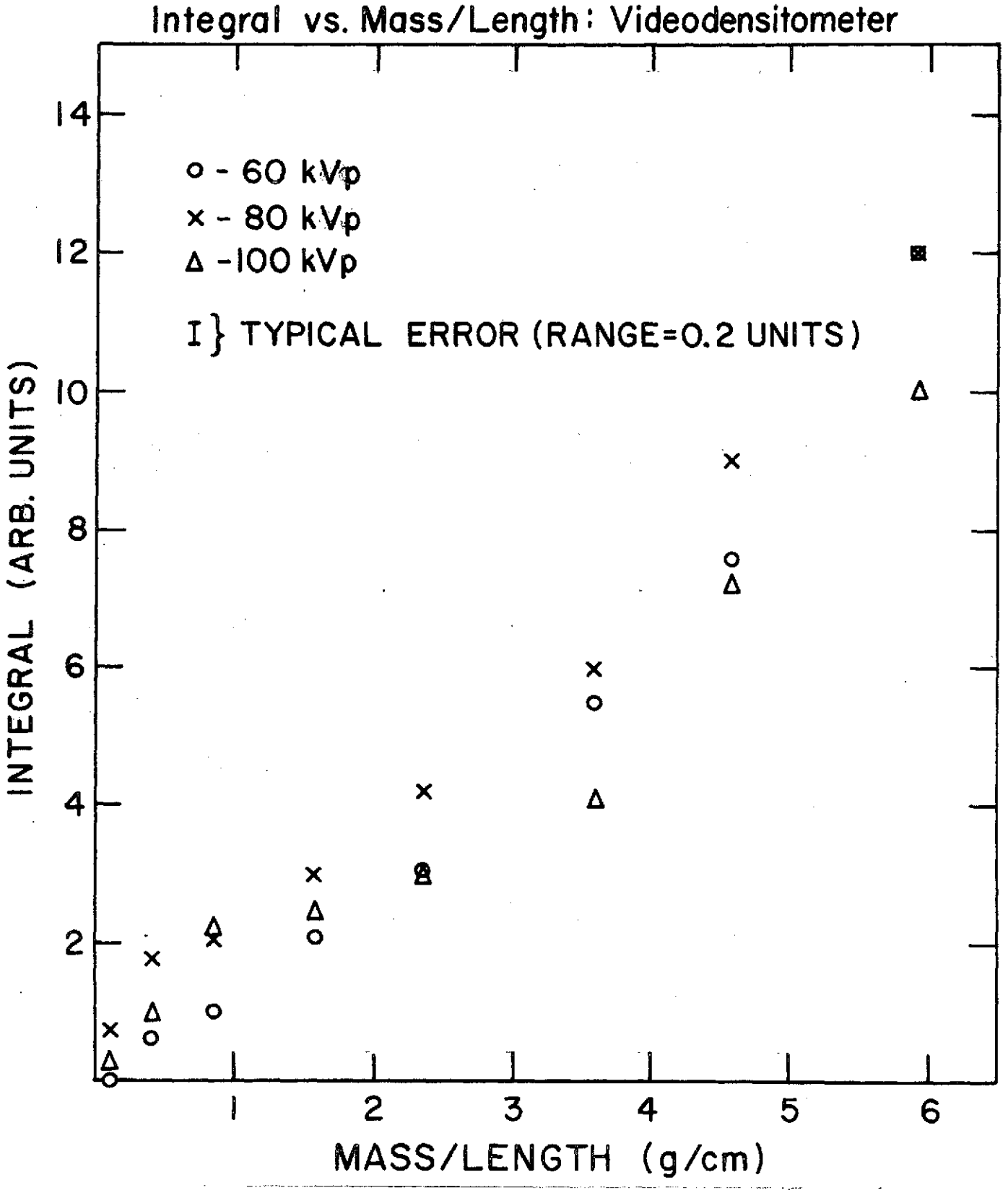

Fig. 1 Estimation of the mass per unit length for lucite rods in chest phantom using the videodensitometer. Ordinates were derived from the densitometer signal; abscissae were determined by measurements of mass and length of cylinders.

The data of Fig. 1 do not indicate any consistent energy dependence of the mass estimate. Also it appears that this data can best be fit by a curvilinear calibration curve. However this has not been attempted in these preliminary investigations since the instrumentation parameters used here are not necessarily those that will be used for any clinical investigations.

QUANTITATION OF MASS/LENGTH: DIGITAL COMPUTATIONS

The second method used to perform the mass determination was to digitize the video signal and perform the necessary integrations with a digital computer. Selected fields of the videotaped study were recorded onto a videodisc so that individual fields could be reviewed and then played continuously during digitization without serious degradation of the image. As with the videodensitometer, the image was viewed on a TV monitor and the area for study delineated, in this case with a light pen. The voltage waveforms of all the portions of all TV lines within this area were digitized by a Biomation Transient Recorder. The digitized waveforms were recorded on magnetic tape for subsequent computer analysis. Again $\ln(I_o/I)$ was taken as the estimate of the object's mass/area where I_o and I now represent the digital values applied to the waveform at points outside of and within the object, respectively. During the digitization process, the images of the smallest cylinders, those with 3.2 and 6.4 mm diameters, were essentially invisible in the playback from the disc recording although they were clearly visible in the original fluoroscopic study and distinguishable in playbacks of the videotape.

Since the TV scan lines were oriented parallel to the axes of the cylinders, a scan path perpendicular to the cylinder axis, from which the mass/length could be determined, was obtained by selecting corresponding digitization points from successive TV lines in a field. There were 162 such digitization points along a TV line representing a distance of about 2.5 cm at the object; there were 63 TV lines included in the digitization corresponding to a distance of about 3.8 cm. Hence the size of a data element at the location of the cylinders was about 0.15 x 0.60 mm^2. A typical scan path is shown in Fig. 2.

To determine the mass/length from the log of the ratio of intensities, it is necessary to use the net intensities transmitted in each case; background subtraction is required. The background level for a particular position in the TV image and for a particular x-ray generator potential was calculated as the average of the digitized values of the first and last points (e.g., TV lines 1 and 63 of Fig. 2) of all scans at that position in images recorded at that potential. A total of 16 points were used in each such average. The background was not constant with position in the TV image but was about 10% greater at the right side of the image compared to the left as viewed on a monitor (Fig. 3).

The I_o level was similarly determined for particular positions and x-ray generator potentials. Forty digitized points chosen from regions of maximum transmission (e.g., near TV lines 10 and 50 in Fig. 2) in the scan paths of the smaller cylinders were averaged after subtracting the corresponding background. An attempt was made to determine I_o by measuring the transmission through a region of the phantom without a tumor cylinder, but values determined in this way were 12 to 15% higher than those determined by the above method.

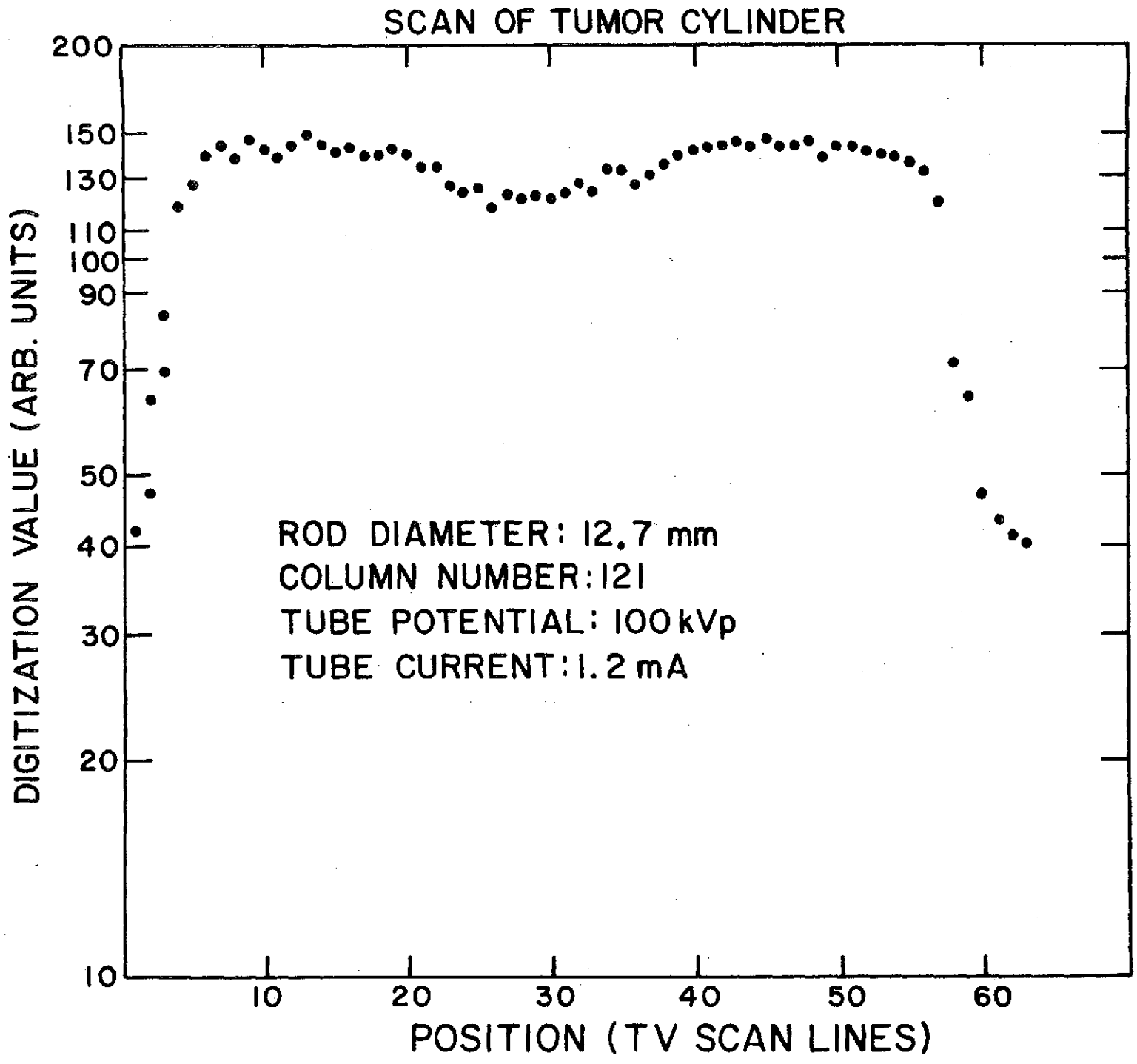

Fig. 2 Typical scan path across lucite cylinder derived from digitization of video signals.

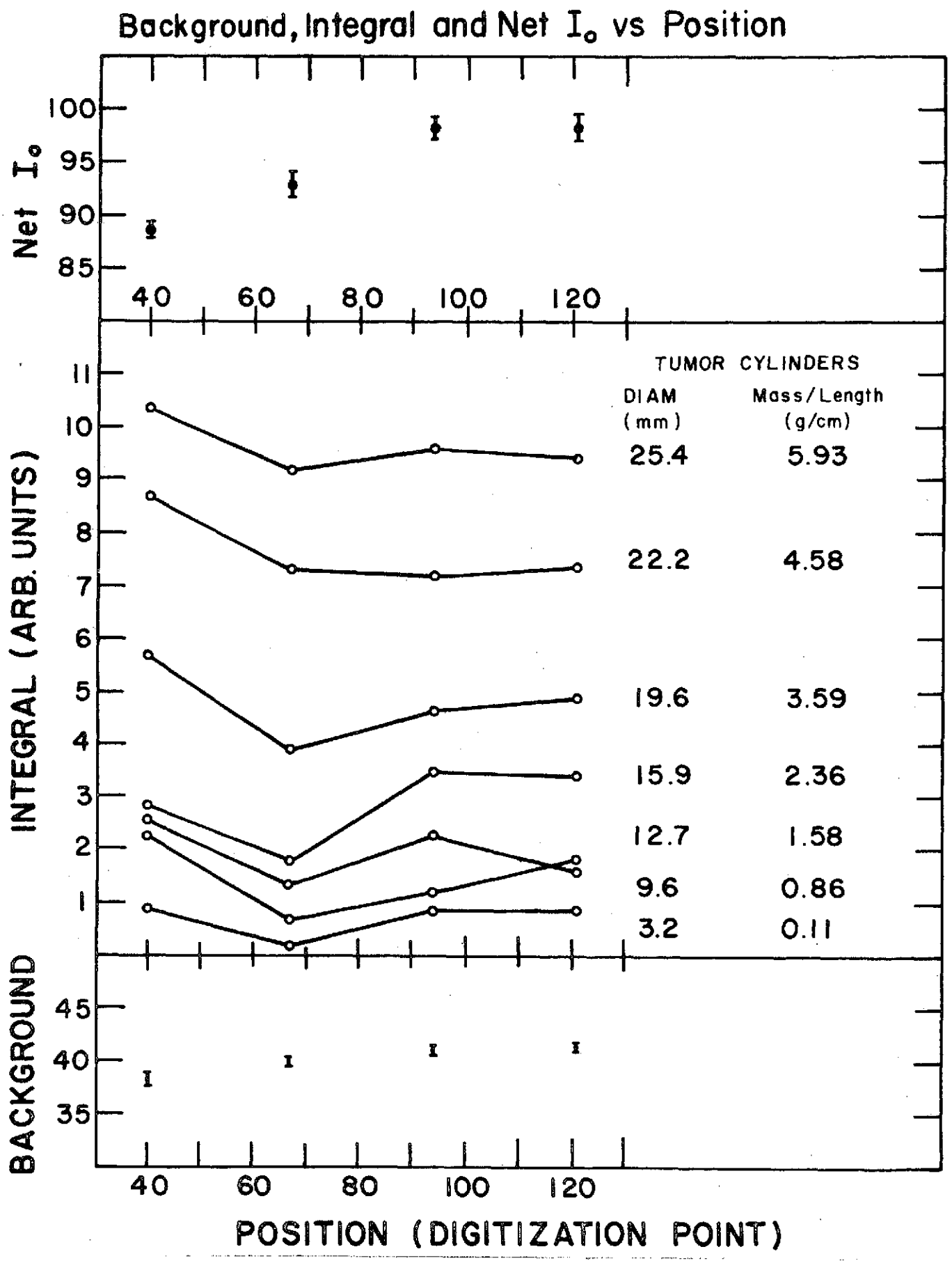

Fig. 3 Variation of background, integral, and net I_o values with position in the TV image. Error bars denote standard error of the mean.

The I_o values also depend on the position in the TV image (Fig. 3). This variation follows the same pattern as the background level with the difference between the two sides of the image, a length of 2.5 cm at the object, being about 10%.

The estimation of mass/length was then made by summing $\ln(I_o/I)$ along a scan path where I_o and I represent net digitized values of the video signal. Values of the integral as a function of position in the field are shown in Fig. 3 for seven of the eight cylinders. When the mass/length at a certain position in the field is calculated using values of background and I_o at the same position, the integrals show no consistent dependence on position.

Unlike the videodensitometer computations the mass/length values determined from the digitized video signals showed the expected dependence on beam energy (Fig. 4). That is, due to the larger subject contrast at lower x-ray energies, mass/length values are typically larger at 60 kVp than at 80 kVp, and those at 80 kVp are in turn larger than those at 100 kVp. In each case the I_o level was approximately the same since the x-ray tube current was adjusted to give the optimum signal-to-noise ratio in the video signal for the studies at each kVp.

The points in Fig. 4 represent the average integral for five adjacent scan paths across each cylinder corresponding to a total width of about 0.75 mm. The standard deviation of any five measurements showed no correlation with size of the cylinder or energy of the x-ray beam. The average value of these standard deviations ($\pm$ 0.21 units) is indicated in Fig. 4; the range of the standard deviations was 0.06 to 0.46 units. Typically for cylinders of about 20 mm diameter the coefficient of variation was in the range of 2 to 7% and for cylinders of about 5 mm diameter this value was in the range of 10 to 20%. However for cylinders having a mass/length less than 1 g/cm (cylinder diameters of 3.2 to 9.6 mm) the integral was essentially independent of the actual mass/length (Fig. 4). This may be due to degradation of the image after the many processes preceding digitization. This effect was not observed for the integrals determined with the videodensitometer (Fig. 1).

The points in Fig. 4, like those in Fig. 1, indicate a curvilinear relationship between the actual mass/length and the calculated integral. The direction of the curvature may be the result of an overestimation of the background. Before calibration equations are defined the nature of the relationship between the videodensitometrically determined integral and the actual mass/length should be investigated further.

SUMMARY AND CONCLUSIONS

These studies have indicated that a roentgen videodensitometric system can be employed to quantitate the measurement of lung tumor size. However there are many variables associated with the measurement which are expected to affect its outcome. These include the x-ray generator kVp and mA and their stability; the control settings of the image intensifier tube, TV camera, and video processing equipment; the size of the window of the videodensitometer or the coarseness of the digitization of the TV signal; the number of times the signal is processed; the position within the TV field at which the measurement is made; and the many problems associated with motion of and repositioning of the patient.

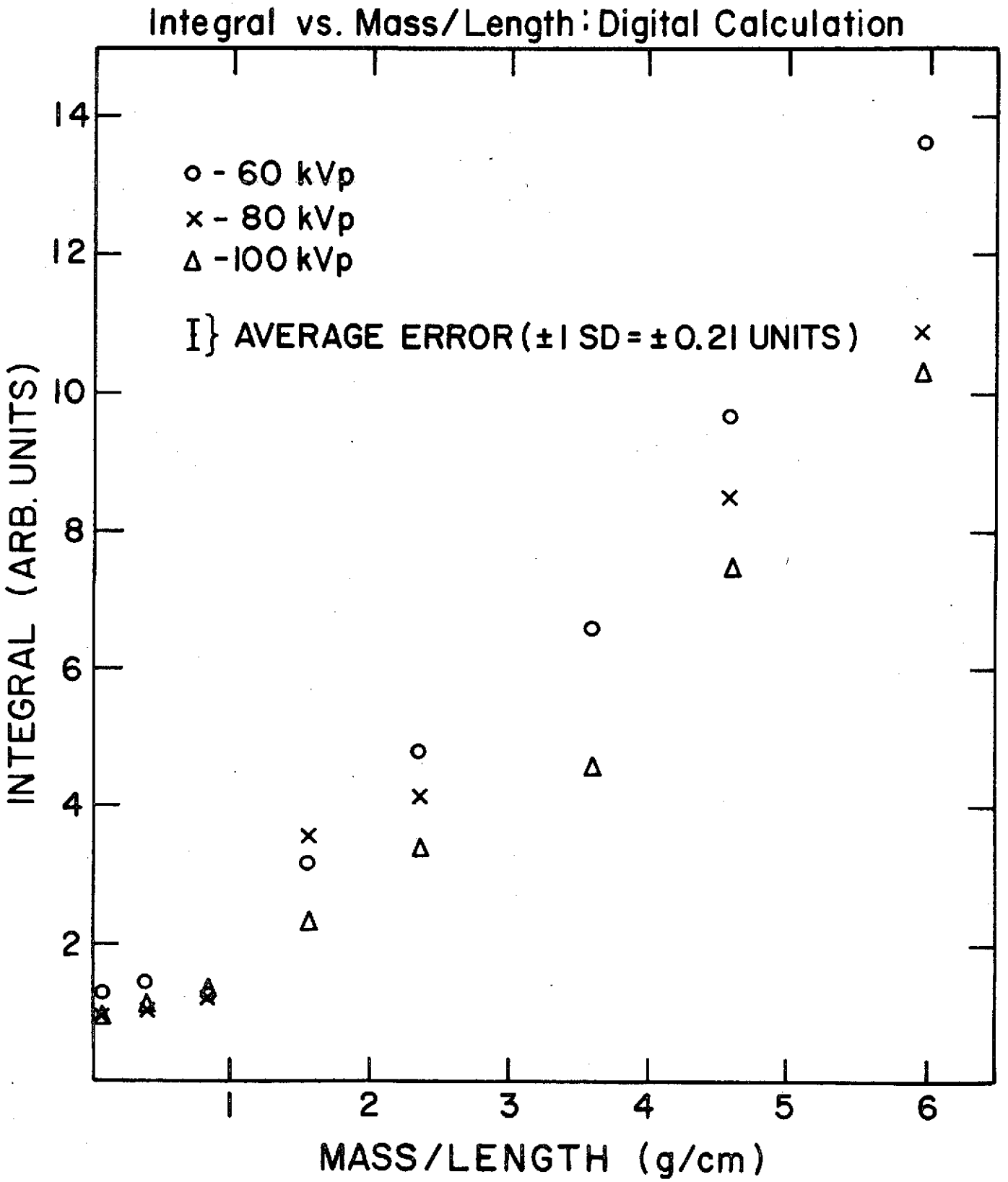

Fig. 4 Estimation of the mass per unit length for lucite rods in chest phantom using digitized video signals.

The energy dependence of the measurement has been investigated with inconclusive results. The estimations of the mass/length from the digitized signals showed the expected decrease of the estimate with increased x-ray generator potential. No consistent results relating to kVp dependence were seen in the determinations using the videodensitometer.

Tests on the digitized signals indicated that the mass/length estimate was independent of the position within the image at which the estimate was made. However, the video signal tended to increase along the path of the TV scan line for objects having constant thickness along this line. The source of this variation needs to be investigated.

The precision of a set of measurements made at the same time was comparable for both the videodensitometer and the digital determinations. The percentage errors for cylinders of about 20 mm diameter were in the range of 2 to 7% while those for cylinders of about 5 mm diameter ranged from 10 to 20%. This precision may be improved by obtaining a larger number of events per data element either by increasing the x-ray tube current or using larger data elements. The former solution is somewhat restricted by the necessity of avoiding saturation of the TV signal processing equipment. The digitization density is however easily variable although a coarser density would be expected to degrade the accuracy of the measurement somewhat. These statements of precision relate only to short-term fluctuations leading to variation within the images recorded at one session. Tests of long-term precision need to be undertaken.

The same videodensitometer window size was used for the measurements on all eight cylinders in order that the measurements could be readily intercompared. Greater sensitivity might be obtained by better matching of the window size to the object size, but a white level must be established for each window size used. The dependence of the mass estimate on the window size needs to be studied.

Another problem is the loss of information due to multiple processing of the image. The digitally calculated integrals became independent of cylinder size for the smallest cylinders. These same cylinders were essentially invisible in the videodisc recorded image from which the digitization was performed. This problem did not occur in the videodensitometer estimations for which the signals were obtained from the videotape. These results indicate that quantitation of the mass of small tumors will require a minimum of image processing.

REFERENCES

1. Sturm, R. E. and E. H. Wood: The Video Quantizer: An Electronic Photometer to Measure Contrast in Roentgen Fluoroscopic Images. Mayo Clinic Proc. 43, No. 11: 803, 1968.

2. Sturm, R. E. and E. H. Wood: Roentgen Image Intensifier, Television Recording System for Dynamic Measurements of Roentgen Density for Circulatory Studies. in Roentgen-, Cine-, and Videodensitometry: Fundamentals and Applications for Blood Flow and Heart Volume Determination, (P. H. Heintzen, ed.). Georg Thiem Verlag, Stuttgart, pp. 23-44, 1971.

3. Wood, E. H., R. E. Sturm and J. J. Sanders: Data Processing in Cardiovascular Physiology with Particular Reference to Roentgen Videodensitometry. Mayo Clinic Proc. 39, No. 11: 849, 1964.

4. Wood, E. H., E. L. Ritman, R. E. Sturm, S. Johnson, P. Spivak, B. K. Gilbert and H. C. Smith: The Problem of Determination of the Roentgen Density, Dimensions and Shape of Homogenous Objects from Biplane Roentgenographic Data with Particular Reference to Angiocardiography. in Proceedings of the San Diego Biomedical Symposium, Vol. 11, Feb. 2-4, 1972.

ACKNOWLEDGMENT

We wish to thank our colleagues at the Mayo Clinic, Rochester, Minnesota, for allowing us to use the roentgen videodensitometry facilities there and for aiding us in these investigations.

This work was supported in part by NIH Training Grant No. 5-T01-CA-05104-11.

COO-1422-156

BONE LOSS IN RHEUMATOID ARTHRITIS ACCELERATED BY CORTICOSTEROID TREATMENT

by

M. N. Mueller, R. Mazess and J. R. Cameron
Departments of Radiology and Medicine
University of Wisconsin

The monoenergetic photon absorptiometric method of determining bone mineral content was used to examine 236 adult caucasian women with rheumatoid arthritis. 109 had a history of corticosteroid therapy; 129 had no exposure to corticosteroids. Bone mineral content measurements were made at two sites on the radius; the midshaft site representing 99% cortical bone, and the distal site representing 85% cortical bone.

Significant bone mineral loss was not observed in the nonsteroid group at either site until the disease duration was more than 12 years. In the steroid group which was matched for disease severity, significant bone mineral loss was observed within two years.

RHEUMATOID ARTHRITIS DISEASE SEVERITY

Distal Left Radius:

		Without Steroid Therapy			With Steroid Therapy		
Diagnostic Severity	Functional Impairment	N	ΔBM Distal Left Radius	Standard Error of Mean	N	ΔBM Distal Left Radius	Standard Error of Mean
Probably Possible	I:II	47	0.03	±0.02			
Definite	II:III	33	0.01	±0.03	20	-0.10	±0.04
Classic	II	15	-0.05	±0.04	18	-0.14	±0.04
Classic	III	32	-0.11	±0.04	53	-0.24	±0.02
Classic	IV				13	-0.32	±0.04

Midshaft Left Radius:

		Without Steroid Therapy			With Steroid Therapy	
Diagnostic Severity	Functional Impairment	N	ΔBM Midshaft Left Radius	Standard Error of Mean	N	ΔBM Midshaft Left Radius	Standard Error of Mean
Probably Possible	I:II	47	0.00	±0.02			
Definite	II:III	32	-0.01	±0.02	20	-0.06	±0.03
Classic	II	15	-0.04	±0.03	19	-0.14	±0.04
Classic	III	32	-0.12	±0.03	56	-0.20	±0.02
Classic	IV				14	-0.33	±0.04

C00-1422-157

EVALUATION OF BONE MASS IN ARTHRITIS

USING MONOENERGETIC PHOTON-ABSORPTIOMETRY

by

M. N. Mueller, M.D.
Departments of Radiology and Medicine
University of Wisconsin

The technique of monoenergetic photon-absorptiometry was developed by Cameron at the University of Wisconsin to quantitatively assess bone mass in vivo. The method is simple, non-destructive, rapid, inexpensive and has a high degree of precision and accuracy. Although there are many reasons why demineralization of bone might be expected to occur in musculoskeletal disorders, prior use of radiographic techniques have not resolved a controversy as to whether osteopenia does indeed occur in rheumatoid arthritis; accordingly, all patients seen in the Arthritis Service of the University of Wisconsin Hospitals were examined. One hundred forty-four adult Caucasian female subjects with a diagnosis of ARA classic or definite rheumatoid arthritis have detailed clinical and laboratory information which has been analyzed to study relationship of bone mineral to several variables associated with the disease. The results are shown in the table below:

DISEASE SEVERITY, NO STEROID	N	ΔB.M.* ± S.D.
Definite, Functional Class II	22	-.02 ± .12
Classic, Functional Class II	13	-.02 ± .12
Classic, Functional Class III, IV	18	-.13 ± .21

DISEASE DURATION, NO STEROID INTERVAL	MEAN DURATION	N	ΔB.M.* ± S.D.
0-4 years	2.1	24	-.02 ± .10
5-9	6.1	14	-.04 ± .18
10-14	11.6	5	-.04 ± .09
15+	19.2	10	-.19 ± .21

DOSE OF STEROID IN PILL YEARS INTERVAL P-Y	MEAN P-Y	N	ΔB.M.* ± S.D.
0-4	2.4	28	-.06 ± .16
5-8	6.5	19	-.14 ± .13
9-12	10.2	12	-.16 ± .16
13-20	13.5	10	-.20 ± .17
21+	28.6	10	-.29 ± .15

*ΔBM = difference between individual patient measurement of bone mineral and normative mean for age and sex.

These studies establish that bone mineral loss does occur in adult Caucasian women with rheumatoid arthritis. Its onset and severity are associated with disease severity and duration of disease. Demineralization is also related to total dose of steroids in prednisone treated patients. Multiple regression analysis techniques are being utilized to assess the relative risks associated with each variable.

Monoenergetic photon-absorptiometry has proven to be a useful technique for investigating bone mass in clinical disease states at single points in time. Of potentially greater interest are sequential measurements at different points in time allowing estimation of the rate of bone mineral loss in individual subjects. These studies are in progress.

COO-1422-158

EARLY RECOGNITION OF OSTEOPOROSIS IN THE AGED FEMALE

Submitted to New England Journal of Medicine

Everett Smith, Steven Babcock and John Cameron
University of Wisconsin
Madison, Wisconsin 53706

Abstract

Fifty clinically osteoporotic females were age matched with fifty "control" females with an average age of seventy-four. The average mid-radial bone mineral value of the control group was (0.76 $\pm$ 0.13 g/cm) and for the osteoporotic group (0.62 $\pm$ 0.12 g/cm). The mean bone mineral content of the osteoporotic group was significantly lower ($P < .001$) than the control group. The mean bone width of both the osteoporotic group and the control was 1.27 cm. A bone mineral discriminant value of 0.68 g/cm separated 76% of the control subjects from the osteoporotic subjects. The mean bone mineral divided by bone width of the osteoporotic group was significantly lower ($P < 0.1$) than the control group. We recommend criteria for the early recognition of osteoporosis based on bone mineral measurements of the radius.

Introduction

Excessive bone loss is a major problem in the aged female. It has been estimated that at least one out of four women in America over the age of 55 has a serious problem with bone loss (1). Early recognition of excessive bone loss is important if preventive measures are to be taken prior to the development of clinical symptoms. Bone loss in the aged female is often not diagnosed until non-traumatized spontaneous collapse of a vertebra, fracture of a distal radius or fracture of a femoral neck has occurred. When these clinical symptoms of osteoporosis occur in the aged, the bone mass is often more than thirty percent less than in women of the same size at age thirty. The increased longevity of the human population suggests that clinical osteoporosis will be an increasing medical problem in the elderly population.

Not all elderly people with excessive bone loss develop clinical symptoms of osteoporosis (2). Nor is the occurrence of spontaneous fractures in the elderly necessarily the result of an accentuation of the normal bone loss. However, the quantity of bone mineral does give a good indication of the resistance of bone to fracture. Criteria based on the amount of bone mineral of the radius are proposed for early recognition of osteoporosis prior to fracture, using the absorptiometry technique.

Methods and Materials

In vivo bone mineral mass measurements were obtained by using the Cameron-Sorenson technique of measuring the absorption of an I-125 mono-energetic x-ray beam (27.3 keV) in bone and soft tissue (3,4). The bone mineral and width of the radius were measured at a point one-third the distance from the olecranon to the head of the ulna. This point on the distal radius (called the standard site) is anatomically uniform and

demonstrates minimal bone mineral width variation on either side of the scanning site.

Bone mineral mass values were determined on fifty women age 52 to 97 (average age 74 $\pm$ 11) who were selected on the basis of clinical osteoporosis, and compared to fifty individually age matched controls. The criteria used to define clinical osteoporosis were a history of non-trauma fractures of the femoral neck, distal radius or a collapsed vertebra (5). The osteoporotic females were members of the local Senior Citizens' Club of Madison, patients of the University of Wisconsin Hospital, or the Manor House of Madison Nursing Home. The age matched controls were drawn from about 200 elderly women from the same sources. In the control group there were no histories of femoral neck or vertebral fractures, chronic endocrine, calcium or phosphorus disorders, or prolonged bed rest.

The bone mineral and width of the radius of the subjects were measured on a single visit over a two-year period. Three scans were made and the mean of the measurements was used in the comparison.

Results

The mean bone mineral contents at the standard site on the radius for the osteoporotic group and the age matched control group were 0.62 g/cm* and 0.76 g/cm, respectively (Table 1). The osteoporotic group was significantly lower than that of the control group indicated by the paired t-test, $P < .001$ (Table 1).

However, mean bone width at the standard site of the radius for both the osteoporotic women and their age matched controls was 1.27 cm (Table 1).

The mean bone mineral divided by bone width values at the standard site of the radius for the osteoporotic women and the age matched control group was 0.49 g/cm^2 and 0.60 g/cm^2, respectively (Table 1). The mean bone mineral divided by bone width for the osteoporotic group was significantly lower than that of the control group as indicated by the paired t-test, $P<.01$ (Table 1).

A bone mineral discriminant value of 0.68 g/cm was determined (Table 2). This value resulted in a seventy-six percent agreement between the absorptiometry measurement and the clinical diagnosis (Table 2). The discriminant value of 0.68 g/cm was above seventy-eight percent of the osteoporotic group and below seventy-four percent of the control group. Using this discriminant value, twenty-two percent of the osteoporotics would be "diagnosed" as normal and twenty-six percent of the normals would be "diagnosed" as clinically osteoporotic.

A bone mineral divided by bone width discriminant value of 0.55 g/cm^2 was determined (Table 2). This value results in a seventy-three percent agreement between the absorptiometry measurement and the medical diagnosis (Table 2). This discriminant value of 0.55 g/cm^2 was above seventy-six percent of the

* The unit g/cm indicates the mass of bone mineral in a 1 cm long section of bone at the measurement site.

osteoporotic group and below seventy percent of the control group. Using the absorptiometry bone mineral divided by bone width discriminant value, twenty-four percent of the osteoporotics would be "diagnosed" as normal and thirty percent of the normals would be "diagnosed" as osteoporotic.

Discussion

The criteria for early recognition of osteoporosis depends on what is considered "normal" bone loss in the aged. The distinction between normal bone loss and extreme bone loss is very clear, while the decision of how to classify a subject who demonstrates bone loss that is marginal, is very difficult. The distinction between the control group (0.76 g/cm) and the osteoporotic group (0.62 g/cm), determined by absorptiometry in this study, was highly significant ($P < .001$). These data parallel that reported by Dr. Smith (6). Using statistical criteria, he demonstrated that women with collapsed vertebrae had significantly less bone mineral in the radius than those without collapsed vertebrae. When the criteria of a discriminant bone mineral value of 0.68 g/cm was used to separate the two groups in our study, the decision as to which group an individual was classified into became less distinct in 24 of the hundred subjects measured.

The original criteria for recognition of clinical osteoporosis in the hundred subjects was determined by the presence of a spontaneous fracture of the femoral neck, vertebra, or distal radius. We propose that absorptiometry measurements be included in the criteria for recognition of osteoporosis. We suggest that any adult Caucasian female who has a bone mineral value below the discriminant value of 0.68 g/cm at the standard measuring site, be considered osteoporotic.

Using this additional criterion, thirteen of the control group would be considered as osteoporotic. These subjects were not recognized as osteoporotic solely because they did not manifest the presence of a spontaneous fracture. Using the combined criterion, 89% of the subjects are correctly classified as non-osteoporotic or osteoporotic.

Eleven of the osteoporotic subjects in this study were classified as "normal" by the absorptiometric system. These eleven osteoporotic subjects may: 1) have had fractures which were not spontaneous, 2) have elevated radial bone mineral because of therapy programs, or 3) have elevated radial bone mineral because of hypermineralization.

The classification of subjects with radial bone mineral below 0.68 g/cm, as osteoporotic is consistent with recent results reported by Wilson (7). He observed that of 25 cadavers, five out of six with indications of femoral neck fracture, pre or post death, had a radial bone mineral at the standard site less than 0.68 g/cm of the nineteen cadavers with bone mineral above 0.68 g/cm at the standard site only one had evidence of a hip fracture (cause unknown). Wilson quantitated the relationship between the bone mineral content of the femoral neck and radius. This quantitation was done by taking three separate bone mineral measurements on the neck of the femur, averaging these values and then correlating the average value with the bone mineral value measured at the standard site of the radius. These in vitro measurements demonstrated a correlation of 0.87 between the bone mineral content

in the radius and the neck of the femur. These data support the usefulness of the radial bone mineral discriminant value of 0.68 g/cm in early recognition of osteoporosis.

The data from our study can be used as a guide to distinguish "normal" from excessive bone loss with age. Early recognition of osteoporosis in the aged will enable therapy to be prescribed prior to development of spontaneous fractures.

Understanding of osteoporosis in the aged requires not only the discriminant bone mineral value as described above, but also the development of standards which will enable data comparison between various hospitals and laboratories nationally and internationally. We suggest the adoption of bone standards similar to those developed by Witt (8) at the University of Wisconsin.

One of the values selected for the international absorptiometry standard should be set at about 1.00 g/cm. The reason for choosing 1.00 g/cm is that it represents about the mean bone mineral value at the standard site obtained by Cameron (9) on a population of young normal Caucasian females (mean age 33.9 ± 3.1). This bone mineral represents the upper mean limit of the normative bone mineral value expressed in gm/cm in the Caucasian female population studied (Fig. 1). Similar bone mineral values of 30 year old females have been observed by other investigators (10, 11, 12). After age thirty, bone mineral decreases in the aging female to an average value of about 0.60 g/cm in ninety year old subjects. Therefore, if we relate the status of all bone mineral values at the standard site as a percentage of the mean bone mineral standard of 1.00 g/cm, a clearer expression of bone loss with age may evolve. This method of reporting would enable one to express bone loss as a fraction or percentage of a normal Caucasian female subject at age thirty. Similar reporting methods have been used in other aging studies (13). Any laboratory using this type of standardization may compare their results to national and international studies.

To enhance early recognition of osteoporotic subjects the following criteria for osteoporosis are suggested:

1. Any individual whose bone mineral mass at the standard measurement site of the radius is more than two standard deviations below the mean for individuals of the same age, sex and bone size, (Fig. 1), or;

2. Any adult Caucasian female whose bone mineral at the standard site of the radius is less than 0.68 g/cm, (32% less than the 30 year old) (Fig. 1); or

3. Any adult Caucasian female whose bone mineral divided by bone width at the standard site of the radius is less than 0.55 g/cm^2 (Fig. 2); or

4. Any individual who has a spontaneous fracture (who has not been diagnosed as having a bone disease which would cause the fracture).

TABLE 1

BONE MINERAL CONTENT, BONE WIDTH, AND BONE MINERAL DIVIDED BY BONE WIDTH OF THE STANDARD SITE OF THE RADIUS FOR 50 OSTEOPOROTIC WOMEN AND 50 AGE MATCHED CONTROLS

N = 50	Mean	S.D.	t-test*
Bone Mineral			
Osteoporotic	0.62 g/cm	0.12	5.54
Control	0.76 g/cm	0.13	$p<0.001$
Bone Width			
Osteoporotic	1.27 cm	0.15	
Control	1.27 cm	0.14	
Bone Mineral/Bone Width			
Osteoporotic	0.49 g/cm^2	0.09	5.11
Control	0.60 g/cm^2	0.09	$p<0.01$

TABLE 2

DISCRIMINANT ANALYSIS FOR THE STANDARD SITE OF THE RADIUS FOR 50 OSTEOPOROTIC WOMEN AND 50 AGE MATCHED CONTROLS

N = 100 cases	Controls	Osteoporosis	Correct Diagnosis	
Bone Mineral (S = 0.68 g/cm)				
BM $\geq$ 0.68 g/cm	37	11	78%	76%
BM $<$ 0.68 g/cm	13	39	74%	
Bone Mineral/Bone Width ($S = 0.55\ g/cm^2$)				
BM/W $\geq 0.55\ g/cm^2$	35	12	70%	73%
BM/W $< 0.55\ g/cm^2$	15	28	76%	

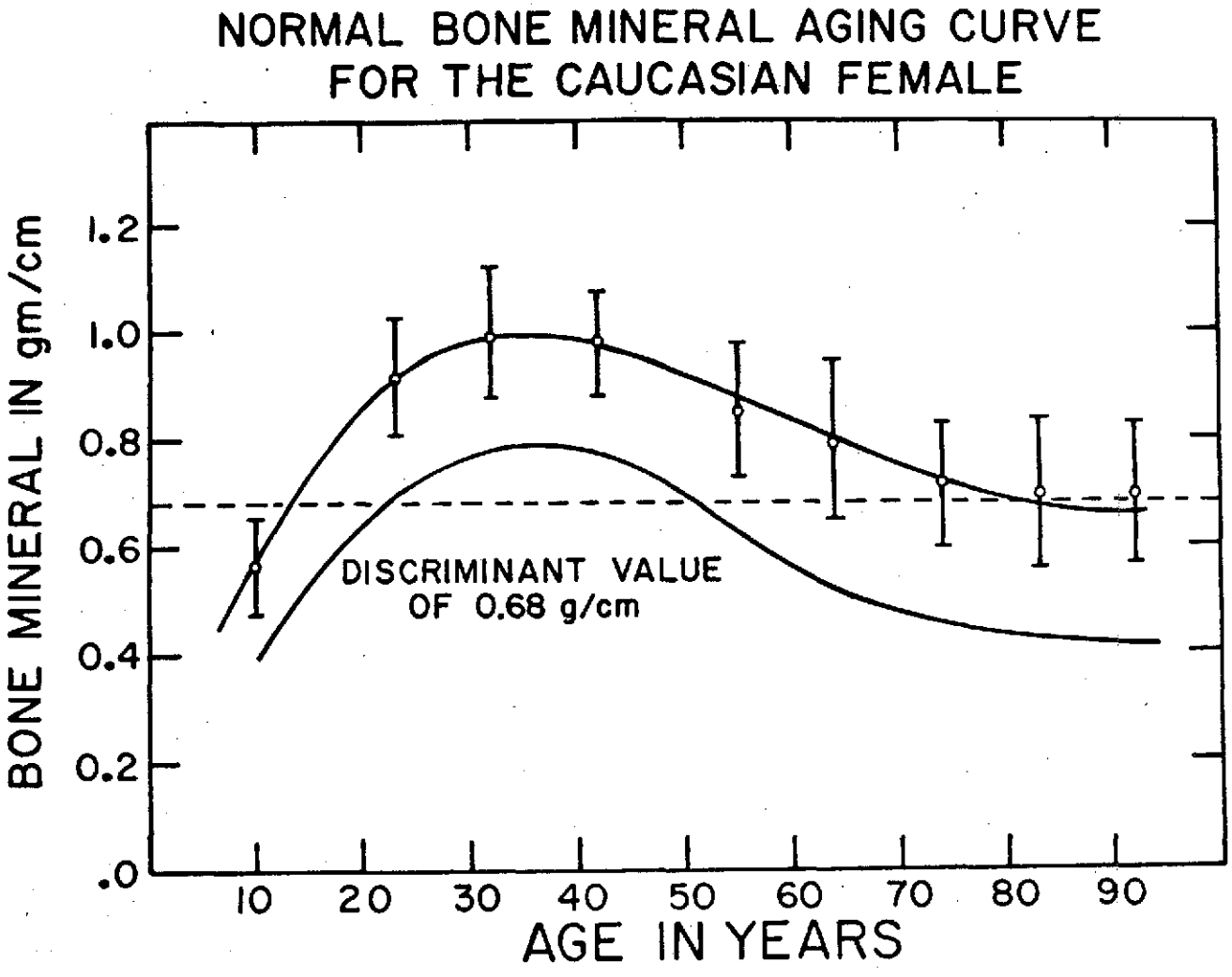

figure 1

Bars represent one standard deviation.
Solid black line represents two standard deviations.
Broken line represents the discriminant value of 0.68 g/cm.

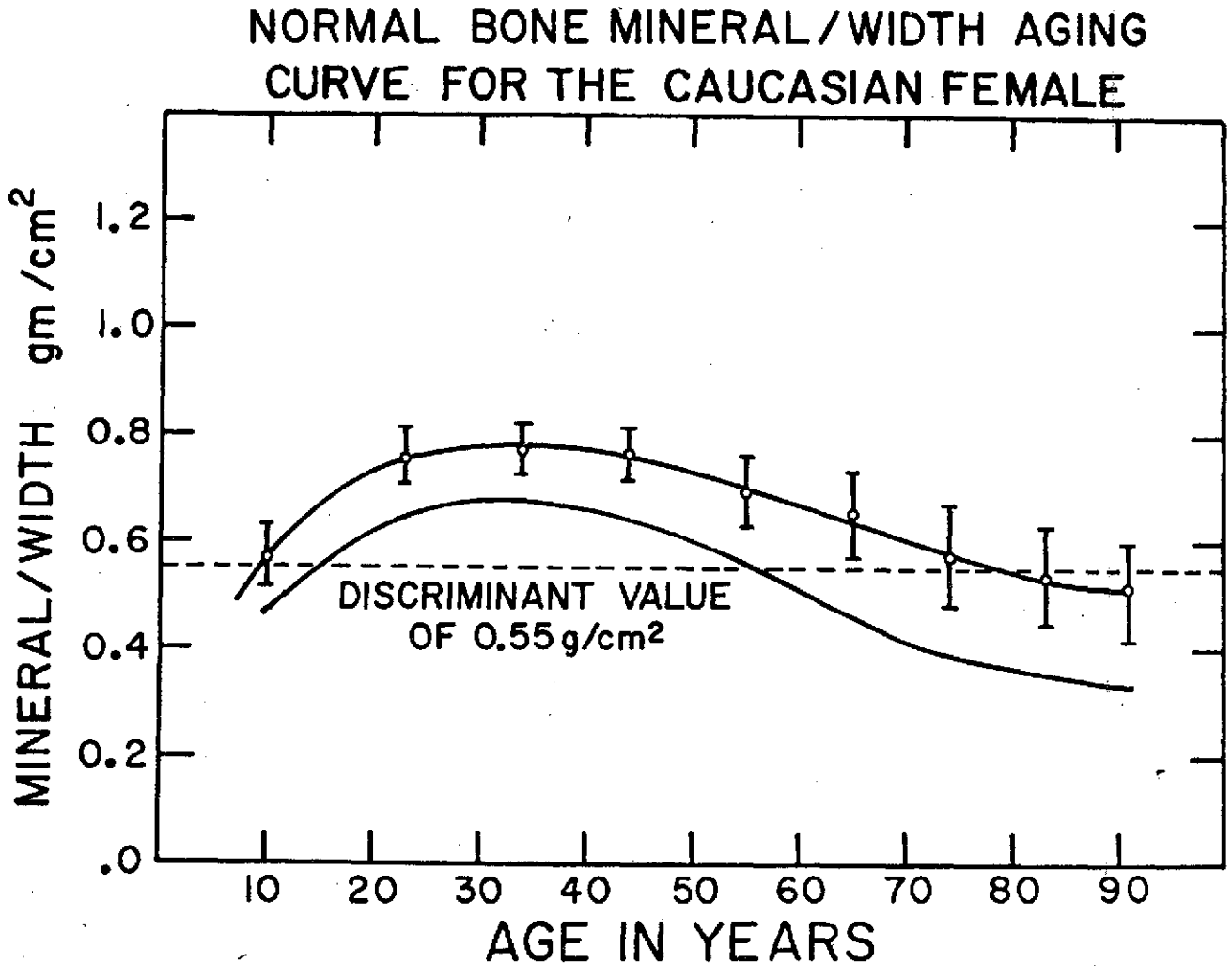

figure 2

Bars represent one standard deviation.
Solid black line represents two standard deviations.
Broken line represents the discriminant values of $0.55 g/cm^2$.

References

1. Davis, M.E., Lanzl, L.H. and Cox, Ann B. The detection, prevention and retardation of menopausal osteoporosis. Osteoporosis Ed. Uriel S. Barzel, Grune and Stratton, Inc., New York, New York, p. 140-149, 1970.

2. Issekutz, B., Blizzard, J.J., Birkhead, H.C. and Rodahl, K. Effects of prolonged bedrest on urinary calcium output. J. of Appl. Physiol. 21: 1013-1020, 1966.

3. Cameron, J.R. and Sorenson, J.A. Measurement of bone mineral in vivo: An improved method. Science 142: 230-232, 1963.

4. Sorenson, J.A. and Cameron, J.R. A reliable in vivo measurement of bone mineral content. J. Bone and Joint Surgery 49A: 3, 481-497, 1967.

5. Urist, M.R., MacDonald, N.S., Noss, M.J. and Skoog, W.A. Rarefying disease of the skeleton: observation dealing with aged and dead bone in patients and osteoporosis in mechanisms of hard tissue destruction. Pub. No. 75, Am. Assoc. for the Adv. of Science, Wash. D.C., 385-446, 1963.

6. Smith, D.M., Johnson, C.C., Jr., Yu, Pao-Lo. In Vivo measurements of bone mass. J.A.M.A. 219: 325-329, 1972.

7. Wilson, C.R. The use of in vivo bone mineral determination to predict the strength of bone. University of Wisconsin, Ph.D. Thesis, 1972.

8. Witt, R.M., Mazess, R.B., and Cameron, J.R. Standardization of bone mineral measurements. Proceedings of Bone Measurement Conference. Edited by J.R. Cameron. CONF-700S1S, 303-307. Clearinghouse for Federal Scientific and Technical Information, National Bureau of Standards, U.S. Department of Commerce. Springfield, Virginia 22151.

9. Cameron, J.R. The bone mineral of the radius in normals. Application of the direct photon absorption technique for measuring bone mineral content in vivo. NASA Grant No. Y-NGR-50-002-051. COO-1422-41, 1969.

10. Garn, S.W., Rohmann, C.G., and Wagner, B. Bone loss as a general phenomenon in man. Fed. Proc. 26: 1729-1736, Nov.-Dec. 1967.

11. Saville, P.E. Changes in bone mass with age and alcoholism. J. Bone and Joint Surg. 47: 492-499, 1965.

12. Trotter, M., Broman, G.E. and Peterson, R.R. Densities of bones of white and negro skeletons. J. Bone and Joint Surg. 42A: 50-58, 1960.

13. Shock, N.W. The physiology of aging. Scientific American 206: 1, 100-110, Jan. 1962.

COO-1422-159

EFFECTS OF PHYSICAL ACTIVITY ON BONE LOSS IN THE AGED*

E. L. Smith and S. W. Babcock
University of Wisconsin
Madison, Wisconsin

In vivo bone mineral absorptiometry measurements were obtained by using the Cameron-Sorenson technique of measuring the absorption of an I-125 monoenergetic beam in bone and soft tissue at the mid-shaft of the radius.

The purpose of this investigation was to study the effects of physical activity in slowing the normal process of osteoporosis and/or increasing bone mineral in the aged. Thirty-nine subjects were involved and included both sexes with an age range of 55 to 94 years. Three groups were studied for 8 months: 21 in a control group, twelve in a physical activity group and 6 in a physical therapy group. The physical activity group participated in an exercise program 45 minutes, 3 times a week for 8 months. The physical therapy group received supervised physical therapy for medical indications during the study. The control group participated in no formal physical activity.

Bone mineral: The physical activity group demonstrated a significant, ($P<.05$) bone mineral increase of 2.6 percent during the 8 month study, while the control group demonstrated no bone mineral change. The physical therapy group demonstrated a significant, ($P<.05$) bone mineral increase of 7.8 percent. The bone mineral change difference between the control group and the physical activity group was not significant at the .05 level. The bone mineral change difference between the control group and the physical therapy group was significant at the ($P<.05$) level. Physical activity as demonstrated by the physical therapy group and suggested by the physical activity group will maintain bone mineral and may stimulate bone mineral increase in the aged.

* Presented at the 20th Annual Meeting of the American College of Sports Medicine, Seattle, Washington, May 1973.